

**TITLE PAGE**

**THE INTERACTION BETWEEN MALARIA PARASITES  
AND HUMAN ENDOTHELIAL CELLS: SINGLE CELL  
STUDIES**

**Thesis submitted in accordance with the requirements of the  
University of Liverpool for the degree of Doctor of Philosophy**

**By**

**Kwannan Nantavisai**

**B.Sc. (Biology) Mahidol University (Thailand)**

**M.Sc. (Microbiology) Mahidol University (Thailand)**

**April 2011**

## **DECLARATION**

This thesis is the result of my own work. The material contained in the thesis has not been presented, nor is currently being presented, either wholly or in part for any other degree or other qualification.

The research work was carried out in The Liverpool School of Tropical Medicine, United Kingdom.

Kwannan Nantavisai (2011)

## ACKNOWLEDGEMENTS

First of all, I would like to thank my supervisor, Professor Stephen Andrew Ward, for giving me an opportunity to work in his laboratory, for his constant support and encouragement throughout my research work and thesis writing. I also would like to express my gratitude to my co-supervisor, Dr. Giancarlo Biagini, for his generous help with confocal microscope, and for his encouragement and suggestion regarding my research and thesis writing.

I wish to extend my special thanks to Professor Alister Craig and Professor Mark Taylor, who are my advisory panel, for their valuable comments and suggestions. Thanks to Dr. Yang Wu, Tadge Szeszak, Dr. Srabasti Chakravorty and Dr. Katie Hughes for their suggestions and help in the laboratory techniques.

Sincerest thanks to Ruth and Jill for teaching me how to culture malaria parasites, for showing me good practice in the laboratory and many more. Thanks to Ashley for teaching me how to operate the fluorescence plate reader, reviewing my thesis draft and his friendship. Thanks to Ally and Alison (Mbekeani) for reviewing my thesis draft and also their friendship.

Special thanks to Dr. Parnpen Viriyavejakul for teaching me how to handle confocal microscope, co-culture techniques and her kindness. I would like to thank my colleagues and friends: Enrique, Paul, Nick, Dave, Sam, Alison (Ardrey), Alasdair, Edwin, Sant, Mohammed, Doss, Archana, Khairul, Thomas, Susan, Teresa, Upali, Tiago, Susanna, Francesca, Murad, Taghreed and Fayza for their company, discussion and all cheerful support. Thanks to Mary and Angela for assisting me in many different ways. Sincere thanks to Peung, Pee Jae and Air for all supporting and encouragement.

Grateful thanks to The Royal Thai Government for providing financial support throughout my study in UK. I also would like to express my gratitude to Prof. Peerepan Tan-ariya, Colonel Associate Prof. Saovanee Leelayoova and Colonel Associate Prof. Mathirut Mungthin who trust and support me in order to study in the UK.

I thank my family: papa and mama for giving me life, for educating me, and for their unconditional love and supporting in whatever I do. My brother and sister for listening to my complaint, for believing in me and for their constant love and encouragement. I cannot come this far without them.

Last, but not least, I thank to the person who is very special in my life, Kachanon Nirunpong, for his constant patience, love, support and everything he has given me for almost ten years.

**Thesis title: The interaction between malaria parasites and human endothelial cells: single cell studies**

**Author: Kwannan Nantavisai, B.Sc, M.Sc.**

### **THESIS ABSTRACT**

Cerebral malaria (CM) is one of the most common lethal complications of the complex syndrome named severe malaria. The pathogenesis of severe malaria is thought to be due to the ability of infected red blood cells to sequester in the small blood vessels of vital organs. Sequestration, resulting from the interaction between parasite proteins on the surface of parasitized red blood cells (PRBC) and host endothelial cell adhesion molecules can cause activation of intracellular signalling pathways in endothelial cells including induction of apoptosis in endothelial cells which may be responsible for the blood-brain barrier breakdown seen in CM.

The aim of the thesis is to get a better understanding of the pathogenesis of cerebral malaria which may lead to new therapeutic interventions for the disease. We used co-culture models to study the interaction between malaria infected erythrocytes and endothelial cells. The results showed that the cytoadherence of infected erythrocytes to endothelial cells can induce apoptosis of endothelial cells which was confirmed by endothelial cell morphological changes, annexin V binding and caspase activity. It was found that the ability of parasites to induce endothelial apoptosis is dependent on the infected erythrocyte membrane remaining intact, but is independent of parasite viability. Apoptosis of endothelial cells induced by malaria parasites has been shown to involve both receptor-mediated (caspase-8) and mitochondrial mediated (caspase-9) pathways. Measurement the mitochondrial membrane potential ( $\Delta\Psi_m$ ) of apoptotic endothelial cells showed the dissipation of the mitochondrial  $\Delta\Psi$  confirming the involvement of a mitochondrial mediated pathway. Further studies to unveil the signalling pathways underlying endothelial apoptosis, using various inhibitors, implicated calcium signalling and NF- $\kappa$ B signalling pathway in apoptosis induced by parasites. Immunocytochemical staining of 4-hydroxynonenal (4-HNE), a marker of oxidative stress, also showed the association of oxidative stress with these events.

To study the endothelial cell membrane receptor mediating PRBC attachment and apoptosis of endothelial cells, the apoptogenic malaria parasites were enriched by panning on endothelial cells. The enriched parasites were shown to have a higher level of cytoadherence and still retained their apoptogenic property. It was found that cytoadherence of the enriched parasites to endothelial cells in our models is probably ICAM-1 independent. Unfortunately, antibodies against CD31, CD36 and CD105 failed to inhibit cytoadherence of parasites. Thus the precise adhesion molecule(s) on endothelial cells which is/are involved in this event remain undefined.

In conclusion, we have shown that cytoadherence of infected erythrocytes can occur by as yet undefined adhesion receptors on the surface of endothelial cells (but which is probably ICAM-1 independent) and this interaction can in turn induce apoptosis. The cell apoptosis involves receptor-mediated and mitochondrial mediated pathways as well as oxidative stress, calcium signalling and NF- $\kappa$ B signalling. The definitive molecular basis for the effects seen in co-culture and the relevance to clinical cerebral malaria require further investigation.



# TABLE OF CONTENTS

<b>DECLARATION .....</b>	<b>ii</b>
<b>ACKNOWLEDGEMENTS .....</b>	<b>iii</b>
<b>THESIS ABSTRACT .....</b>	<b>iv</b>
<b>TABLE OF CONTENTS .....</b>	<b>v</b>
<b>LIST OF ABBREVIATIONS .....</b>	<b>xii</b>
<b>LIST OF FIGURES .....</b>	<b>xvi</b>
<b>LIST OF TABLES .....</b>	<b>xix</b>
<b>CHAPTER 1: INTRODUCTION .....</b>	<b>1</b>
<b>1.1 MALARIA .....</b>	<b>1</b>
1.1.1 <i>Plasmodium falciparum</i> life cycle.....	1
1.1.2 <i>P. falciparum</i> cytoadherence .....	3
1.1.2.1 Host adhesion receptors .....	4
1.1.2.2 <i>P. falciparum</i> erythrocyte membrane protein 1 (PfEMP-1) .....	7
1.1.2.3 Effects of cytoadherence on endothelial cells.....	8
1.1.3 Cerebral malaria .....	9
<b>1.2 APOPTOSIS .....</b>	<b>15</b>
1.2.1 Pathways involved in apoptosis.....	16
1.2.1.1 The extrinsic apoptotic pathway .....	16
1.2.1.2 The intrinsic apoptotic pathway .....	18
1.2.1.3 Endoplasmic reticulum stress apoptotic pathway .....	19
1.2.1.4 JNK and p38 MAPK pathways.....	20
1.2.1.5 p53 .....	22
1.2.1.6 NF- $\kappa$ B .....	24
1.2.1.7 Calcium signalling .....	25

1.2.2 Oxidative stress and apoptosis.....	27
1.2.3 Toll-like receptors (TLR) .....	28
<b>THESIS OBJECTIVES .....</b>	<b>31</b>
<b>CHAPTER 2: GENERAL MATERIALS AND METHODS .....</b>	<b>32</b>
<b>2.1 Malaria culture.....</b>	<b>32</b>
2.1.1 Malaria parasite isolate.....	32
2.1.2 Preparation of complete medium.....	32
2.1.3. Preparation of serum.....	32
2.1.4 Preparation of uninfected erythrocytes.....	32
2.1.5 Sub-culturing of malaria parasite .....	33
2.1.6 Gas Phase.....	33
2.1.7 Parasite cryopreservation.....	33
2.1.8 Parasite retrieval .....	34
2.1.9 Parasite synchronisation .....	34
<b>2.2 Human Umbilical Vein Endothelial Cell (HUVEC) culture .....</b>	<b>35</b>
2.2.1 Primary human umbilical endothelial cells .....	35
2.2.2 Medium preparation .....	35
2.2.3 Preparation of seeding vessels.....	35
2.2.4 HUVEC retrieval .....	36
2.2.5 Standard HUVEC culture .....	36
2.2.6 Sub-culturing of HUVEC .....	36
2.2.7 HUVEC cryopreservation .....	37
<b>CHAPTER 3: POST-ADHESIVE INDUCTION OF APOPTOSIS IN HUMAN ENDOTHELIAL CELLS BY MALARIA INFECTED ERYTHROCYTES .....</b>	<b>38</b>
<b>3.1 INTRODUCTION.....</b>	<b>38</b>
<b>3.2 MATERIALS AND METHODS .....</b>	<b>41</b>

3.2.1 Preparation of HUVEC for co-culturing .....	41
3.2.2 Preparation of malaria parasites for co-culturing .....	41
3.2.3 Co-culture of HUVEC with malaria parasites.....	42
3.2.4 Induction of apoptosis by camptothecin.....	42
3.2.5 Determination of apoptotic cells using confocal laser scanning microscope .....	42
3.2.6 Comparison between live and dead malaria parasites in inducing apoptosis in HUVEC .....	44
3.2.6.1 Malaria parasites killed by artesunate treatment.....	44
3.2.6.2 Malaria parasites killed by heat .....	44
3.2.6.3 Heat-killed parasites binding to endothelial cells .....	45
3.2.6.4 Artesunate-killed malaria parasites binding to endothelial cells .....	46
3.2.7 The importance of parasite ligand binding preference in parasite induced HUVEC apoptosis .....	46
3.2.8 Blocking parasite induced HUVEC apoptosis with caspase inhibitors....	47
3.2.9 Caspase-8 and caspase-9 activities in malaria parasites induced apoptosis in HUVEC .....	48
3.2.9.1 Preparation of cell lysate.....	48
3.2.9.2 Luminescence activities of caspase-8 and caspase-9.....	49
3.2.10 Statistical analysis .....	49
<b>3.3 RESULTS.....</b>	<b>50</b>
3.3.1 Cytoadherence of PRBC and RBC to HUVEC.....	50
3.3.2 Cytoadherence-mediated PRBC induced apoptosis of HUVEC.....	52
3.3.3 The role of ligand binding preference and PRBC induced HUVEC apoptosis.....	55
3.3.4 Establishing the role of parasite viability and PRBC induced HUVEC apoptosis.....	56

3.3.5 The HUVEC binding potential of heat-killed and artesunate-killed malaria parasites .....	58
3.3.6 Blockage of PRBC-induced apoptosis of HUVEC with pan-caspase inhibitor Z-VAD-FMK, caspase-8 inhibitor Z-IETD-FMK and caspase-9 inhibitor Z-LEHD-FMK.....	60
3.3.7 Caspase-8 and caspase-9 activities in PRBC-induced HUVEC.....	63
<b>3.4 DISCUSSION .....</b>	<b>66</b>
<b>CHAPTER 4: MEASURING THE EFFECT OF MALARIA PARASITE BINDING ON THE MITOCHONDRIAL MEMBRANE POTENTIAL OF HUMAN ENDOTHELIAL CELLS.....</b>	<b>70</b>
<b>4.1 INTRODUCTION.....</b>	<b>70</b>
<b>4.2 MATERIALS AND METHODS .....</b>	<b>72</b>
4.2.1 Preparation of HUVEC for co-culturing .....	72
4.2.2 Preparation of malaria parasites for co-culturing .....	72
4.2.3 Co-culture of HUVEC with malaria parasites.....	73
4.2.4 Measurement of endothelial cell mitochondrial membrane potential ( $\Delta\Psi_m$ ) by confocal laser scanning microscope.....	73
4.2.5 Statistical analysis .....	74
<b>4.3 RESULTS.....</b>	<b>75</b>
4.3.1 Binding of PRBC to HUVEC.....	75
4.3.2 Mitochondrial membrane potential of HUVEC attached to PRBC.....	76
<b>4.4 DISCUSSION .....</b>	<b>79</b>
<b>CHAPTER 5: MALARIA PARASITE CYTOADHERENCE INDUCES OXIDATIVE STRESS IN HUMAN ENDOTHELIAL CELLS.....</b>	<b>81</b>
<b>5.1 INTRODUCTION.....</b>	<b>81</b>
<b>5.2 MATERIALS AND METHODS .....</b>	<b>84</b>
5.2.1 Preparation of HUVEC for co-culturing .....	84

5.2.2 Preparation of malaria parasites for co-culturing .....	84
5.2.3 Co-culture of HUVEC with malaria parasites .....	85
5.2.4 Immunocytochemistry for the detection of 4-HNE formation .....	85
5.2.5 Determination of 4-HNE formation using confocal laser scanning microscope.....	86
<b>5.3 RESULTS.....</b>	<b>87</b>
5.3.1 Malaria parasites induced the formation of 4-HNE in HUVEC.....	87
5.3.2 Effect of iron chelator on the formation of 4-HNE in HUVEC co-cultured with malaria parasites .....	87
<b>5.4 DISCUSSION .....</b>	<b>93</b>
<b>CHAPTER 6: EFFECT OF CELL SIGNALLING INHIBITORS ON MALARIA PARASITE-INDUCED HUMAN ENDOTHELIAL CELL APOPTOSIS .....</b>	<b>95</b>
<b>6.1 INTRODUCTION.....</b>	<b>95</b>
<b>6.2 MATERIALS AND METHODS .....</b>	<b>98</b>
6.2.1 Preparation of HUVEC for co-culturing .....	98
6.2.2 Preparation of malaria parasites for co-culturing .....	98
6.2.3 Co-culture of HUVEC with malaria parasites.....	99
6.2.4 Inhibitor treatment.....	99
6.2.5 Determination of apoptotic cells using confocal laser scanning microscope .....	102
6.2.6 Statistical analysis .....	102
<b>6.3 RESULTS.....</b>	<b>103</b>
6.3.1 Cytoadherence of PRBC and to HUVEC.....	103
6.3.2 Effect of various apoptotic inhibitors on apoptosis of HUVEC attached to PRBC.....	105
<b>6.4 DISCUSSION .....</b>	<b>110</b>

<b>CHAPTER 7: CHARACTERISATION OF HUMAN ENDOTHELIAL CELL SURFACE MEMBRANE RECEPTORS ELICITING CYTOADHERENCE-INDUCED APOPTOSIS.....</b>	<b>117</b>
<b>7.1 INTRODUCTION.....</b>	<b>117</b>
<b>7.2 MATERIAL AND METHODS.....</b>	<b>119</b>
7.2.1 HUVEC-bound malaria parasites selection.....	119
7.2.1.1 Preparation of HUVEC for parasites selection.....	119
7.2.1.2 Preparation of malaria parasites for parasites selection.....	119
7.2.1.3 HUVEC-bound malaria parasites selection .....	120
7.2.1.4 Determination of percentage binding between HUVEC and enriched parasites and percentage apoptosis of HUVEC attached to enriched parasites .....	120
7.2.2 Determination the effect of TNF- $\alpha$ on apoptosis of HUVEC .....	122
7.2.3 HUVEC immunofluorescence staining for ICAM-1 expression analysis by FACS .....	122
7.2.4 ICAM-1 inhibition.....	123
7.2.5 CD31, CD36 and CD105 inhibition .....	124
7.2.6 Statistical analysis .....	125
<b>7.3 RESULTS.....</b>	<b>126</b>
7.3.1 Attachment between HUVEC and PRBC .....	126
7.3.2 Apoptosis of HUVEC attached to PRBC .....	127
7.3.3 Effect of TNF- $\alpha$ on apoptosis of HUVEC.....	128
7.3.4 Quantitative measurement of ICAM-1 expression.....	130
7.3.5 Inhibition of binding of PRBC to ICAM-1 on HUVEC.....	132
7.3.6 Inhibition of binding of PRBC to CD31, CD36 and CD105 on HUVEC .....	138
<b>7.4 DISCUSSION .....</b>	<b>141</b>

<b>CHAPTER 8: GENERAL DISCUSSION .....</b>	<b>145</b>
<b>REFERENCES .....</b>	<b>155</b>

## LIST OF ABBREVIATIONS

μl	microlitre
μM	micromolar
4-HNE	4-hydroxy-2-noneal
AIF	apoptosis inducing factor
Apaf-1	apoptosis activating factor-1
ATP	adenosine triphosphate
ATS	acidic terminal segment
BBB	blood-brain barrier
CIDR	cysteine-rich interdomain regions
CLSM	confocal laser scanning microscope
CM	cerebral malaria
CORMs	carbon monoxide releasing molecules
CR1	complement receptor 1
CSA	chondroitin sulphate A
CSF	cerebrospinal fluid
CSP	circumsporozoite protein
DBL	Duffy binding like domains
DFO	desferrioxamine
DISC	death-inducing signalling complex
DNA	deoxyribonucleic acid
eCAMs	endothelial cell adhesion molecules
ER	endoplasmic reticulum
ERAD	ER-associated protein degradation
FACS	fluorescence activated cell sorter
FADD	Fas-associated death domain protein
FasL	Fas ligand



FasR	Fas receptor
GA	gentamicin, amphotericin-B
GPI	glycosylphosphatidylinositols
h	hour
Hdm2	human double minute-2
hEGF	human recombinant epidermal growth factor
hFGF-B	human Fibroblast growth factor basic
HO	heme oxygenase
HSPGs	heparan sulphate proteoglycans
HUVEC	human umbilical endothelial cell
IAP	inhibitors of apoptosis protein
ICAM-1	intercellular adhesion molecule 1
IFN- $\gamma$	interferon gamma
IKK	I $\kappa$ B kinase
IL-1 $\beta$	interleukin-1 beta
Ins(1,4,5)P <sub>3</sub>	inositol - 1, 4, 5 - triphosphate
JNK	c-Jun N-terminal kinase
LFA-1	lymphocyte function-associated antigen 1
mAb	monoclonal antibody
MAPK	mitogen-activated protein kinase
Mdm2	mouse double minute-2
min	minute
ml	millilitre
mm	millimetre
mM	millimolar
MOMP	mitochondrial outer membrane permeabilization
MyD88	myeloid differentiation factor 88
NCAM	neural cell adhesion molecule

NF- $\kappa$ B	nuclear factor kappa B
NIK	NF- $\kappa$ B-inducing kinase
NTS	N terminal segment
$^{\circ}\text{C}$	degree Celsius
PCR	polymerase chain reaction
PECAM-1	platelet/EC adhesion molecule 1
PfEMP-1	<i>Plasmodium falciparum</i> erythrocyte membrane protein 1
PI	propidium iodide
PMCA	plasma membrane $\text{Ca}^{2+}$ ATPase
PRBC	parasitized red blood cells
PSGL-1	P-selectin glycoprotein ligand-1
PTP	permeability transition pore
PUFAs	polyunsaturated fatty acids
R <sup>3</sup> -IGF-1	human Recombinant Insulin-like Growth Factor
RBC	red blood cells
RNA	ribonucleic acid
ROS	reactive oxygen species
SAPKs	stress-activated protein kinases
SE	standard error
SERCA	sarco-endoplasmic reticulum $\text{Ca}^{2+}$ ATPase
sFas	soluble Fas
SOD1	superoxide dismutase
SR	sarcoplasmic reticulum
TLR	Toll-like receptor
TM	trans-membrane domain
TNFR	tumor necrosis factor receptor
TNF- $\alpha$	tumor necrosis factor alpha
TRADD	TNF receptor-associated death domain

TSP	thrombospondin
UPR	unfolded protein response
UV	ultra violet
VCAM-1	vascular cell adhesion molecule 1
VEGF	vascular Endothelial Growth Factor
$\Delta\Psi_m$	mitochondria transmembrane electrical potential

## LIST OF FIGURES

<b>Figure 1.1</b> Life cycle of <i>P. falciparum</i> .....	3
<b>Figure 1.2</b> <i>P. falciparum</i> erythrocyte membrane protein 1 (PfEMP-1); protein architecture and binding domains.....	8
<b>Figure 1.3</b> Diagram showing two major apoptotic pathways: extrinsic and intrinsic pathways .....	19
<b>Figure 1.4</b> The three-tiered regulatory cascade (MAPK, MAPKK and MAPKKK levels) and cellular responses elicited by JNK and p38 MAPK.....	22
<b>Figure 1.5</b> p53 activation and modulation of downstream events .....	23
<b>Figure 1.6</b> NF- $\kappa$ B signalling pathways.....	25
<b>Figure 1.7</b> Calcium signalling .....	26
<b>Figure 1.8</b> TLR-mediated immune response .....	29
<b>Figure 3.1</b> Comparison amount of binding of PRBC and RBC to HUVEC at different time points .....	51
<b>Figure 3.2</b> Confocal images of HUVEC incubated with RBC and PRBC after 3 h....	51
<b>Figure 3.3</b> Comparison of apoptosis (%) of HUVEC when attached or unattached during co-incubation with PRBC .....	53
<b>Figure 3.4</b> Confocal images of various morphological changes of HUVEC after incubation with PRBC or camptothecin.....	54
<b>Figure 3.5</b> Comparison of HUVEC binding between ITG and C24 parasite lines .....	55
<b>Figure 3.6</b> Apoptosis of HUVEC induced by two parasites isolates (C24 and ITG)..	56
<b>Figure 3.7</b> Cell viability of control, heat-killed and artesunate-killed malaria parasites .....	58
<b>Figure 3.8</b> Cytoadherence of control parasites (viable parasites), heat-killed parasites and artesunate-killed parasites to HUVEC.....	59
<b>Figure 3.9</b> Apoptosis of HUVEC attached and unattached to control parasites, heat-killed parasites and artesunate-killed parasites.....	59
<b>Figure 3.10</b> Comparison amount of binding between PRBC and HUVEC in control group and caspase inhibitors treated groups.....	61
<b>Figure 3.11</b> Effect of caspase inhibitors on PRBC-induced HUVEC apoptosis.....	62
<b>Figure 3.12</b> Cytoadherence of PRBC to HUVEC in control group and in the presence of caspase inhibitors .....	63

<b>Figure 3.13</b> Caspase-8 activity in HUVEC .....	64
<b>Figure 3.14</b> Caspase-9 activity in HUVEC .....	65
<b>Figure 4.1</b> Comparison amount of binding of PRBC to HUVEC at different co-incubation time points .....	75
<b>Figure 4.2</b> Confocal images of HUVEC stained with JC-1 dye.....	77
<b>Figure 4.3</b> Comparison the percentage green fluorescence cell of HUVEC with and without attached PRBC at different co-incubation time points.....	78
<b>Figure 5.1</b> Confocal images of HUVEC stained with anti-4-hydroxynoneal antibody. ....	89
<b>Figure 5.2</b> Confocal images of PRBC-adhered HUVEC stained with anti-4-hydroxynoneal antibody .....	90
<b>Figure 5.3</b> Confocal images of PRBC-adhered HUVEC stained with anti-4-hydroxynoneal antibody in the presence and absence of DFO .....	91
<b>Figure 6.1</b> Comparison amount of binding between PRBC and HUVEC in control group and inhibitors treated groups.....	104
<b>Figure 6.2</b> Apoptosis of HUVEC attached to PRBC in control groups and apoptotic inhibitors treated groups.....	107
<b>Figure 6.3</b> Confocal images of HUVEC attached to PRBC in control group and in presence of inhibitors .....	108
<b>Figure 7.1</b> Comparison amount of binding of PRBC to HUVEC in the control parasites, the first and the second enriched parasites .....	126
<b>Figure 7.2</b> Apoptosis of HUVEC induced by cytoadherence of control (non-enriched), the first enriched and the second enriched parasites .....	127
<b>Figure 7.3</b> Comparison of apoptosis (%) of HUVEC attached and unattached to PRBC in control, the first enriched parasite and the second enriched parasite group.....	128
<b>Figure 7.4</b> HUVEC morphology of unstimulated HUVEC and TNF- $\alpha$ stimulated HUVEC under inverted and confocal microscope .....	129
<b>Figure 7.5</b> The degree of apoptosis in unstimulated and TNF- $\alpha$ stimulated HUVEC groups .....	130
<b>Figure 7.6</b> ICAM-1 expression on HUVEC measured by FACS.....	131

<b>Figure 7.7</b> Cytoadherence of the enriched parasite and the ICAM-1 selected parasites to unstimulated HUVEC and TNF- $\alpha$ stimulated HUVEC in the presence or absence of anti-ICAM-1 mAb .....	134
<b>Figure 7.8</b> Apoptosis of unstimulated HUVEC and TNF- $\alpha$ stimulated HUVEC attached to the enriched parasites or the ICAM-1 selected parasites in the presence or absence of anti-ICAM-1 mAb .....	136
<b>Figure 7.9</b> The morphology of HUVEC in TNF- $\alpha$ stimulated group attached to enriched parasites or ICAM-1 selected parasites .....	137
<b>Figure 7.10</b> Cytoadherence of enriched parasites induced apoptosis of HUVEC in presence or absence of cell receptors specific antibodies .....	140
<b>Figure 8.1</b> The proposed mechanism of PRBC-induced endothelial apoptosis. ....	151

## LIST OF TABLES

<b>Table 3.1</b> Comparison of cell viability and localisation of parasite in control, heat-killed and artesunate-killed malaria parasites.....	57
<b>Table 3.2</b> Caspase-8 and Caspase-9 activities .....	65
<b>Table 6.1</b> Summary apoptotic pathway inhibitors used in the experiments and their targets .....	101
<b>Table 6.2</b> Comparison the percentage attachment of PRBC to HUVEC in control and inhibitor treated groups.....	103
<b>Table 6.3</b> Comparison the percentage apoptosis of HUVEC attached to PRBC in control and inhibitor treated groups .....	106
<b>Table 7.1</b> The percentage of adhesion of the enriched parasites and the ICAM-1 selected parasites to unstimulated HUVEC and TNF- $\alpha$ stimulated HUVEC in the presence or absence of anti-ICAM-1 mAb.....	133
<b>Table 7.2</b> The percentage apoptosis of unstimulated HUVEC and TNF- $\alpha$ stimulated HUVEC attached to the enriched parasites and the ICAM-1 selected parasites in the presence or absence of anti-ICAM-1 mAb.....	135
<b>Table 7.3</b> The percentage of binding between the enriched parasites and HUVEC in the presence or absence of anti-CD31 mAb, anti-CD36 mAb, and anti-CD105 pAb. ....	139
<b>Table 7.4</b> The percentage of apoptosis of the HUVEC attached to the enriched parasites in the presence or absence of CD31 mAb, CD36 mAb, and CD105 pAb. .	139

## CHAPTER 1: INTRODUCTION

---

### 1.1 MALARIA

Malaria is caused by protozoan parasites of the genus *Plasmodium*. There are five species of *Plasmodium* that infect human and cause disease which are: *Plasmodium falciparum*, *Plasmodium vivax*, *Plasmodium malariae*, *Plasmodium ovale* (de Souza & Riley, 2002) and *Plasmodium knowlesi* (Cox-Singh et al., 2008, Singh et al., 2004). Using PCR genotyping techniques, human infection with *P. knowlesi*, which is commonly misdiagnosed by microscopy as *P. malariae*, has been identified (Cox-Singh et al., 2008, Singh et al., 2004). Recently, *P. knowlesi* has been reported to cause severe disease in a human host (Cox-Singh et al., 2010). Based on the dimorphism in defined genes, *P. ovale* has been divided into classic and variant types (Win et al., 2004). There is recent evidence indicating that these two parasite types might be in fact two distinct species which were named *P. ovale curtisi* (classic type) and *P. ovale wallikeri* (variant type) (Sutherland et al., 2010). However, among the human malaria parasites, *P. falciparum* is the only species which sequesters in microvasculature and causes the most severe form of the disease, cerebral malaria (de Souza & Riley, 2002).

#### 1.1.1 *Plasmodium falciparum* life cycle

The vector of *P. falciparum* transmission is the female *Anopheles* mosquito. To facilitate the ingestion of blood, the mosquito injects saliva which contains vasodilators and anti-coagulants on biting a mammalian host. If the mosquito is infected with *P. falciparum*, sporozoites which reside in its salivary glands are injected into the host skin. From there, they travel through the blood stream to the liver.



Sporozoites interact with heparan sulphate proteoglycans (HSPGs) on the liver cells via their surface protein, circumsporozoite protein (CSP) prior to invasion. Once inside the liver, the sporozoite passes through several hepatocytes before establishing in one, where it forms a parasitophorous vacuole. Within this, the sporozoite develops and multiplies forming thousands of merozoites. These are released into the blood stream where they invade red blood cells (RBC) (Prudencio *et al.*, 2006). The merozoites attach to the RBC surface and must undergo apical reorientation in order to make its apical pole attach to RBC surface. After that, a junction between the invading merozoite and the RBC membrane is formed. The movement of the junction around the penetrating merozoite allows the merozoite to enter into the RBC forming a parasitophorous vacuole (Gaur *et al.*, 2004). Inside the host RBC, the merozoite develops through ring, trophozoite, and schizont stage parasites. In *P. falciparum*, the mature trophozoite stages express parasite-derived adhesion surface molecules on the surface of their RBC which can bind to host endothelial cell adhesion receptors resulting in sequestration of parasitized red blood cells (PRBC) in microvasculature. After completion of the blood stage cycle, merozoites are released, which rapidly infect other RBC. Some parasites differentiate into sexual erythrocytic stages (gametocytes). The gametocytes: male (microgametocytes) and female (macrogametocytes), are ingested by a female *Anopheles* mosquito during a blood meal. In the mosquito's stomach, the male and female gametocytes fuse and develop into motile ookinete which invade a single epithelial cell in the mosquito's midgut. The ookinete then differentiates into an oocyst producing thousands of sporozoites. Sporozoites move to mosquito's salivary glands ready to infect another host in the next blood meal (Cirimotich *et al.*, 2010, Scherf *et al.*, 2008).

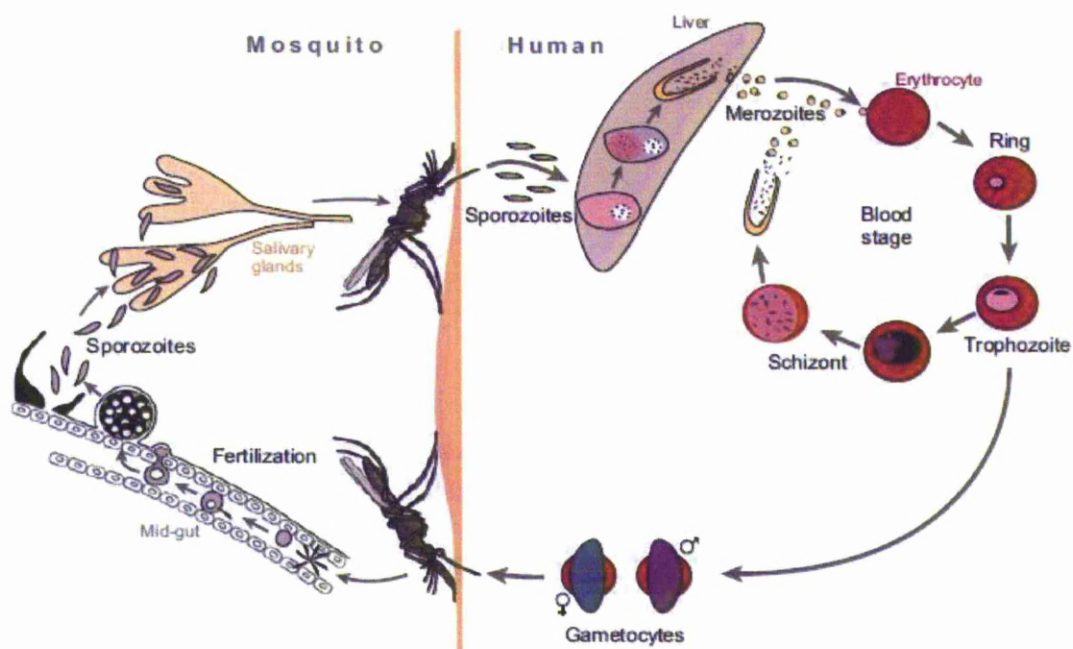


**Figure 1.1** Life cycle of *P. falciparum* (Scherf et al., 2008).

### 1.1.2 *P. falciparum* cytoadherence

During the trophozoite and schizont stages, parasites disappear from the peripheral circulation and sequester in the microvascular beds in vital organs such as the brain where it can cause the severe disease, cerebral malaria (Newton *et al.*, 2000). Sequestration of PRBC is a result of cytoadherence of PRBC to the endothelial cells lining blood vessels. Endothelial cells express many different receptors on their surface. Some of them are increasingly expressed in response to activation by inflammatory cytokines including TNF- $\alpha$  which is known to be up-regulated in malaria (Chakravorty *et al.*, 2008). Many endothelial cell receptors have been reported to serve as ligands for PRBC adhesion. In most cases, adhesion between PRBC and host receptors has been shown to be mediated by *P. falciparum* erythrocyte membrane protein 1 (PfEMP-1), which is the protein displayed on the surface of the PRBC

(Rowe *et al.*, 2009). The detail regarding some of the endothelial cell receptors involved in cytoadherence and PfEMP-1 as well as the effects of cytoadherence on endothelial cells is briefly described in sections 1.1.2.1, 1.1.2.2 and 1.1.2.3, respectively.

#### **1.1.2.1 Host adhesion receptors**

The molecules on endothelial cells that have been reported to participate in adhesion of PRBC include: thrombospondin; CD36; ICAM-1 (intercellular adhesion molecule 1), VCAM-1 (vascular cell adhesion molecule 1); PECAM-1 (platelet/EC adhesion molecule)/CD31 and NCAM (neural cell adhesion molecule); P-selectin and E-selectin; and chondroitin sulphate A (CSA) (Rowe *et al.*, 2009). A brief detail of each molecule is described below.

##### ***Thrombospondin (TSP)***

Thrombospondin (TSP) is a large adhesive glycoprotein which is released into plasma in response to platelet activation by thrombin (Rowe *et al.*, 2009). TSP has been implicated in binding under both static assay (Roberts *et al.*, 1985) and flow conditions (Rock *et al.*, 1988). The possible candidates of parasite ligands for TSP are PfEMP-1 (Baruch *et al.*, 1996), red-cell-derived phosphatidylserine (Eda & Sherman, 2002) and altered Band 3 protein (Eda *et al.*, 1999).

##### ***CD36***

CD36 is an 88 kDa highly glycosylated, cell surface class B scavenger receptor expressed on endothelial and epithelial cells, macrophages, monocytes, platelets, erythrocyte precursors and adipocytes (Greenwalt *et al.*, 1992). It has been revealed

that most patient isolates tested have some ability to bind to CD36 (Chakravorty *et al.*, 2008). However, the role of CD36 in malaria pathogenesis remains unclear (Serghides *et al.*, 2003). Studies conducted in Africa showed no difference in CD36-binding ability between parasite isolates from severe and uncomplicated malaria patients (Newbold *et al.*, 1997, Rogerson *et al.*, 1999). In contrast, other studies showed a positive correlation between CD36 binding and severe malaria (Ho *et al.*, 1991, Ockenhouse *et al.*, 1991). A recent study demonstrated that platelet-expressed CD36 can act as a bridge mediating binding of PRBC to endothelial cells lacking in CD36 (Wassmer *et al.*, 2004).

### ***ICAM-1***

ICAM-1 (CD54) is a member of the immunoglobulin superfamily, expressed on endothelial cells and leukocytes (Rowe *et al.*, 2009). Adhesion to ICAM-1 has been suggested to be linked with cerebral malaria. Post-mortem studies showed increased parasite sequestration in the brain of patients with severe malaria who also showed increased ICAM-1 expression (Turner *et al.*, 1994). Isolates from CM patients have also shown the ability to adhere *in vitro* to ICAM-1 (Newbold *et al.*, 1997). The binding site for PRBC on ICAM-1 is the N-terminal external Ig domain of the protein which is distinct from the binding sites for its natural ligand LFA-1 (lymphocyte function-associated antigen 1) (Berendt *et al.*, 1992, Ockenhouse *et al.*, 1992a). ICAM-1 levels on many types of endothelial cells can be stimulated by cytokines, including TNF- $\alpha$  and IL-1 (interleukin 1) which are up-regulated during malaria infection (Chakravorty *et al.*, 2008). Furthermore, ICAM-1 levels can also be stimulated directly by the PRBC (Tripathi *et al.*, 2006, Viebig *et al.*, 2005).

### ***VCAM-1***

VCAM-1 (CD106) is also a member of the immunoglobulin superfamily and is expressed on endothelial cells in response to inflammatory mediators. PRBC isolated from patients with severe complicated malaria have been shown to bind to VCAM-1 (Ockenhouse *et al.*, 1992b). However, a study with African isolates showed low levels of VCAM-1 binding and did not appear to be associated with severity of the disease (Newbold *et al.*, 1997).

### ***PECAM-1***

Platelet endothelial cell adhesion molecule 1 (PECAM-1 or CD31) is another glycosylated member of the Ig superfamily. It is expressed on endothelial cells, monocytes, platelets and granulocytes. The protein is normally concentrated at the endothelial junction in the microvasculature, but stimulation with IFN- $\gamma$  can redistribute the receptor to the surface of endothelium, leading to an increase in binding. PRBC have been shown to bind to PECAM-1 transfected cells and directly to recombinant PECAM-1 absorbed onto plastic (Treutiger *et al.*, 1997).

### ***P-selectin***

P-selectin (CD62P), a glycoprotein, is expressed on activated platelets and endothelial cells and is important for leukocyte trafficking. This protein has been shown to mediate rolling of PRBC on endothelial cells and facilitates adhesion to CD36 (Udomsangpetch *et al.*, 1997, Yipp *et al.*, 2007). The site of binding for PRBC on P-selectin has not been mapped, however, it is thought to be on the lectin domain but distinct from that of the natural ligand, PSGL-1 (Ho *et al.*, 1998). Another member

of the selectin family that has been suggested to implicate in PRBC cytoadherence is E-selectin (Ockenhouse et al., 1992b).

### **CSA**

Chondroitin sulphate A (CSA) is the carbohydrate found on placental syncytiotrophoblasts. Adhesion of PRBC to CSA has been linked to a specific disease, placental malaria which leads to maternal anaemia, low birth weight and increase in neonatal mortality (Chakravorty et al., 2008).

### ***Other cytoadherence receptors***

Other endothelial receptors which have been proposed to be involved in cytoadherence of PRBC include integrin  $\alpha v \beta 3$  (Siano *et al.*, 1998), fibronectin (Eda & Sherman, 2004), NCAM (Pouvelle *et al.*, 2007) and gC1qR-HABP1-p32 (Biswas *et al.*, 2007). However, neither the PRBC ligand for these receptors or the role of these receptors in severe malaria has been established yet (Rowe et al., 2009).

#### **1.1.2.2 *P. falciparum* erythrocyte membrane protein 1 (PfEMP-1)**

PfEMP-1 is a parasite derived polypeptide of high molecular mass (200 to 350 kDa) which is implicated in cytoadherence to many host endothelial cells adhesion receptors. This protein is encoded by *var* genes of which only one out of a family of 60 *var* genes in a parasite is expressed at a any specific time (Kirchgatter & Del Portillo, 2005). To evade host adaptive immunity, *P. falciparum* undergoes antigenic variation. This results in switching expression to an alternative *var* gene, leading to an expression of an antigenically distinct PfEMP-1 protein (Chakravorty *et al.*, 2008, Smith *et al.*, 2001). The variation in different PfEMP-1 proteins determines the ability

of parasites to adhere to distinct host receptors, mediating sequestration in various tissues (Montgomery *et al.*, 2007).

PfEMP-1 is composed of an N terminal segment (NTS), variable numbers of Duffy binding like domains (DBL;  $\alpha$ - $\epsilon$ ), one or two cysteine-rich interdomain regions (CIDR;  $\alpha$ - $\gamma$ ), a trans-membrane (TM) domain, a C2 domain and a conserved intra-cellular acidic terminal segment (ATS) (Pasternak & Dzikowski, 2009) (Fig 1.2). At the N terminal end of the protein is a semi-conserved head structure consisting of a DBL $\alpha$  domain couple to CIDR domain. This head structure has been suggested to recognize at least eight different receptors including CD36, CD31 and complement receptor 1 (CR1) (Smith *et al.*, 2001) (Fig 1.2). The DBL $\beta$  type domain, which is normally found in tandem with a C2 domain, is known to bind to ICAM-1 (Springer *et al.*, 2004).

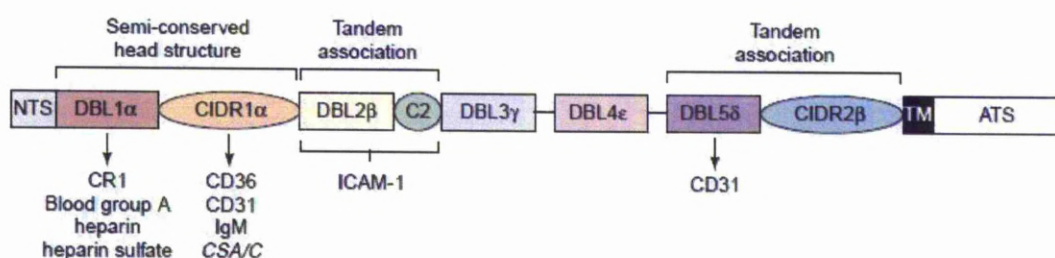


**Figure 1.2** *P. falciparum* erythrocyte membrane protein 1 (PfEMP-1); protein architecture and binding domains (modified from Smith *et al.*, 2001).

### 1.1.2.3 Effects of cytoadherence on endothelial cells

Cytoadherence of PRBC to endothelial cells is not a passive process but can cause activation of intracellular signalling pathways in endothelial cells. The interaction between PRBC and endothelial cells can lead to activation of MAP kinase signalling

pathways, including ERK1/2, JNK (c-Jun N-terminal kinase) and p38 pathways (Jenkins *et al.*, 2007) as well as a Rho kinase signalling pathway (Taoufiq *et al.*, 2008). Following the interaction of endothelial cells with the PRBC, nuclear translocation of the transcription factor NF- $\kappa$ B in endothelial cells, as part of the signalling cascade responsible in up-regulation of ICAM-1, has been described. This may explain the localization of ICAM-1 on brain endothelium in post-mortem CM brain samples and may also lead to greater adhesion of PRBC to endothelial cells (Tripathi *et al.*, 2006). Another suggested consequence of PRBC cytoadherence to endothelium is the induction of apoptosis in endothelial cells, which may be responsible for the blood-brain barrier breakdown seen in CM (Pino *et al.*, 2005). This event is described in detail in section 1.1.3.

### **1.1.3 Cerebral malaria**

Cerebral malaria (CM) is one of the most common lethal complications of the complex syndrome named severe malaria. The incidence of this neurological syndrome is hard to assess, but the records of hospital admissions indicate that CM occurs in about 1% of all *P. falciparum* infections. However, this is responsible for more than two million deaths annually among children under 5 years old in Sub-Saharan Africa (Combes *et al.*, 2006). The symptoms of CM can range from confusion or stupor to obtundation and deep coma (Medana & Turner, 2006). Post-mortem brain histopathology reveals that CM is characterised by a blockade of brain microvessels due to an accumulation of PRBC, leucocytes and platelets. Other common findings in post-mortem CM patients brain examinations include brain swelling as well as petechial and ring haemorrhages in both cerebral and cerebellar cortices (Haldar *et al.*, 2007).



There are broadly three hypotheses that have been raised to explain the pathogenesis of CM, i.e. sequestration of PRBC (Berendt *et al.*, 1994), inflammation (Clark & Rockett, 1994) and hemostasis dysfunction (van der Heyde *et al.*, 2006). However, neither one of these hypotheses by itself can explain all of the observed physiological and clinical manifestations of the disease. It has been proposed that the pathogenesis of CM can be better explained by an integration of all three hypotheses. In this unifying hypothesis, parasite antigens (including surface molecules on PRBC, merozoites and malaria toxins released during replication) activate the inflammatory response and platelets leading to increased levels of endothelial cell adhesion molecules (eCAMs). This, in turn, leads to a further increase in the level of PRBC sequestration in the brain microvasculature. By unknown mechanisms, the acute sequestration of PRBC in the brain microvasculature is thought to cause disruption of the blood-brain barrier (BBB) (van der Heyde *et al.*, 2006), which is the specialized interface between the vascular space and the brain parenchyma playing a role in regulating solute and cellular transport into the brain (Hawkins & Davis, 2005).

There are studies supporting the notion that the BBB integrity is compromised in CM. A loss of endothelial cell junctional protein ZO-1, occludin and vinculin, in vessels containing sequestered PRBC, was shown by immunohistochemistry on post-mortem brain tissues from Vietnamese adults (Brown *et al.*, 1999) and Malawian children (Brown *et al.*, 2001) with CM. The leakage of the plasma protein fibrinogen into the perivascular space was detected in Vietnamese adults (Brown *et al.*, 1999). Perivascular macrophages in both adults and children expressed scavenger receptor and sialoadhesin, which are normally not expressed in the normal central nervous system. Sialoadhesin is only induced on these cells in the presence of plasma proteins.

Taken together, these results provide clear evidence of BBB breakdown, especially in vessels containing PRBC sequestration (Brown *et al.*, 1999, Brown *et al.*, 2001). Furthermore, retinal haemorrhages have been found in patients with cerebral malaria and are a major component of malarial retinopathy (Beare *et al.*, 2006, Glover *et al.*, 2010, White *et al.*, 2009b). The retina is embryologically derived from the same neuroectoderm as the brain and has an analogous cellular structure and blood-tissue barrier, these finding perhaps support the notion of the BBB breakdown (Maude *et al.*, 2009). The evidences of structural and functional breakdown of the BBB have also been shown in animal models. By measuring the movement of the dye Evans blue and radio-isotope labelled albumin, plasma protein leakage into the brain was detected in experimental cerebral malaria (Chang-Ling *et al.*, 1992, Thumwood *et al.*, 1988). Electron microscopy also showed endothelial damage in brain tissue of animals with CM (Thumwood *et al.*, 1988). The effect of malaria parasites on the functional changes in permeability of BBB was assessed *in vitro* by measuring the electrical resistance of barrier-forming cell-cell contacts. Co-culture of brain endothelial cells together with PRBC or malaria antigen-activated leukocytes resulted in reduction of endothelial barrier function (Treeratanapiboon *et al.*, 2005, Tripathi *et al.*, 2007). The BBB structural changes caused by malaria parasites were also assessed by immunostaining of the tight junction proteins ZO-1, which showed disruption of tight junctional complexes in endothelial cells co-cultured with malaria antigen-activated leukocytes (Treeratanapiboon *et al.*, 2005).

Recently, malaria parasite-induced apoptosis of endothelial cells has been proposed to be one of the factors leading to the breakdown of the BBB (Medana & Turner, 2007, Pino *et al.*, 2005). In support of this, Pino and colleagues have shown that the physical

contact between PRBC and endothelial cells results in induction of caspase 8- and caspase 9- dependent apoptosis of endothelial cells (Pino *et al.*, 2003b). Apoptosis of endothelial cells induced by PRBC has also been showed to be mediated through an oxidative stress pathway (Pino *et al.*, 2003a, Taoufiq *et al.*, 2006). The Rho kinase pathway also plays a role in apoptosis of endothelial cells induced by PRBC, as Fasudil, the Rho kinase inhibitor, prevented endothelial cell apoptosis induced by either laboratory or field isolates (Taoufiq *et al.*, 2008, Zang-Edou *et al.*, 2010). A study which investigated the capacity of field isolates of malaria parasites, derived from patients with clinical malaria, to induce apoptosis in endothelial cells, found that patients with neurological manifestation were more likely to harbour apoptogenic parasites (Toure *et al.*, 2008).

Apoptosis is one of the processes which lead to the formation of apoptotic bodies or microparticles (MP) (Coltel *et al.*, 2006). It has been found that MP is associated with severe malaria. Levels of endothelial microparticles (EMP) have been shown to be dramatically higher in the plasma of patients suffering from the acute phase of CM than in plasma of patients with severe malarial anaemia, uncomplicated malaria or healthy control plasma (Combes *et al.*, 2004).

In contrast to the finding of Pino and colleagues (Pino *et al.*, 2003b), there are some evidences that the physical interaction between PRBC and endothelial cell might not be essential for induction of endothelial cells apoptosis. Soluble factors from PRBC have been found to induce apoptosis in both human brain vascular endothelial and neuroglia cells (Wilson *et al.*, 2008). Co-culture of endothelial cells with patient sera from severe *P. falciparum* malaria or *P. falciparum* culture supernatant in the presence

or absence of neutrophils led to higher endothelial apoptosis rates compared with control sera or control supernatants (Hemmer *et al.*, 2005, Hemmer *et al.*, 2008).

In addition to PRBC itself, the deleterious effect of platelets, which are often co-localized with sequestered PRBC in the CM brain (Grau *et al.*, 2003), on the BBB integrity has been suggested. Platelets have been shown to enhance PRBC binding to endothelial cells by acting like bridges (Wassmer *et al.*, 2004), potentiating PRBC-induced alterations of the endothelial monolayer integrity and enhancing endothelial apoptosis (Wassmer *et al.*, 2006a, Wassmer *et al.*, 2006b). The apoptosis of the BBB endothelial cells in the brain areas where both PRBC and platelets are bound, may be responsible for some of the brain haemorrhages observed during post-mortem CM brain analysis (Combes *et al.*, 2006).

The clinical studies and murine CM models also provided the link between CM and apoptosis. Immunohistochemistry studies of brain tissue derived from patients with CM showed that 40% of these cases had caspase-3 activation (Medana *et al.*, 2001). The significant elevation of Fas ligand (FasL) and soluble Fas (sFas) was found in post-mortem cerebrospinal fluid (CSF) samples and plasma samples, respectively, taken from CM mortality cases (Armah *et al.*, 2007, Jain *et al.*, 2008). Microarray analysis of global gene expression patterns in the brain of mice with CM demonstrated that apoptosis appeared to implicate in pathogenesis of experimental CM (Lovegrove *et al.*, 2007, Miu *et al.*, 2008). In addition, immunohistochemistry analysis of caspase-3 activation revealed the brain endothelial cells apoptosis in experimental murine models of CM (Lackner *et al.*, 2007, Potter *et al.*, 2006a). Despite these data, there are important differences between murine CM models and human CM. For example, there is little or no PRBC sequestration in brain microvasculature of murine model whereas

the hallmark of human CM is sequestration of PRBC in brain microvasculature. These findings perhaps provide a clue regarding pathogenesis of human CM (John, 2007, White *et al.*, 2009a). Although the apoptotic effects of PRBC on endothelial cells has been demonstrated, the fine mechanism(s) and signalling pathway(s) underpinning this event remain elusive and need to be defined.

## 1.2 APOPTOSIS

Apoptosis or programmed cell death is the process that normally occurs during development, aging, and as a homeostatic mechanism to maintain cell populations in tissues. Apoptosis also participates in defence mechanisms such as in immune reactions as well as the pathogenesis of diseases, for example neurodegenerative diseases, cardiovascular diseases, immunological diseases and cancer (Zimmermann & Green, 2001).

During apoptosis, cells undergo many morphological changes including cellular shrinkage, membrane blebbing, nuclear chromatin condensation and fragmentation. Finally, when extensive plasma membrane blebbing occurs, cells break into membrane-surrounded fragments which are called apoptotic bodies. Apoptotic bodies, which are subsequently phagocytosed by macrophages, parenchymal cells or neoplastic cells and degraded within phagosomes, contain cytoplasm with tightly packed organelles with or without a nuclear fragments (Elmore, 2007, Vermeulen *et al.*, 2005). Several biochemical modifications, for example, protein cleavage, protein cross-linking and DNA breakdown are also exhibited in apoptotic cells (Elmore, 2007). DNA breakdown to 180-200 bp lengths of DNA fragments by endonucleases generates a characteristic so-called DNA ladder which can be detected by agarose gel electrophoresis with an ethidium bromide stain and ultraviolet illumination (Bortner *et al.*, 1995). To allow quick phagocytosis with minimal compromise to the surrounding tissue, apoptotic cells undergo another biochemical change, the expression of cell surface markers resulting in the phagocytic recognition by adjacent cells. This can be achieved by exposure of phosphatidylserine, which is normally presented on the

cytoplasmic side of the plasma membrane, on the outer leaflet of the plasma membrane (Bratton *et al.*, 1997).

### **1.2.1 Pathways involved in apoptosis**

The central initiators and executioners of apoptosis are caspases. Caspases are normally present in healthy cells as inactive proenzymes with little or no protease activity. To date, approximately 14 mammalian caspases have been identified and these can be broadly categorised into three groups. The first group is inflammatory caspases; including caspase-1, -4, -5, -11, -12, -13 and -14 which are associated with inflammation instead of apoptosis. The second group, linking upstream signalling pathways with downstream execution steps, is apoptotic initiator caspases; which include caspase-2, -8, -9 and -10. The last group is the apoptotic effector or executioner caspases; which are activated by upstream caspases and perform the downstream execution steps of apoptosis by cleaving multiple cellular substrates, consisting of caspase-3, -6 and -7 (Jin & El-Deiry, 2005, Rai *et al.*, 2005).

To date, apoptosis has been suggested to occur through two main apoptotic pathways, i.e. the extrinsic or death receptor pathway and the intrinsic or mitochondrial pathway. However, the apoptotic process is also affected by many other signalling pathways including endoplasmic reticulum stress-induced apoptosis, MAPK/JNK pathway and NF- $\kappa$ B pathway (Jin & El-Deiry, 2005).

#### **1.2.1.1 The extrinsic apoptotic pathway**

Activation of the extrinsic pathway of apoptosis is initiated by binding of a specific protein ligand to cell surface transmembrane receptors. The transmembrane receptors, also called death receptors, trigger external apoptotic signalling and are members of

the tumor necrosis factor (TNF) receptor gene superfamily. The best characterised ligands and corresponding death receptors include FasL/FasR, TNF- $\alpha$ /TNFR1, Apo3L/DR3, Apo2L/DR4 and Apo2L/DR5. However, among these ligand/receptor interactions, the best characterised of the sequence in the extrinsic phase of apoptosis are FasL/FasR and TNF- $\alpha$ /TNFR1 (Elmore, 2007). Upon binding of ligand to death receptors, cytoplasmic adapter proteins, which display corresponding death domains that bind with the receptors, are recruited. The binding of Fas ligand to Fas receptor recruits the adapter protein FADD to the receptor, and the binding of TNF ligand to TNF receptor allows the binding of the adapter protein TRADD which subsequently recruits FADD and RIP. FADD then binds to procaspase-8 resulting in the formation of a death-inducing signalling complex (DISC), which leads to autoproteolytic processing of caspase-8. The activated caspase-8 can activate a series of downstream caspases, which result in cleavage of structural and regulatory intracellular proteins, finally leading to apoptosis (Schultz & Harrington, 2003).

In this pathway, cells can be divided into two types depending on their requirement in the mitochondrial pathway. In type I cells, activated caspase-8 is sufficient to directly activate other members of the caspases family and lead to apoptosis. In type II cells, caspase-8 mediates cleavage of Bid which induces the translocation and insertion of Bax and/or Bak into the mitochondrial outer membrane. This causes the release of several proteins from the mitochondrial intermembrane space, for example, cytochrome *c*, which forms a complex called the apoptosome with apoptosis-activating factor-1 (Apaf-1) and procaspase-9. This leads to the activation of caspase-9, which can activate the executioner caspase-3 (Jin & El-Deiry, 2005, Orrenius *et al.*, 2003) (Fig1.3).



### **1.2.1.2 The intrinsic apoptotic pathway**

This cell death pathway is controlled by the Bcl-2 family of proteins. All protein members in this family share at least one of four conserved Bcl-2 homology (BH) domains (BH1, BH2, BH3 and BH4). This family can be divided into two groups according to their function. The first group consists of antiapoptotic members including Bcl-2, Bcl-XL, Bcl-w, A1 and Mcl-1. The second group is made up of proapoptotic members, consisting of two subgroups: one subgroup sharing 3 BH domains (BH1, BH2 and BH3) with Bcl-2 including Bax, Bak and Bok; and a subgroup sharing only the BH3 domain with Bcl-2 including Bik, Hrk, Bim, Blk, Bad and Bid. Antiapoptotic members act as repressors of apoptosis by blocking release of cytochrome *c*, while proapoptotic members act as promoters (Cory & Adams, 2002).

In response to apoptotic stimuli, there is formation of the mitochondrial permeability transition pore (PTP) which is a multiprotein complex, consisting of both inner and outer membrane proteins. This pore formation leads to loss of the mitochondrial transmembrane potential and release of apoptotic inducing factors from the intermembrane space into the cytosol. The apoptotic-inducing factors released from the mitochondria include cytochrome *c*, Smac/DIABLO and HrtA2/Omi. Cytochrome *c* forms the apoptosome complex with Apaf-1 and procaspase-9, leading to activation of caspase-9 (Vermeulen et al., 2005). Smac/DIABLO and HrtA2/Omi interact with IAP (inhibitors of apoptosis protein) resulting in apoptosis (Schimmer, 2004, van Loo *et al.*, 2002). In addition, other apoptotic inducing factors such as AIF and endonuclease G are also released from the mitochondria. After release from the mitochondria, AIF and endonuclease G translocate to the nucleus and cause DNA fragmentation (Joza *et al.*, 2001, Li *et al.*, 2001) (Fig1.3).

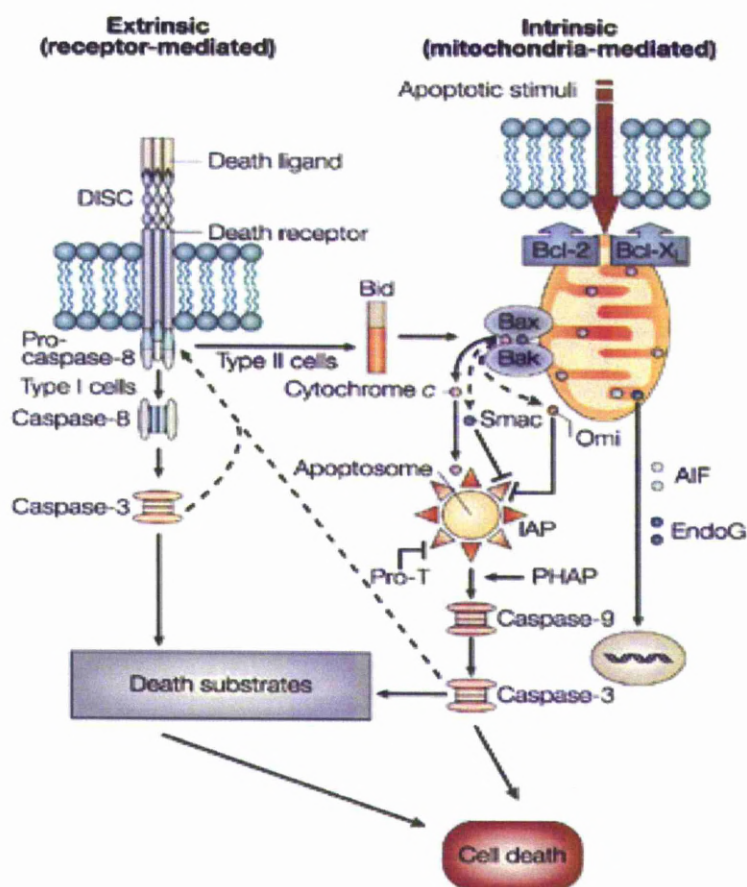


**Figure 1.3** Diagram showing two major apoptotic pathways: extrinsic and intrinsic pathways (modified from Orrenius et al., 2003).

### 1.2.1.3 Endoplasmic reticulum stress apoptotic pathway

In mammalian cells, the main functions of the endoplasmic reticulum (ER) are folding, modifying and sorting of newly synthesized proteins, as well as calcium storage and signalling. Disturbance in any of these functions can result in ER stress (Breckenridge *et al.*, 2003). In response to the accumulation of misfolded proteins or disruption of calcium homeostasis, the signalling pathway called unfolded protein response (UPR) is activated. The activation of the UPR signalling pathway results in: reduction of

protein synthesis to prevent additional accumulation of unfolded protein; induction of ER chaperones and folding catalysts; and activation of ER-associated protein degradation (ERAD) which decreases the folding load in the ER by enhancing degradation of slowly folding protein in the ER. However, if this stress cannot be resolved, it results in caspase-12 triggering which may activate caspase-9 and execute apoptosis (Rao *et al.*, 2004, Schroder & Kaufman, 2005).

Furthermore, calcium release from the ER into the cytosol can act as a messenger that coordinates between the mitochondria and the ER. In the cell-death process triggered by staurosporine and ceramide, a small amount of cytochrome *c* released from mitochondria diffuses to ER and binds to InsP<sub>3</sub> receptors. This enhances calcium release from the ER which causes release of cytochrome *c* from all mitochondria inducing the formation of the apoptosome leading to caspase activation (Mattson & Chan, 2003).

#### **1.2.1.4 JNK and p38 MAPK pathways**

The c-Jun N-terminal kinase (JNK) and p38 MAPK, which are also known as stress-activated protein kinases (SAPKs), are members of the mitogen-activated protein kinase (MAPK) superfamily. These kinases transduce multiple signals from the cell surface to the nucleus in response to a variety of stimuli (Cowan & Storey, 2003). The activation of JNK and p38 MAPK occurs in response to various cellular and environmental stresses including change in osmolarity or metabolism, DNA damage, heat shock, ischemia, inflammatory cytokines, UV irradiation and oxidative stress (Wada & Penninger, 2004).

JNK and p38 MAPK are the terminal kinases of a three-tiered activation system, i.e., MAPKKK, MAPKK and MAPK (Fig 1.4). Kinases that activate JNK include MKK4 and MKK7, and upstream of these kinases are a number of other kinases including TAK, MLK-3, MEKK1, 4 and ASK. After activation, JNK translocates across the nuclear membrane and phosphorylates c-Jun and other nuclear transcription factors such as tumor suppressor p53 and MADD (a cell death domain protein) (Cowan & Storey, 2003). The upstream kinases activating p38 MAPK include MKK3 and MKK6 which, in turn are activated by MEKK, MLK and ASK1. The p38 MAPK regulates two major groups of proteins which are transcription factors such as p53 and protein kinases such as MAPK-activated kinase 2 (Wagner & Nebreda, 2009).

Both JNK and p38 MAPK are involved in regulation of various cellular events, including apoptosis. The role of JNK and p38 MAPK in apoptosis is controversial as they have been implicated in both pro-apoptotic effects (Deng *et al.*, 2003, Grethe *et al.*, 2004, Newhouse *et al.*, 2004) and anti-apoptotic effects (Matusali *et al.*, 2009, Yu *et al.*, 2004). The role of JNK and p38 MAPK in apoptosis may depend on cell type and the nature of the death stimulus (Liu & Lin, 2005, Wada & Penninger, 2004).

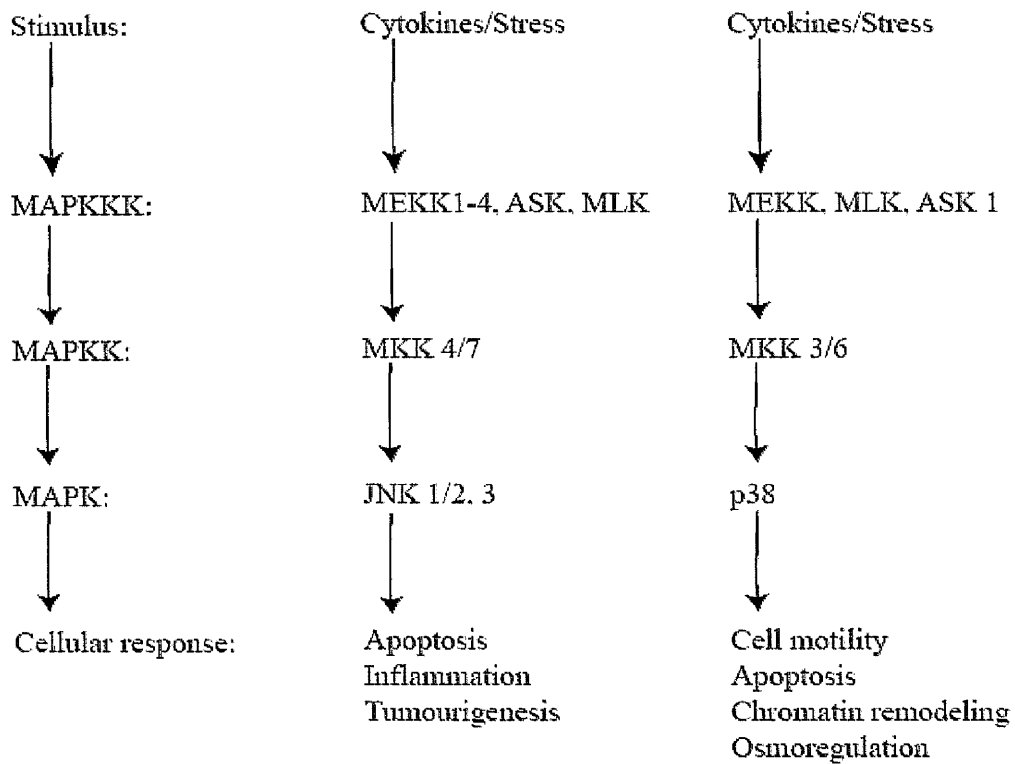


**Figure 1.4** The three-tiered regulatory cascade (MAPK, MAPKK and MAPKKK levels) and cellular responses elicited by JNK and p38 MAPK (modified from Cowan & Storey, 2003).

#### 1.2.1.5 p53

The p53, also known as tumor suppressor protein 53, is a transcription factor which plays a role in the response of cells to stress such as DNA damaging agents, hypoxia or oncogene activation (Amaral *et al.*, 2009). The p53 has a very short half-life and is presented at very low levels within cells. This is maintained by p53 inhibitors, Mdm2 (mouse double minute-2) or Hdm2 in humans which function in inhibiting the transcriptional activity of p53 and promoting its degradation by proteosomes. This protein is transiently stabilised and activated in response to stress stimuli. Depending

on cell or stress signal types p53 activation can lead to cell cycle arrest, DNA repair, cellular senescence or apoptosis (Fig 1.5) (Haupt *et al.*, 2003, Vousden & Lu, 2002). The p53 can promote apoptosis by both transcription dependent and transcription independent mechanisms. In transcription-dependent apoptosis, p53 regulates the expression of component of both extrinsic and intrinsic pathways including Fas (CD 95/ APO-1), DR5, Bax, NOXA, PUMA and Bid (Haupt *et al.*, 2003, Pietsch *et al.*, 2008). In transcription-independent apoptosis, p53 can directly induce apoptosis by translocation to the mitochondria leading to the release of cytochrome *c* and pro-caspase-3 activation (Marchenko *et al.*, 2000, Nemajero *et al.*, 2005).

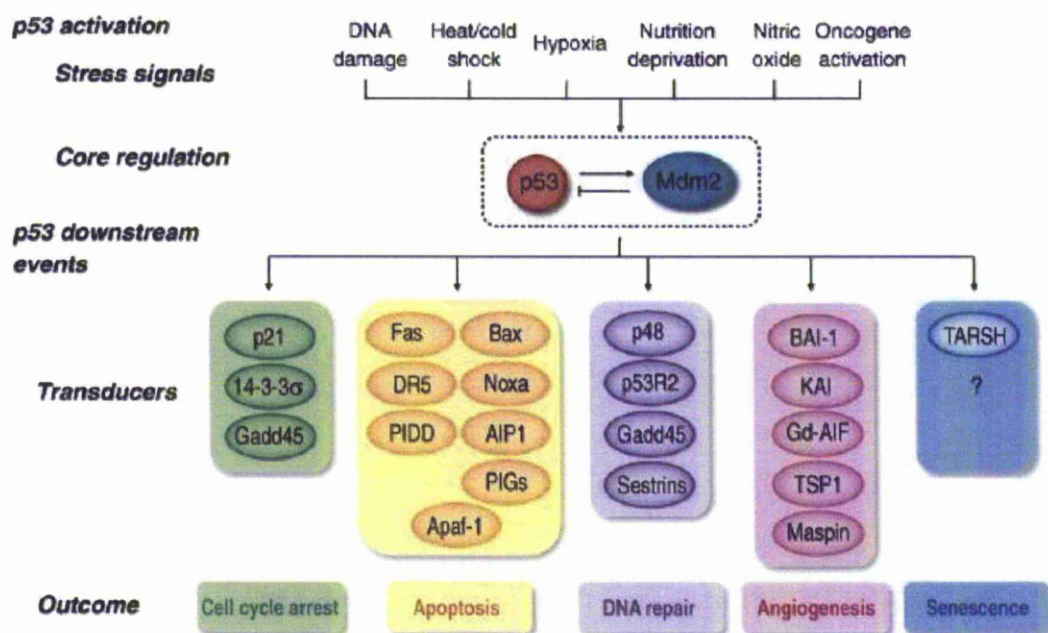


**Figure 1.5** p53 activation and modulation of downstream events (modified from Amaral *et al.*, 2009)

### 1.2.1.6 NF- $\kappa$ B

The nuclear factor kappa B (NF- $\kappa$ B) regulates several biological processes, for example, inflammation, immunity and apoptosis. Five members of the NF- $\kappa$ B family have been identified. These are p50, p52, p65 (also known as REL-A), c-REL, and REL-B. p50 and p52 are derived from proteolytic cleavage of p105 and p100, respectively (Hayden & Ghosh, 2008). The activation of NF- $\kappa$ B is regulated by I $\kappa$ B proteins which are bound to NF- $\kappa$ B under basal conditions and hold NF- $\kappa$ B in the cytoplasm. The I $\kappa$ B family consists of seven members, i.e., I $\kappa$ B $\alpha$ , I $\kappa$ B $\beta$ , I $\kappa$ B $\gamma$ , I $\kappa$ B $\epsilon$ , Bcl-3 and the precursor proteins p100 and p105 (Wang *et al.*, 2009).

Stimulation of cells with tumor necrosis factor- $\alpha$  (TNF- $\alpha$ ), interleukin-1 $\beta$  (IL-1 $\beta$ ) or Toll-like receptor (TLR) ligands leads to the activation of classical or canonical pathway of NF- $\kappa$ B activation. Following the stimulation, the I $\kappa$ B molecules are phosphorylated by I $\kappa$ B kinase (IKK) complex, leading to polyubiquitination by the SCF- $\beta$ TrCP E3 ligase complex. Ubiquitinated I $\kappa$ B is degraded by the proteasome. This results in the translocation of p50/p65 NF- $\kappa$ B dimer to nucleus and the activation of gene transcription. The non-canonical or alternative pathway occurs when a subset of TNF receptor (TNFR) superfamily members including those for BAFF, CD40 ligands and lymphotoxin- $\beta$  are activated. This pathway depends on NF- $\kappa$ B-inducing kinase (NIK) and the IKK $\alpha$  subunit. The phosphorylation of p100 by IKK $\alpha$  leads to the ubiquitination and proteasomal processing to p52. This allows the translocation of the p52/REL-B dimer into the nucleus to activate gene transcription (Skaug *et al.*, 2009, Wang *et al.*, 2009) (Fig 1.6).

The role of NF- $\kappa$ B in apoptosis has been studied in various cell types under a variety of stimuli. A number of reports support an anti-apoptotic effect of NF- $\kappa$ B (Lin *et al.*,



1995, Liu *et al.*, 1996, Van Antwerp *et al.*, 1996, Wang *et al.*, 1996). However, besides these anti-apoptotic effects, there are many reports that reveal an implication of NF- $\kappa$ B in the induction of apoptosis (Connolly *et al.*, 2000, Hansberger *et al.*, 2007, Kuhnel *et al.*, 2000, Stark *et al.*, 2007).

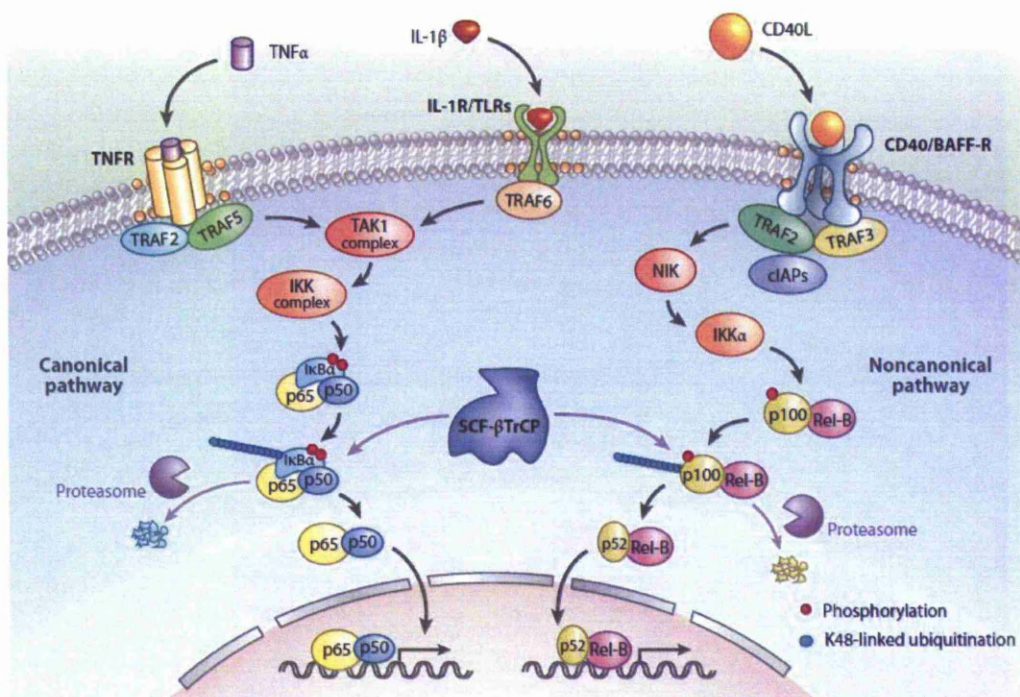


**Figure 1.6** NF- $\kappa$ B signalling pathways (Skaug *et al.*, 2009).

### 1.2.1.7 Calcium signalling

Calcium ( $\text{Ca}^{2+}$ ) is a universal signalling molecule, regulating many aspects of cellular function and is one of the key elements of apoptotic signalling pathways. The concentration of  $\text{Ca}^{2+}$  inside cells is determined by the 'on' reactions which introduce  $\text{Ca}^{2+}$  into the cytoplasm and 'off' reactions which removed  $\text{Ca}^{2+}$  from the cytoplasm by the action of buffers, pumps and exchangers (Berridge *et al.*, 2000). During the 'on' reaction, stimuli induce the entry of external  $\text{Ca}^{2+}$  through channels located on the



plasma membrane as well as the formation of second messengers including inositol - 1, 4, 5 - triphosphate (Ins(1,4,5)P<sub>3</sub>) that release Ca<sup>2+</sup> stored within the endoplasmic/sarcoplasmic reticulum (ER/SR). Most of Ca<sup>2+</sup> released into the cytoplasm by the 'on' reactions are bound to buffers, while a small proportion binds to the effectors which activate various cellular processes. During the 'off' reactions, various exchangers and pumps remove Ca<sup>2+</sup> from the cytoplasm. The Na<sup>+</sup>/Ca<sup>2+</sup> exchanger (NCX) and the plasma membrane Ca<sup>2+</sup> ATPase (PMCA) pump Ca<sup>2+</sup> out of the cell, while the sarco-endoplasmic reticulum Ca<sup>2+</sup> ATPase (SERCA) pumps Ca<sup>2+</sup> back into the ER/SR. The mitochondria also plays a role during the recovery process by sequestration of Ca<sup>2+</sup> through a uniporter which is then slowly released back into cytoplasm and removed by the SERCA and the PMCA (Fig 1.7) (Berridge *et al.*, 2003, Berridge *et al.*, 2000, Bootman *et al.*, 2001).

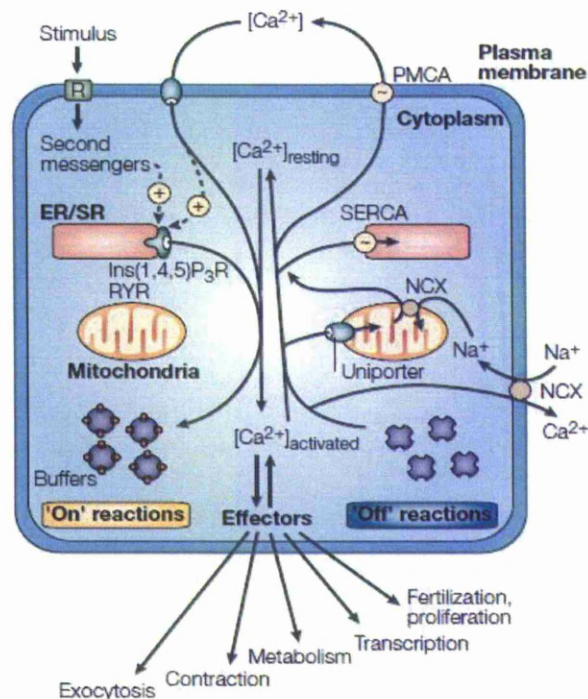


**Figure 1.7** Calcium signalling (modified from Berridge *et al.*, 2003)

There is much evidence to indicate the involvement of alterations in the cytosolic  $\text{Ca}^{2+}$  concentration and/or intracellular  $\text{Ca}^{2+}$  compartmentalization, including the ER, in the regulation of apoptosis. An increase in intracellular  $\text{Ca}^{2+}$  induced by artesunate contributed to apoptosis in endothelial cells (Wu *et al.*, 2004). Treatment of human intestinal cells with BAPTA-AM, an intracellular  $\text{Ca}^{2+}$  chelator, inhibited apoptosis induced by rotavirus infection (Chaibi *et al.*, 2005). Treatment of various types of cell with thapsigargin, the inhibitor of endoplasmic reticular  $\text{Ca}^{2+}$  ATPase or with  $\text{Ca}^{2+}$  ionophores results in apoptosis (Jiang *et al.*, 1994, Kaneko & Tsukamoto, 1994, Levick *et al.*, 1995, Martikainen & Isaacs, 1990).

### **1.2.2 Oxidative stress and apoptosis**

In aerobic organisms, the participation of oxygen in redox reactions cannot be avoided, and this results in the generation of a variety of reactive oxygen species (ROS) including  $\text{O}_2^-$ ,  $\text{H}_2\text{O}_2$ , hydroxyl radical ( $\cdot\text{OH}$ ), and nitric oxide/peroxynitrate ( $\text{NO}/\text{ONOO}^-$ ). A number of these molecules possess a beneficial role in the cell such as signal transduction and the bactericidal activity of phagocytes. However, when an excess amount of these agents is presented in the cell, it becomes toxic to the cell. To protect the cell from the toxicity of ROS, the mammalian cell has developed antioxidative defence mechanisms. When an imbalance between the production of ROS and the antioxidative system occurs, cells become oxidatively stressed. Oxidative stress can result in injury to all important cellular components, for example, proteins, DNA and membrane lipid (lipid peroxidation) which can result in cell death (Clutton, 1997, Yang *et al.*, 2003).

The implication of oxidative stress in the induction of apoptosis has been shown in many studies. For instance, Guha and colleagues showed that malarial infection induced the generation of hydroxyl radical ( $\bullet\text{OH}$ ) in the liver. They suggested that  $\bullet\text{OH}$  may be responsible for the induction of oxidative stress and apoptosis of hepatocyte as these events were able to be prevented by administration of free radical and  $\bullet\text{OH}$  specific scavengers to infected animals (Guha *et al.*, 2006). Oxidative stress has also been shown to induce apoptosis in endothelial cells which can be suppressed by treatment with antioxidant agents (Aoki *et al.*, 2001, Warren *et al.*, 2000).

### **1.2.3 Toll-like receptors (TLR)**

Toll-like receptors (TLR) are a family of evolutionary conserved pathogen recognition receptors. These receptors play a major role in innate immune responses in the defence against bacteria, viruses, parasites and other pathogens. To date, 10 members of TLR in human and 13 in mouse have been identified. All TLR have their respective ligands, for example, LPS of gram negative bacteria is recognised by TLR4 and double stranded RNA (dsRNA) is recognised by TLR3 (Fig 1.8). After recognition of microbial pathogens, TLR triggers intracellular signalling pathways (the myeloid differentiation factor 88 (MyD88)-dependent and/or MyD88-independent pathways) which result in the induction of inflammatory cytokines (Kawai & Akira, 2006, Takeda *et al.*, 2003). Almost all TLR share a common adaptor protein, MyD88, in their signalling pathways, except TLR3. TLR4 is a unique receptor which initiates signalling through both MyD88-dependent and MyD88-independent pathways (Fig 1.8) (Akira & Takeda, 2004).

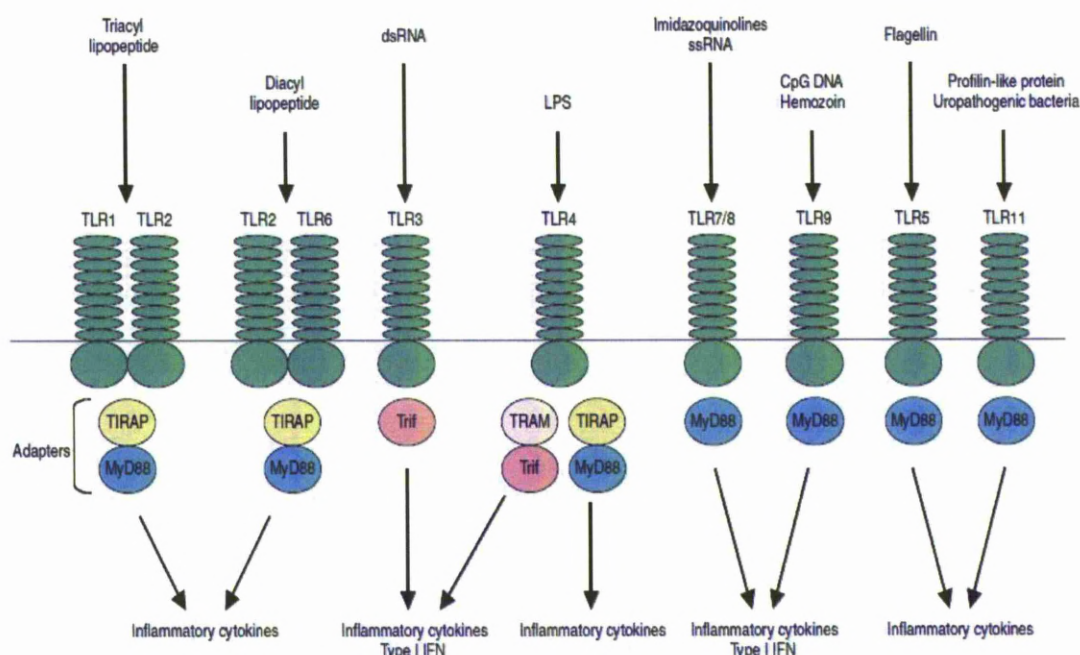


**Figure 1.8** TLR-mediated immune response (Kawai & Akira, 2006).

In addition to the function of TLR in initiating the innate inflammatory immune response, TLR engagement can also result in the induction of apoptosis. TLR2 mediated apoptosis in differentiated THP-1 cells and monocyte-derived macrophages induced by *Mycobacterium tuberculosis* glycolipoprotein (Lopez *et al.*, 2003). TLR3 has been shown to be involved in apoptosis of human breast cancer cells induced by dsRNA (Salaun *et al.*, 2006). Chlamydial heat shock protein 60 induces trophoblast cell apoptosis through triggering of TLR4 (Equils *et al.*, 2006). Other TLR including TLR5, TLR8 and TLR9 have also been implicated in apoptosis (Fischer *et al.*, 2005, Ma *et al.*, 2006, Zeng *et al.*, 2006).

The importance of toll-like receptors in immunity against malaria infection has been established. Coban and co-workers have reported that hemozoin purified from *Plasmodium falciparum* functions as a TLR9 ligand and activates innate immune

response, resulting in production of cytokines and chemokines. These responses were impaired in TLR9- and MyD88-deficient mice. The author suggested that the innate immune response activated by hemozoin is TLR9-mediated and MyD88-dependent (Coban *et al.*, 2005). The same author also illustrated that DNA-free hemozoin can bind to TLR9 and induce conformational changes of TLR9 as those induced by the canonical TLR9 ligand, CpG-DNA (Coban *et al.*, 2010). However, Parroche and colleagues suggested that hemozoin itself was immunologically inert but enhanced innate responses by delivering malarial DNA to TLR9 (Parroche *et al.*, 2007). Besides hemozoin, *Plasmodium* glycosylphosphatidylinositols (GPI) membrane anchor for functionally important proteins on the cell surface, is another TLR ligand inducing proinflammatory response (Gowda, 2007). GPI are recognised mainly by a TLR2/6 heterodimer as well as TLR2/1 heterodimer, and to a lesser extent by TLR4 (Krishnegowda *et al.*, 2005).

## THESIS OBJECTIVES

---

A single cell imaging approach has been adopted to characterise PRBC-endothelial post-adhesive events. Specifically, the phenomenon of adhesion-mediated apoptosis has been studied to;

1. Provide a description of PRBC induce apoptosis of HUVEC at the single-cell level
2. Provide insights into the signalling mechanisms involved in adhesion-mediated apoptosis
3. Provide insights of the host-cell receptors involved in adhesion-mediated apoptosis.

## CHAPTER 2: GENERAL MATERIALS AND METHODS

---

### 2.1 Malaria culture

#### 2.1.1 Malaria parasite isolate

The *Plasmodium falciparum* isolate used in this study was ITG which is a strong ICAM-1 binder (Gray *et al.*, 2003). This isolate was a gift from Prof. Alister Craig (Liverpool School of Tropical Medicine, UK). The parasite was grown and maintained in culture using a modified method of Trager and Jensen (Trager & Jensen, 1976).

#### 2.1.2 Preparation of complete medium

A complete medium was prepared by adding 12.5 ml 1 M HEPES (N-(2-Hydroxyethyl) piperazine-N'-(2-ethanesulfonic acid)) pH 7.4 (Sigma), 0.2 ml gentamicin solution (50 mg/ml) (Sigma) and 37.5 ml pooled human AB serum to 500 ml RPMI-1640 medium supplemented with L-glutamine and sodium bicarbonate (Sigma).

#### 2.1.3. Preparation of serum

Blood was collected from the gastroenterology ward, Royal Liverpool Hospital, UK. Serum from multiple donors was pooled together in a sterile glass flask, before aliquots of 37.5 ml were prepared in 50 ml centrifuge tubes. Serum aliquots were stored at -80 °C. Prior to use, serum was thawed in a water bath at 37 °C.

#### 2.1.4 Preparation of uninfected erythrocytes

Group O Rhesus positive human whole blood was collected from National Blood Service, Royal Liverpool Hospital, UK. Before adding to culture flasks, blood was

resuspended in RPMI-1640 medium supplemented with L-glutamine and sodium bicarbonate (Sigma) followed by centrifugation at 3,000 rpm for 5 min. The supernatant and buffy coat layers were removed by aspiration. This process was repeated three times. Washed erythrocytes were stored at 4 °C and used within a week to prevent haemolysis.

### **2.1.5 Sub-culturing of malaria parasite**

Parasites were routinely sub-cultured to keep them alive and avoid over-growth. The parasitemia was checked by preparing a thin blood film and counting parasites using a light microscope. After determination of parasitemia, parasite suspensions were transferred to 50 ml centrifuge tube and centrifuged at 2,000 rpm for 5 min. The supernatant was discarded. The parasite pellet was diluted to the appropriate parasitemia in 35 ml of complete medium in T75 cm<sup>2</sup> culture flasks (Nunc) or 12 ml complete medium in T25 cm<sup>2</sup> culture flasks (Nunc). Subsequently, washed uninfected erythrocytes were added to achieve a haematocrit of 1%.

### **2.1.6 Gas Phase**

Following preparation of the sub-cultures, flasks were flushed with mixed gas (4% O<sub>2</sub>, 3% CO<sub>2</sub> in N<sub>2</sub>) (BOC, UK). The duration of gassing was 1 min for a T75 cm<sup>2</sup> culture flask (Nunc) and 30 sec for a 25 cm<sup>2</sup> culture flask (Nunc).

### **2.1.7 Parasite cryopreservation**

Ring stage parasites ( $\geq$  5% parasitemia) were centrifuged at 2,000 rpm for 5 min and resuspended in an equal volume of cryoprotectant solution (70 ml glycerol, 180 ml



4.2% w/v sorbitol in 0.9% w/v sodium chloride solution). Aliquots (1ml) were placed into labelled screw-capped cryotubes (Nunc), and placed in liquid nitrogen storage.

#### **2.1.8 Parasite retrieval**

Cryopreserved parasites were removed from the liquid nitrogen storage, thawed at 37 °C, resuspended in an equal volume of retrieval solution (3.5% sodium chloride) and left stand for 5 min at room temperature. The suspension was then centrifuged at 2,000 rpm for 5 min. The supernatant was removed and the pellet was resuspended in 10 ml complete medium. The suspension was centrifuged and the supernatant discarded. The pellet was resuspended in 15 ml complete medium together with 0.5 ml uninfected erythrocytes in a T25 cm<sup>2</sup> culture flask (Nunc).

#### **2.1.9 Parasite synchronisation**

Malaria parasites were synchronised to generate cells in the same stage of the asexual life cycle. Parasite culture was synchronised using sorbitol (Lambros & Vanderberg, 1979). Synchronisation uses the principle of osmotic lysis to selectively remove mature forms of the parasites, leaving the younger ring stage parasites. Parasite culture with a mixed population of both mature (trophozoites and schizonts) and ring stages was centrifuged at 2,000 rpm for 5 min. The pellet was resuspended in 5X volume of 5% w/v sorbitol (Sigma) for 20 min. Synchronised parasites were resuspended in an excess volume of complete medium and centrifuged to wash off sorbitol and particulates.

## **2.2 Human Umbilical Vein Endothelial Cell (HUVEC) culture**

### **2.2.1 Primary human umbilical endothelial cells**

Primary pooled human umbilical cells were purchased from Lonza (Switzerland) as cryopreserved cells. The method for HUVEC cultivation followed the manufacturer's instructions. Briefly, a cryovial of primary HUVEC was resuspended in 12 ml endothelial cell complete medium (Lonza). The resuspended endothelial cell was seeded into three gelatin-coated T25 cm<sup>2</sup> vented cap flasks (Nunc) (4 ml per seeding vessel). This first passage is designated as passage 1. HUVEC were cultured to passage 3, after which they were frozen in liquid nitrogen as described in section 2.2.7.

### **2.2.2 Medium preparation**

For HUVEC culturing the EGM-2 BulletKit was utilised (Lonza). This kit contains a 500 ml bottle of EBM-2 endothelial medium and supplement (EGM-2 SingleQuot). The EGM-2 SingleQuot supplement contains 10 ml fetal calf serum (FCS), 0.2 ml hydrocortisone, 2.0 ml hFGF-B (human Fibroblast Growth Factor Basic), 0.5 ml VEGF (Vascular Endothelial Growth Factor), 0.5 ml R<sup>3</sup>-IGF-1 (Human Recombinant Insulin-like Growth Factor), 0.5 ml Ascorbic Acid (Vitamin), 0.5 ml hEGF (human recombinant Epidermal Growth Factor), 0.5 ml GA (gentamicin, amphotericin-B) 1000 and 0.5 ml heparin. This supplement was added to a bottle of EBM-2 to make complete medium.

### **2.2.3 Preparation of seeding vessels**

The seeding vessels (T75 cm<sup>2</sup> or T25 cm<sup>2</sup> vented cap flask (Nunc)) were coated with 2% gelatin solution (Sigma) diluted to 1% gelatin in 1X phosphate buffer saline

solution (PBS). The amount of gelatin solution used was 2 ml for a T25 cm<sup>2</sup> flask and 4 ml for a T75 cm<sup>2</sup> flask. The coated vessels were left at 37 °C for at least 30 min. Excess gelatin was removed before seeding.

#### **2.2.4 HUVEC retrieval**

A cryovial of HUVEC at passage 3 was removed from the liquid nitrogen storage and plunged into a 37 °C water bath until almost completely defrosted. Final defrosting was completed at room temperature. The thawed HUVEC were immediately transferred to 8.5 ml of pre-warmed complete media and mixed thoroughly by inverting the tube and pipetting. The cell suspension was distributed between three gelatin-coated T25 cm<sup>2</sup> vented cap flasks (3 ml per flask). Cells were allowed to settle for 2 hr or overnight in a 37 °C, 5% CO<sub>2</sub>, humidified incubator. After the cells had settled, medium was replaced with fresh medium and cultured as per 2.2.5.

#### **2.2.5 Standard HUVEC culture**

HUVEC do not tolerate rapid temperature fluctuations or nutrient-deficient medium and hence endothelial media was pre-warmed to 37 °C before use. HUVEC were monitored daily under an inverted microscope for cell growth and contamination. The culture medium was changed every other day after seeding to maintain sufficient nutrient levels. The amount of medium used was 4 ml for a T25 cm<sup>2</sup> vented cap flask and 10 ml for a T75 cm<sup>2</sup> vented cap flask. Cells were maintained until nearly confluent.

#### **2.2.6 Sub-culturing of HUVEC**

Once HUVEC reached 80-90% confluence, three T25 cm<sup>2</sup> vented cap flasks with gelatin were prepared for each confluent T25 cm<sup>2</sup> flask. The medium was removed

from the culture vessel and HUVEC were washed once with 1X PBS to remove complex proteins that neutralize trypsin (3 ml for T25 cm<sup>2</sup> vented cap flask and 8 ml for a T75 cm<sup>2</sup> vented cap flask). PBS was then removed from the culture vessel. Trypsin-EDTA solution (Sigma) was added to the flask. The flask was examined under inverted microscope until all cells were rounded up (about 1 min). As soon as all cells were rounded up, the flask was tapped sharply. Cells were checked again for complete detachment under an inverted microscope. When cells were deemed sufficiently detached, Trypsin-EDTA was neutralised with an equal volume of endothelial complete medium. The suspension was transferred to a 15 ml tube and centrifuged at 1,500 rpm for 5 min and the resultant supernatant was discarded. The pellet was resuspended in 0.5-1 ml complete medium and gently mixed by pipetting. Cells were diluted to a final volume of 2-3 ml in complete medium and the number of cells determined using a haemocytometer. The suspension was then adjusted to the required volume and added to the culture vessels. The seeded culture vessels were placed in a humidified incubator (37 °C, 5% CO<sub>2</sub>). Medium was replaced one day post-seeding and every other day thereafter.

### **2.2.7 HUVEC cryopreservation**

When HUVEC reached confluence, they were trypsin detached (as described above), centrifuged and the pellet was resuspended in 3 ml of cryoprotective solution which comprised 8 parts fetal bovine serum, 1 part DMSO and 1 part complete medium. The cell suspension was aliquoted to 3 cryotubes and placed at -20 °C until frozen. Cryovials were then transferred to -80 °C overnight and finally stored in liquid nitrogen until required.

## **CHAPTER 3: POST-ADHESIVE INDUCTION OF APOPTOSIS IN HUMAN ENDOTHELIAL CELLS BY MALARIA INFECTED ERYTHROCYTES**

---

### **3.1 INTRODUCTION**

Apoptosis (programmed cell death) is a process triggered in response to specific stimuli. This process can mainly occur through two pathways. The first pathway involves the interaction between a death receptor, such as TNF receptor-1 or FAS receptor, and its ligand (extrinsic pathway) which lead to the activation of caspase-8. Another pathway depends on the participation of mitochondria (intrinsic pathway) which results in the triggering of caspase-9 (Schultz & Harrington, 2003). The detail of apoptotic pathways are described in section 1.2.1 of Chapter 1.

The potential role of apoptosis in the pathology of malaria has been suggested by a number of laboratories. Post-mortem studies conducted in Vietnamese patients showed that 40% of cerebral malaria (CM) patients had activation of caspase-3, a marker of apoptosis (Medana *et al.*, 2001). The significant elevation of Fas ligand (FasL) was found in post-mortem cerebrospinal fluid (CSF) samples from CM mortality cases (Armah *et al.*, 2007). Soluble Fas (sFas) levels were significantly increased in plasma samples taken from CM patients when compared with plasma samples taken from healthy controls or mild malaria patients (Jain *et al.*, 2008). Furthermore, a study to investigate the capacity of field isolates to induce endothelial cell apoptosis found that patients who have neurological manifestations were more likely to harbour apoptogenic strains (Toure *et al.*, 2008).

The study of Pino and colleagues, which co-cultured human endothelial cells with PRBC, illustrated that physical interactions between endothelial cells and PRBC are necessary to induce apoptosis of endothelial cells (Pino et al., 2003b). However, some studies have demonstrated induction of endothelial cell apoptosis indirectly in the absence of a physical interaction with PRBC. For instance, the study by Wilson and colleagues illustrated that soluble factors from *P. falciparum*-infected erythrocytes can induce apoptosis in both human brain vascular endothelial and neuroglia cells (Wilson et al., 2008). The co-incubation of human endothelial cells with sera from malaria patients in the presence of neutrophils resulted in apoptosis of human endothelial cells (Hemmer et al., 2005).

The study which assessed whole-brain transcriptional responses in experimental murine CM showed the expression of apoptotic-related genes in CM-susceptible (C57BL/6) mice compared with CM-resistant (BALB/c) mice. This was confirmed by the histological analysis of mouse brain which demonstrated higher numbers of apoptotic cells in C57BL/6 mice compared with BALB/c mice (Lovegrove et al., 2007). Studying the brains of mice with CM, Lackner and co-workers found activation of caspase-3 in different central nervous system cells of animals with CM (Lackner et al., 2007). Another study in deficient Fas and Fas ligand mice infected with *P. berghei* ANKA showed that these animals were protected from fatal CM (Potter et al., 2006b).

Although the murine model has been widely used as a model for the study of human CM, there are markedly different histopathological features between murine and human CM. For instance, there is little or no intracerebral sequestration of PRBC in the murine model, whereas intense intracerebral sequestration is associated with human CM (White et al., 2009a). As described above, there are conflicts as to whether

cytoadherence of PRBC is essential for induction of apoptosis (Hemmer et al., 2005, Pino et al., 2003b, Wilson et al., 2008). In this chapter, we adopted an *in vitro* single-cell imaging approach to determine PRBC-endothelial post-adhesive events. This approach surpasses other techniques as it allows us to closely observe the essential of PRBC cytoadherence in induction of endothelial cell apoptosis without signal interfering from the cells without PRBC cytoadherence.

## **3.2 MATERIALS AND METHODS**

### **3.2.1 Preparation of HUVEC for co-culturing**

HUVEC used in the experiments were from passage 4-6. HUVEC culture methodologies have been described in detail in Chapter 2 section 2.2. When HUVEC reached to 80-90% confluence, cells were trypsinised and seeded on 40 mm diameter gelatin coated coverslip (Bioptechs) placed in petri dish (Nunc). The seeding density was 15,000-20,000 cells/cm<sup>2</sup>. Approximately 500 µl of cell suspension was gently loaded onto the coated coverslips. Cells were allowed to settle for 1 h at 37 °C, 5% CO<sub>2</sub> in a humidified incubator. The medium was then removed and 2 ml of pre-warmed fresh medium was added. Cells were then further cultured until they reached 80-90% confluence.

### **3.2.2 Preparation of malaria parasites for co-culturing**

*P. falciparum* strains ITG and C24 were cultured as described in Chapter 2 section 2.1. Parasites were cultured until they reached 5-8% parasitemia (trophozoite or schizont stages). Parasites were then submitted to a magnetic separation technique in order to obtain 80-90% parasitemia. This method is based on the paramagnetic property of mature parasites due to the stacking of the iron content of the haemozoin product of haemoglobin breakdown (Paul *et al.*, 1981). Briefly, the parasite suspension was centrifuged at 2000 rpm for 5 min. The parasite pellet was re-suspended in 10 ml of binding solution (1X PBS containing 2% BSA (Sigma) and 20 mM glucose (Sigma)). The CS column was placed on a VarioMACS magnet (Miltenyi Biotec) and pre-washed once with binding solution. The column was not allowed to dry at any time during the procedure. The parasite suspension was applied to the top of the column



and the column was washed with binding solution until the flow through was clear. The column was removed from the magnet and the concentrated parasites were eluted by adding 10 ml of binding solution to the top of the column. The eluent was centrifuged at 2000 rpm for 5 min. The pellet was washed three times with parasite culture media.

### **3.2.3 Co-culture of HUVEC with malaria parasites**

The concentrated parasites were re-suspended in 1% FCS in medium 199 to a parasitemia of 50% in 1% haematocrit. Endothelial medium was removed from HUVEC grown on coverslips at 80-90% confluence and the cells were gently washed once with 1X PBS. Parasite suspension (2 ml) was then added to the HUVEC monolayer and co-cultured for 3, 6 or 24 h at 37 °C, 5% CO<sub>2</sub> in a humidified incubator. In control groups, uninfected RBC were re-suspended in 2 ml of 1% FCS in medium 199 to get a 1% haematocrit and applied onto HUVEC monolayer washed with 1X PBS. The co-culture dishes were agitated either clockwise or counter clockwise every 10-15 min to allow more cell-to-cell contact until the third hour.

### **3.2.4 Induction of apoptosis by camptothecin**

For the positive control, HUVEC cultured on coverslips were treated with camptothecin (Sigma) at a concentration of 5 µM for 24 h in order to induce apoptosis.

### **3.2.5 Determination of apoptotic cells using confocal laser scanning microscope**

After 3 h of co-cultivation, the co-culture medium was discarded. HUVEC in all groups of experiments were washed twice with 1X PBS to remove unbound uninfected red blood cells or parasites. Apoptosis of HUVEC was detected using annexin V,

Alexa fluor 488 conjugate (Molecular Probes). Annexin V is a  $\text{Ca}^{2+}$  dependent phospholipid-binding protein. It binds to phosphatidylserine translocated from the inner plasma membrane to the external side in apoptotic cells. To exclude necrotic cells, propidium iodide (PI) (Sigma) which stains nucleic acids was used (Fadok *et al.*, 1992, Vermes *et al.*, 1995). Double staining of annexin V and propidium iodide was performed by adding 8  $\mu\text{l}$  of annexin V and 2  $\mu\text{l}$  of 2.5  $\mu\text{g/ml}$  PI into 2 ml of annexin-binding buffer (10 mM HEPES, 140 mM NaCl and 2.5 mM  $\text{CaCl}_2$ , pH 7.2). Cells were incubated within this mixture at 37 °C, 5%  $\text{CO}_2$  in humidified incubator for 20 min. The coverslips were gently washed once with annexin-binding buffer. The coverslips were assembled into a Biopetechs FCS2 perfusion chamber (Biopetechs), perfused with annexin-binding buffer and observed with Zeiss Pascal confocal laser scanning microscope (CLSM). Cells were viewed through a Plan-Apochromat 63x 1.2 numerical aperture (N.A.) water objective. Fluorescence signals from annexin V and PI were obtained by single excitation with argon ion laser at 488 nm and collection of emitted light through a 505-530 nm band pass filter and a 650 nm long pass filter, respectively. At least 500 cells were counted for each replicate and scored according to the appearance of cells, i.e. attached/unattached to PRBC, blebbing and/or annexin V/PI staining. Endothelial cells undergoing apoptosis were characterised by blebbing of the cell membrane and/or staining positive for annexin V or annexin V positive alone. HUVEC that showed uptake of annexin V together with PI or uptake of PI alone were considered as necrotic cells (Jacobi *et al.*, 2005).

The level of attachment between HUVEC and PRBC, apoptosis resulting from PRBC cytoadherence and apoptosis of HUVEC without cytoadherence were shown in percentage as calculated by:

- a. The level of attachment between HUVEC and PRBC:

$$\frac{\text{number of HUVEC attached to PRBC}}{\text{total number of cell count}} \times 100$$

- b. The level of apoptosis resulting from cytoadherence:

$$\frac{\text{number of apoptotic HUVEC attached to PRBC}}{\text{number of HUVEC attached to PRBC}} \times 100$$

- c. The level of apoptosis of HUVEC without cytoadherence:

$$\frac{\text{number of apoptotic HUVEC unattached to PRBC}}{\text{total number of cell count}} \times 100$$

### **3.2.6 Comparison between live and dead malaria parasites in inducing apoptosis in HUVEC<sup>a</sup>**

To further understand the process of malaria parasite induced apoptosis of HUVEC, we investigated the apoptotic potential of live and dead parasites. The parasites were killed using two different methods, i.e. heat killing and artesunate killing.

#### **3.2.6.1 Malaria parasites killed by artesunate treatment**

Malaria parasites (ITG strain) at ~5% parasitemia (at mature trophozoite stages) were incubated with 500 nM artesunate (Mepha) for 4 h. The parasites were centrifuged at 3000 rpm for 5 min and then washed once with complete media.

#### **3.2.6.2 Malaria parasites killed by heat**

Mature stage malaria parasites were heat-killed by subjecting the parasite pellet to 60 °C for 20 min in a water bath. The pellet was washed twice with complete media.

---

<sup>a</sup> In collaboration with Dr. Parnpen Viriyavejakul

In order to determine the viability of the parasites, 200 µl each of the artesunate-killed or heat-killed parasites were incubated separately with equal volumes of annexin-binding buffer containing 2.5 µg/ml propidium iodide for 20 min. A control consisting of untreated PRBC was prepared in parallel. Wet smear preparations were produced and visualised under the confocal microscope through the Plan-Apochromat 63x 1.4 N.A. water objective. Cell viability was calculated and expressed as the percentage of the total number of cells counted. Parasites stained with PI were considered as dead parasites.

The remaining parasites from the heat-killed and artesunate-killed parasites were transferred to culture flasks and grown in continuous culture for 4 weeks to confirm that all parasites were dead.

#### **3.2.6.3 Heat-killed parasites binding to endothelial cells**

HUVEC were grown on coverslips as described in section 3.2.1. Malaria parasites (ITG strain) were prepared as described in section 3.2.2 with some modifications. After the parasite pellet was washed with complete media, they were re-suspended to get 50% parasitemia in 1% haematocrit in M199 supplemented with 1% FCS. The sample was divided into two tubes of 2 ml each. One suspension was heat-killed by immersing the tube into a 60 °C for 20 min in a water bath. The other tube served as a control (live parasites). Live and heat-killed parasite suspensions were then added to the HUVEC monolayer and co-cultured for 3 h at 37 °C, 5% CO<sub>2</sub> in a humidified incubator. The co-culture dishes were agitated either clockwise or counter clockwise every 10-15 min to allow more cell-to-cell contact until the third hour. Apoptotic

endothelial cells were determined with the aid of confocal microscopy as described in section 3.2.5.

#### **3.2.6.4 Artesunate-killed malaria parasites binding to endothelial cells**

Malaria parasites (ITG strain) and HUVEC were prepared for co-culturing as described in section 3.2.1 and 3.2.2. The washed parasite pellet was re-suspended in M199 supplemented with 1% FCS to get 50% parasitemia in 1% haematocrit. The parasites were divided into two tubes each of 2 ml. One tube was subjected to artesunate-killed by incubation with 500 nM artesunate for 4 h. The other tube was served as a control (live parasites). Parasites in both groups were co-cultured with HUVEC for 3 h at 37 °C, 5% CO<sub>2</sub> in a humidified incubator. The co-culture dishes were agitated either clockwise or counter clockwise every 10-15 min to allow more cell-to-cell contact until the third hour. The determination of apoptotic endothelial cells was performed with the aid of confocal microscopy as described in section 3.2.5.

#### **3.2.7 The importance of parasite ligand binding preference in parasite induced HUVEC apoptosis<sup>a</sup>**

The ITG parasite used in previous experiments has a preference to bind to ICAM-1 (Ockenhouse *et al.*, 1991). In contrast, *P. falciparum* isolate used in these experiments was C24, which strongly bind to CD36 on endothelial cells (Gray *et al.*, 2003).

HUVEC and malaria parasites were prepared as previously described in section 3.2.1 and 3.2.2, respectively. Both parasite lines were added on HUVEC monolayer and co-cultured for 3 h at 37 °C, 5% CO<sub>2</sub> in a humidified incubator. After 3 h of co-culture, HUVEC were stained with annexin V and propidium iodide as described in section

---

<sup>a</sup> In collaboration with Dr. Parnpen Viriyavejakul

3.2.5. Apoptotic HUVEC were determined using confocal microscopy as described in section 3.2.5.

### **3.2.8 Blocking parasite induced HUVEC apoptosis with caspase inhibitors**

The general caspase inhibitor (Z-VAD-FMK) (Promega) was used to confirm that the apoptotic process seen in HUVEC occurred via a caspase dependent mechanism. In addition, more-specific caspase inhibitors, Z-IETD-FMK (caspase-8 inhibitor) (R&D systems) and Z-LEHD-FMK (caspase-9 inhibitor) (R&D systems) (Meguro et al., 2001), were also used in the experiments to determine the cellular pathway involved in apoptosis of HUVEC.

HUVEC and parasites were prepared as described in section 3.2.1 and 3.2.2, respectively. The concentrated parasites were re-suspended in 1% FCS in medium 199 to a parasitemia of 50% in 1% haematocrit. Endothelial medium was removed from HUVEC grown on coverslips at 80-90% confluence and the cells were gently washed once with 1X PBS. Parasite suspension was then added to the HUVEC monolayer and co-cultured for 3 h at 37 °C, 5% CO<sub>2</sub> in a humidified incubator. The co-culture dishes were agitated either clockwise or counter clockwise every 10-15 min to allow more cell-to-cell contact until the third hour.

For apoptotic inhibition assay, Z-VAD-FMK at 20 µM, Z-IETD-FMK at 100 µM and Z-LEHD-FMK at 100 µM were added at the same time as co-culturing. After 3 h of co-cultivation, the co-culture medium was discarded. HUVEC were washed twice with 1X PBS and stained with annexin V and propidium iodide as described in section 3.2.5. Apoptosis of endothelial cells was determined as described in section 3.2.5.

### **3.2.9 Caspase-8 and caspase-9 activities in malaria parasites induced apoptosis in HUVEC<sup>a</sup>**

To confirm the involvement of two apoptotic pathways (the extrinsic and intrinsic pathways) that have been observed from our single cell studies, luminescence-based assays were conducted to determine the activities of caspase-8 and caspase-9 from induced HUVEC. The assay kits used in this experiment contain the substrates of caspase-8 or caspase-9. Upon cleavage of the substrates by the respective caspases, aminoluciferin is liberated and can contribute to the generation of light in a luminescence reaction. The resulting luminescent signal is directly proportional to the amount of caspase activity present in the sample.

#### **3.2.9.1 Preparation of cell lysate**

HUVEC were grown in T25 cm<sup>2</sup> vented cap flask as described in Chapter 2 section 2.2. Malaria parasites were culture and subjected to magnetic separation as described in Chapter 2 section 2.1 and section 3.2.2, respectively. Experimental samples consisted of cell lysates collected from control HUVEC, HUVEC incubated with camptothecin, HUVEC co-cultured with normal red blood cells and HUVEC co-cultured with parasitized red blood cells. Camptothecin was used at 10 µM. Uninfected red blood cells were used at 1% haematocrit, and parasitized red blood cells were used at 50% parasitemia at 1% haematocrit. After 24 h of co-culturing, the suspension was removed and centrifuged at 14,000 rpm for 45 min at 4 °C to spin down microparticles and floating cells. Adherent HUVEC were washed three times with iced cold 250 mM sucrose (Sigma) in 10 mM Tris solution (Sigma) (pH 7.4) with

---

<sup>a</sup> In collaboration with Dr. Parnpen Viriyavejakul

gentle rocking of the culture vessels to remove as much RBC and PRBC materials as possible. Cells were harvested in 15 ml of sucrose-Tris solution using a cell scraper. The suspension was spun down at 1,500 rpm for 5 min. The supernatant was discarded and the precipitate was combined with microparticles and floating cells.

#### **3.2.9.2 Luminescence activities of caspase-8 and caspase-9**

Caspase-Glo 8 and Caspase-Glo 9 assays (Promega) were used to determine the activities of caspase-8 and caspase-9, respectively. The 1:1 ratio of Caspase-Glo 8 or Caspase-Glo 9 assays to sample volume was used. Then, the mixture was incubated for 1 h at room temperature. Luminescence of each sample was measured using the Wallac 1450 MicroBeta Trilux Liquid Scintillation and Luminescence counter. The counting time was set at 20 s per sample.

#### **3.2.10 Statistical analysis**

Results were expressed as mean  $\pm$  standard error of individual experimental groups. Statistical analysis was performed with GrapPad InStat version 3.05. Data were analysed by Mann-Whitney U test. A value of  $p < 0.05$  was considered significant.



### 3.3 RESULTS

#### 3.3.1 Cytoadherence of PRBC and RBC to HUVEC

The level of binding between malaria parasites and HUVEC at 3, 6 and 24 h of co-culturing were  $3.98\% \pm 0.41$  (SE),  $4.84 \pm 0.80$  (SE) and  $3.60\% \pm 0.61$  (SE), respectively (Fig. 3.1). In control groups, co-culturing RBC together with HUVEC, the percentages of binding between RBC and HUVEC were  $0.00\% \pm 0.00$  (SE),  $0.13\% \pm 0.08$  (SE) and  $0.60\% \pm 0.40$  (SE) after 3, 6 and 24 h of co-incubation, respectively (Fig. 3.1).

There were statistically significant differences between the amount of attached PRBC and attached RBC for 3 and 6 h of co-culturing ( $p < 0.05$ ). However, the numbers of attached PRBC and attached RBC at 24 h co-culturing was not statistically significant different. This might due to the lesser number of replicates ( $n = 3$ ) compared to experiments with 3 h and 6 h ( $n > 6$ ) co-culture. This situation occurred because there was technical difficulty in counting apoptotic HUVEC after cells had been co-cultured with PRBC for 24 h.

The absence of attachment between RBC and HUVEC is illustrated in figure 3.2A, whilst PRBC-HUVEC cytoadherence is illustrated in Fig. 3.2B. Cell membrane blebbing and annexin V staining of attached HUVEC can also clearly be seen for PRBC-dependent cytoadherence.

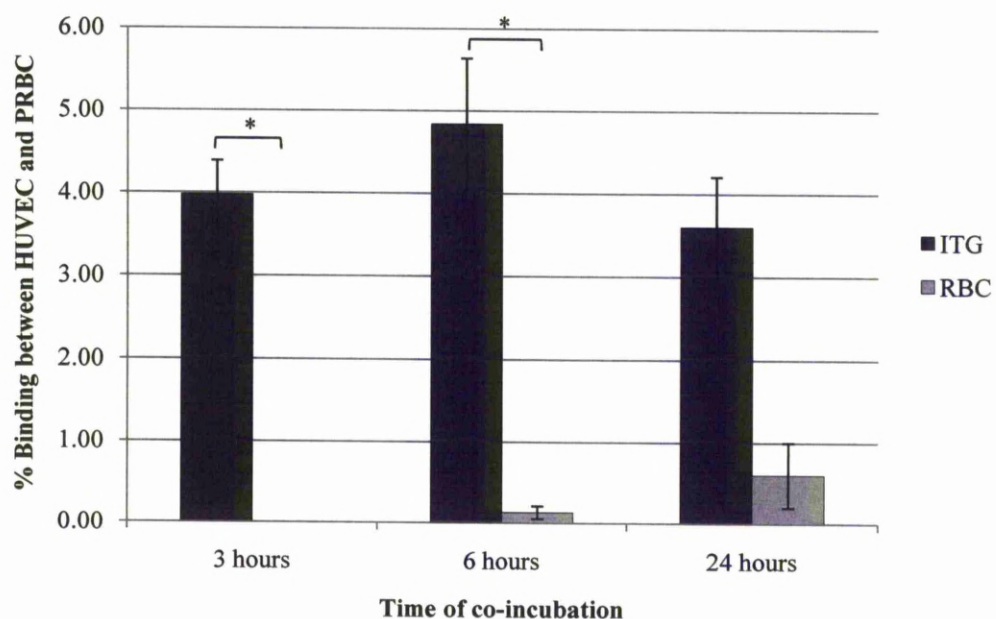


**Figure 3.1<sup>a</sup>** Comparison amount of binding of PRBC and RBC to HUVEC at different time points. Data are mean  $\pm$  SE of at least three experiments. \* denotes statistical difference ( $p < 0.05$ ).

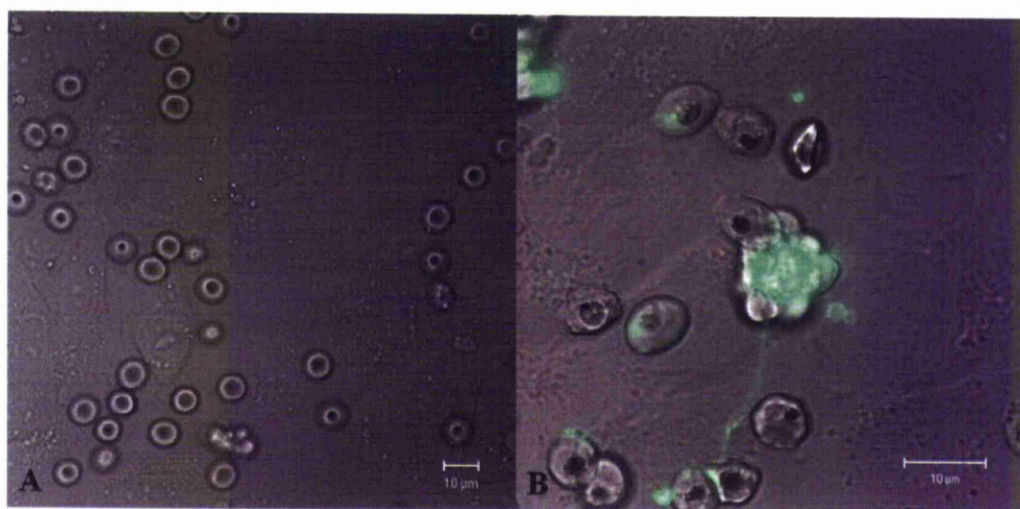


**Figure 3.2** Confocal images of HUVEC incubated with (A) RBC and (B) PRBC after 3 h.

<sup>a</sup> In collaboration with Dr. Parnpen Viriyavejakul

### 3.3.2 Cytoadherence-mediated PRBC induced apoptosis of HUVEC

HUVEC undergoing apoptosis were characterised by blebbing of the cell membrane and/or staining positive for annexin V or annexin V positive alone. HUVEC positively stained with PI were considered as necrotic cells. Various features of HUVEC apoptosis and samples of cells stained positively with PI were showed in Fig 3.4 (A-E).

In positive control experiments, HUVEC were induced to apoptosis by using the topoisomerase I inhibitor camptothecin (Simak *et al.*, 2002). Treatment of HUVEC with camptothecin caused profound changes in HUVEC morphology and staining compared to untreated cells. Cells became detached, together with cell membrane blebbing and/or positive staining with annexin V Fig 3.4 (F). These phenomena were also found in HUVEC that attached to PRBC. HUVEC with attached PRBC showed detachment from coverslip, cell membrane blebbing and/or annexin V positive as well as the formation of apoptotic bodies (microparticles) (Fig 3.4 (A-D)).

The degree of apoptosis resulting from cytoadherence was also assessed. The data demonstrated that after 3, 6 and 24 h of co-incubation,  $88.77\% \pm 1.35$  (SE),  $71.65\% \pm 10.83$  (SE) and  $67.44\% \pm 9.22$  (SE) of HUVEC with attached PRBC demonstrated signs of apoptosis, respectively (Fig 3.3). Relative to attached cells, very few HUVEC that were unattached displayed signs of apoptosis after either 3, 6 or 24 h of co-culture ( $p < 0.05$ ).

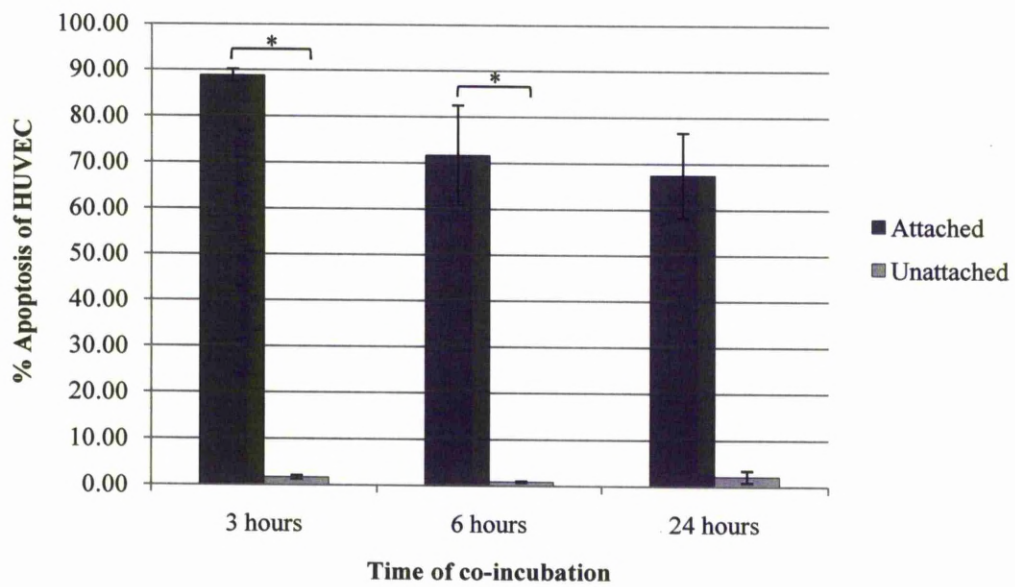


**Figure 3.3<sup>a</sup>** Comparison of apoptosis (%) of HUVEC when attached or unattached during co-incubation with PRBC. Data are mean  $\pm$  SE of at least three experiments. \* denotes statistical difference ( $p < 0.05$ ).

<sup>a</sup> In collaboration with Dr. Parnpen Viriyavejakul

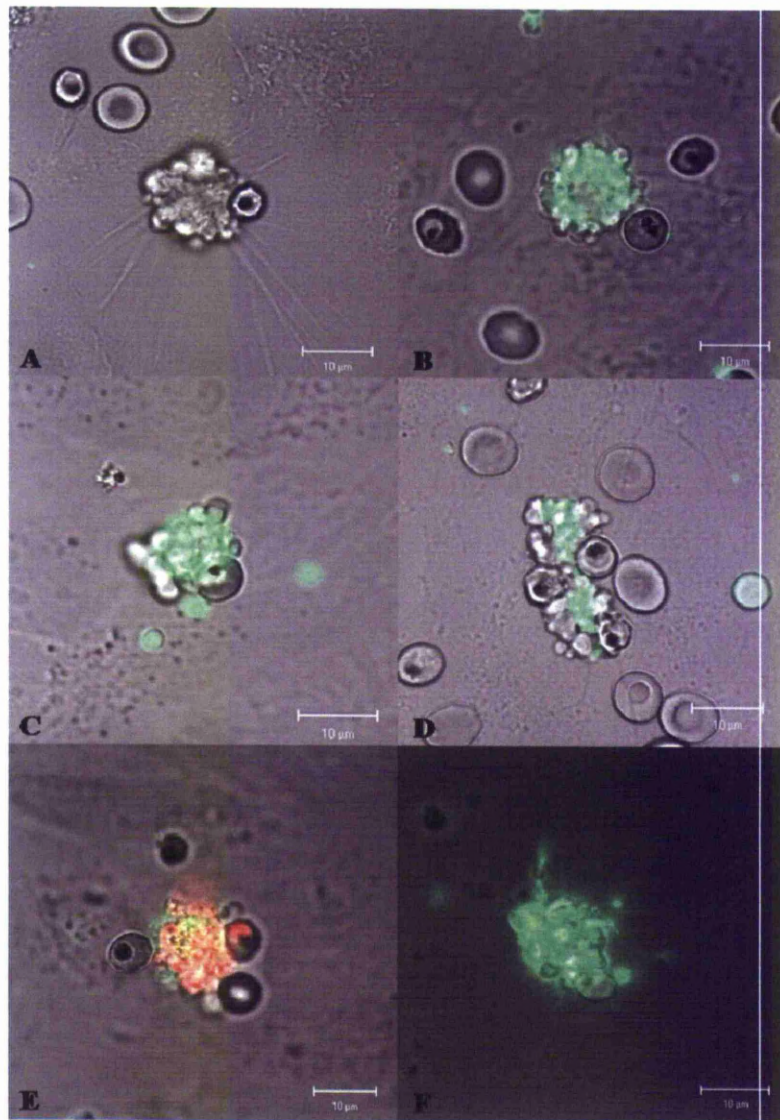


**Figure 3.4** Confocal images of various morphological changes of HUVEC after incubation with PRBC (A-E) or camptothecin (F). (A) Cell membrane blebbing alone of HUVEC attached to PRBC; (B) Blebbing and annexin V positive HUVEC with attached PRBC; (C) Blebbing, annexin V positive and microparticles stained with annexin V of HUVEC attached to PRBC; (D) Blebbing and annexin V positive of HUVEC with multiple binding of PRBC; (E) Necrotic HUVEC showing blebbing, annexin V and propidium iodide positive; (F) Blebbing and annexin V positive of HUVEC treated with camptothecin.



### 3.3.3 The role of ligand binding preference and PRBC induced HUVEC apoptosis

In this experiment, two parasite strains were used to co-incubate with HUVEC, namely ITG and C24. As stated previously, C24 malaria parasites are known to bind to CD36 receptors whilst ITG parasites are known binders of ICAM-1. The C24 parasite line was shown to have reduced binding to HUVEC compared to ITG parasites (C24 binding was measured at  $0.59\% \pm 0.13$  (SE) compared to  $3.59\% \pm 0.64$  for ITG, Fig 3.5). However interestingly, when comparing the percentage of bound cells that became apoptotic, there was no statistically significant difference between the two parasite lines (Fig 3.6).

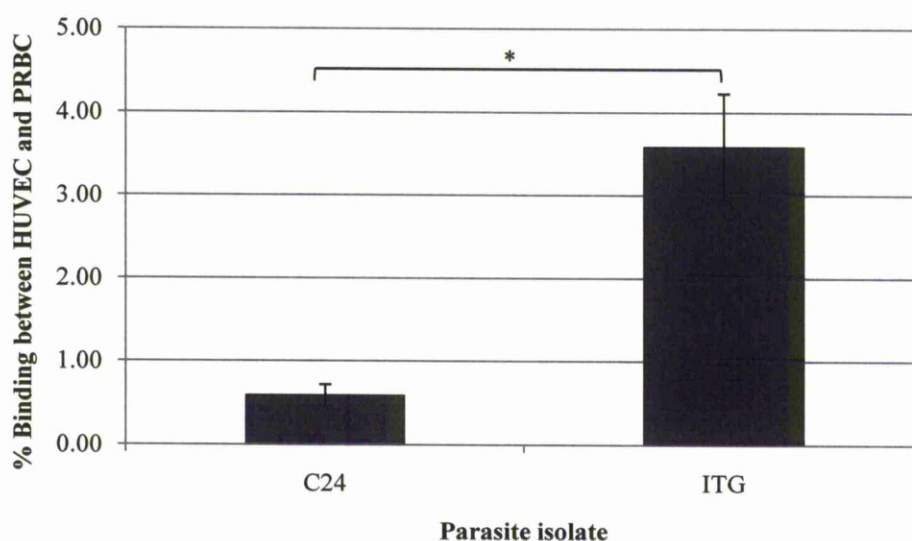


**Figure 3.5<sup>a</sup>** Comparison of HUVEC binding between ITG and C24 parasite lines. Data are mean  $\pm$  SE of at least five experiments. \* denotes statistically significant difference ( $p < 0.05$ ).

<sup>a</sup> In collaboration with Dr. Parnpen Viriyavejakul

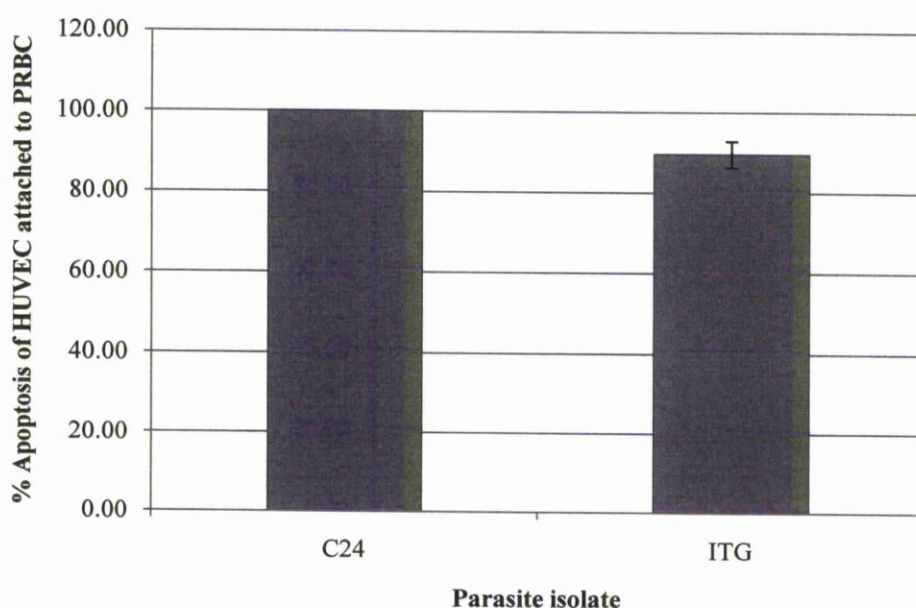


**Figure 3.6<sup>a</sup>** Apoptosis of HUVEC induced by two parasites isolates (C24 and ITG). Data are mean  $\pm$  SE of at least five experiments.

### 3.3.4 Establishing the role of parasite viability and PRBC induced HUVEC apoptosis

The aim of this experiment was to investigate the role of parasite viability on malaria parasite-induced apoptosis of HUVEC. Two procedures, i.e. heat-killing and artesunate-killing were used to kill parasites. The viability and appearance of the parasites were compared with the control/untreated parasites.

In the control group, almost all parasites were localised within RBC, whereas many of parasites killed by heat and artesunate appeared as ghost red cells and many appeared as free parasites. Table 3.1 summarises parasite viability and localisation of the

<sup>a</sup> In collaboration with Dr. Parnpen Viriyavejakul

parasites from control, heat-killed and artesunate-killed groups. Cell viability of malaria parasites in control group (live parasites) was  $93.92\% \pm 1.14$  (SE). In heat-killed and artesunate-killed malaria parasites, cell viability of parasites was  $0.62\% \pm 0.36$  (SE) and  $0.87\% \pm 0.27$  (SE), respectively (Fig 3.7). Unsuprisingly, there was a statistically significant difference in parasite viability between control group and both modes of parasite killing ( $p < 0.05$ ).

To confirm that parasites died after treatment with either heat or artesunate, both heat-killed and artesunate-killed malaria parasites were kept in continuous culture for four weeks. However, parasites in both groups failed to grown in culture.

	Cell viability (%) $\pm$ SE	In RBC (%) $\pm$ SE	In ghost (%) $\pm$ SE	Free parasite (%) $\pm$ SE
Control	93.92 $\pm$ 1.14	97.15 $\pm$ 0.38	0.00 $\pm$ 0.00	2.85 $\pm$ 0.38
Heat-killed	0.62 $\pm$ 0.36	10.97 $\pm$ 2.05	31.28 $\pm$ 5.82	57.75 $\pm$ 6.87
Artesunate-killed	0.87 $\pm$ 0.27	51.48 $\pm$ 3.82	30.10 $\pm$ 3.10	18.41 $\pm$ 2.00

**Table 3.1<sup>a</sup>** Comparison of cell viability and localisation of parasite in control, heat-killed and artesunate-killed malaria parasites. Data are mean  $\pm$  SE of four experiments.

---

<sup>a</sup> In collaboration with Dr. Parnpen Viriyavejakul



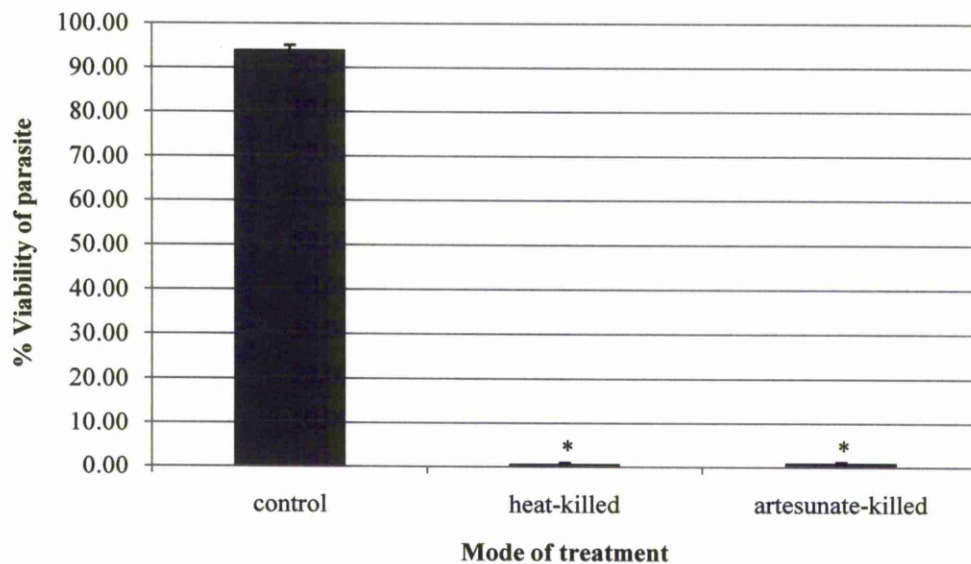


**Figure 3.7<sup>a</sup>** Cell viability of control, heat-killed and artesunate-killed malaria parasites. Data are mean  $\pm$  SE of four experiments. \* denotes statistically significant difference when compare to control ( $p < 0.05$ ).

### 3.3.5 The HUVEC binding potential of heat-killed and artesunate-killed malaria parasites

The mean percent of control parasites (viable parasites), heat-killed parasites and artesunate-killed parasites bound to HUVEC were  $4.57\% \pm 0.85$  (SE),  $0.44\% \pm 0.06$  (SE) and  $3.76\% \pm 0.50$  (SE), respectively (Fig 3.8). However, the percentage of bound cells that became apoptotic was similar for all treatments, irrespective of viability (Fig 3.9).

<sup>a</sup> In collaboration with Dr. Parnpen Viriyavejakul

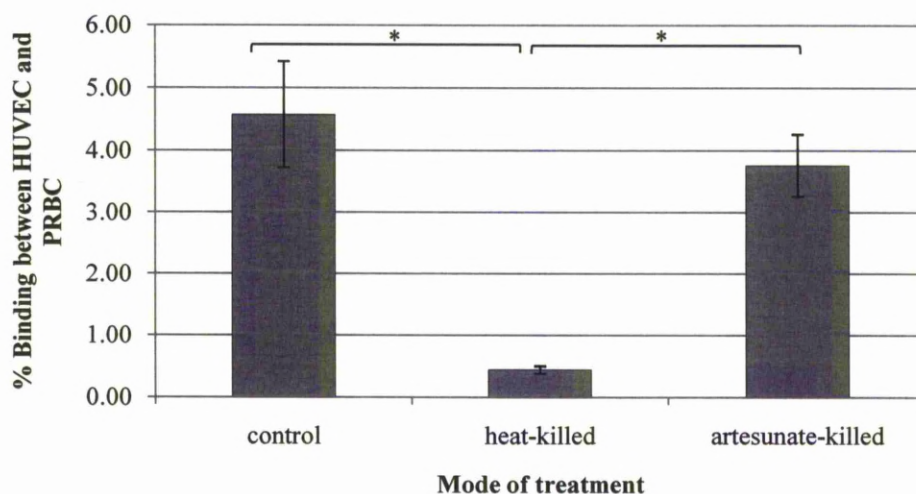


**Figure 3.8<sup>a</sup>** Cytoadherence of control parasites (viable parasites), heat-killed parasites and artesunate-killed parasites to HUVEC. Data are mean  $\pm$  SE of at least five experiments. \* denotes statistically significant difference ( $p < 0.05$ ).

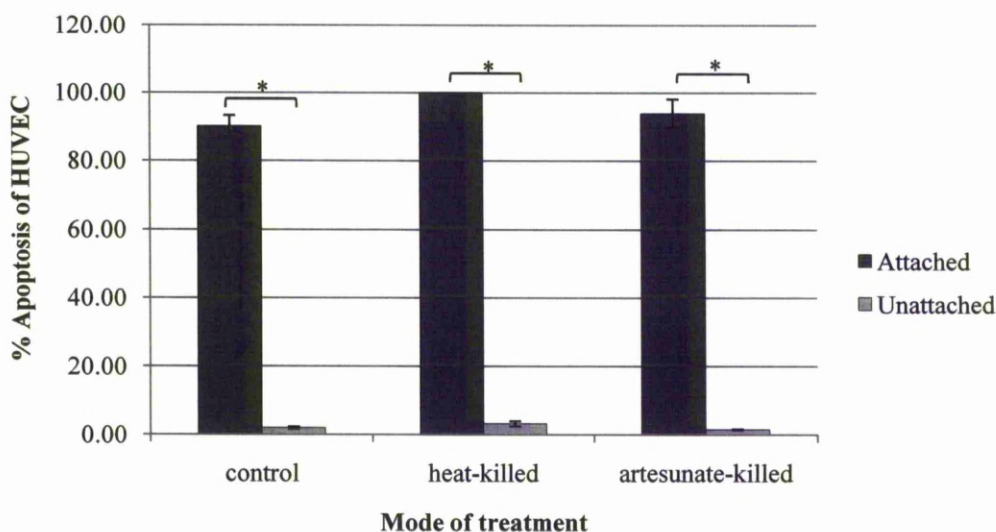


**Figure 3.9<sup>a</sup>** Apoptosis of HUVEC attached and unattached to control parasites, heat-killed parasites and artesunate-killed parasites. Data are mean  $\pm$  SE of at least five experiments. \* denotes statistically significant difference ( $p < 0.05$ ).

<sup>a</sup> In collaboration with Dr. Parnpen Viriyavejakul

### **3.3.6 Blockage of PRBC-induced apoptosis of HUVEC with pan-caspase inhibitor Z-VAD-FMK, caspase-8 inhibitor Z-IETD-FMK and caspase-9 inhibitor Z-LEHD-FMK.**

There was no noticeable effect on morphology of HUVEC after addition of 20  $\mu$ M pan-caspase inhibitor, 100  $\mu$ M caspase-8 inhibitor or 100  $\mu$ M caspase-9 inhibitor to the co-culture. In addition, Z-VAD-FMK, Z-IETD-FMK or Z-LEHD-FMK had no effect on the binding ability of PRBC to HUVEC (Fig. 3.10). The mean percentage of PRBC binding to HUVEC for control group of Z-VAD-FMK was  $6.31\% \pm 0.67$  (SE) versus  $5.55\% \pm 0.71$  (SE) in Z-VAD-FMK treated group. The mean percentage of PRBC binding to HUVEC for control group of Z-IETD-FMK was  $5.74\% \pm 0.34$  (SE) versus  $6.09\% \pm 0.33$  (SE) in Z-IETD-FMK treated group. The mean percentage of PRBC binding to HUVEC of Z-LEHD-FMK treated group was  $5.59\% \pm 0.55$  (SE) versus  $5.23\% \pm 0.39$  (SE) in control group.

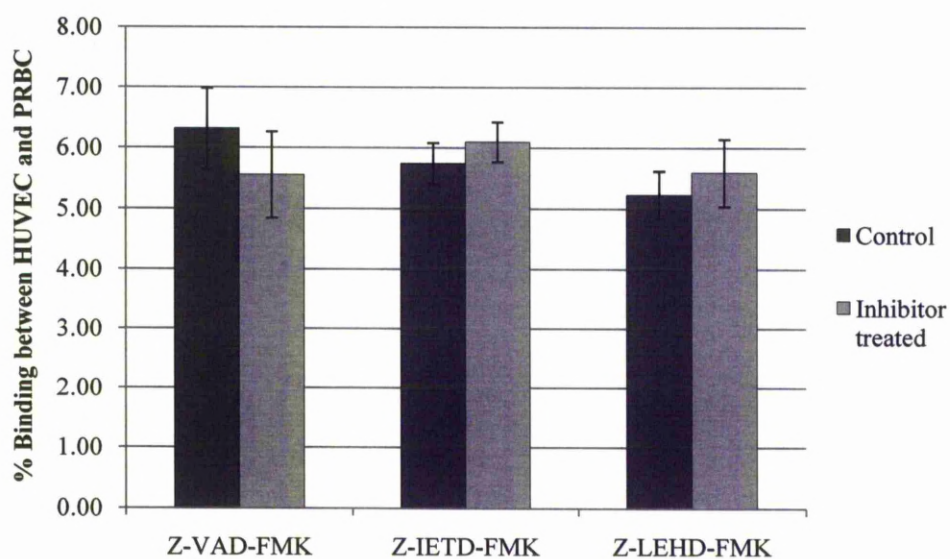


**Figure 3.10** Comparison amount of binding between PRBC and HUVEC in control group and caspase inhibitors treated groups. Data are mean  $\pm$  SE of at least three experiments.

However, the ability of attached PRBC to induced apoptosis of HUVEC was significantly decreased in the presence of pan-caspase inhibitors, caspase-8 inhibitor or caspase-9 inhibitor (Fig 3.11).

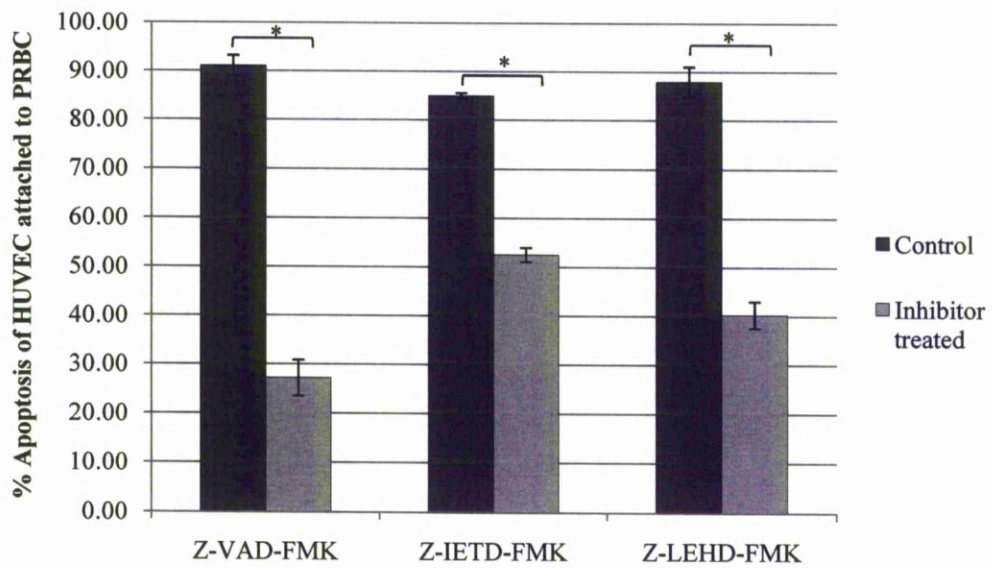


**Figure 3.11** Effect of caspase inhibitors on PRBC-induced HUVEC apoptosis. Data are mean  $\pm$  SE of at least three experiments. \* denotes statistically significant difference ( $p < 0.05$ ).

The absence of annexin V staining and membrane blebbing in inhibitor-treated groups compared to control groups is clearly demonstrated in Fig 3.12.



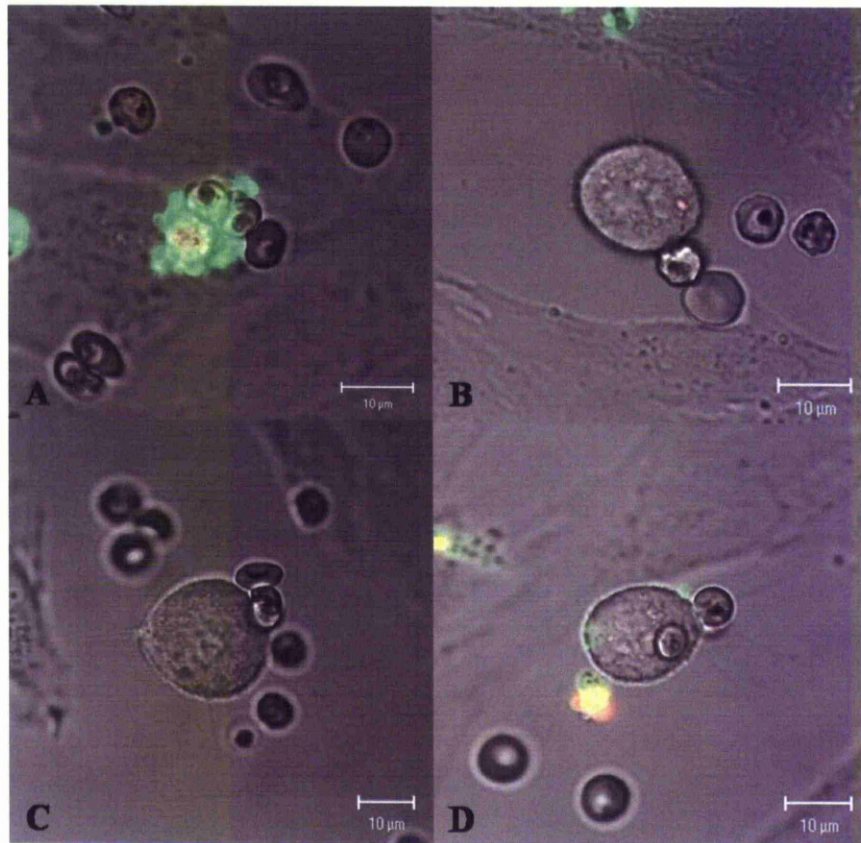


**Figure 3.12** Cytoadherence of PRBC to HUVEC in control group and in the presence of caspase inhibitors. (A) Apoptotic HUVEC attached to PRBC shows cell membrane blebbing and annexin V positive; (B) HUVEC attached to PRBC in the presence of pan-caspase inhibitor (Z-VAD-FMK); (C) HUVEC attached to PRBC in the presence of caspase-8 inhibitor (Z-IETD-FMK); (D) HUVEC attached to PRBC in the presence of caspase-9 inhibitor (Z-LEHD-FMK).

### 3.3.7 Caspase-8 and caspase-9 activities in PRBC-induced HUVEC

The activities of caspase-8 and caspase-9 in HUVEC treated with camptothecin (an inducer of apoptosis) or following co-culture with PRBC or RBC, compared to control (untreated) groups are given in Fig 3.13 and Fig 3.14, respectively. The mean  $\pm$  SE of

caspase-8 and caspase-9 activities are illustrated in Table 3.2. As expected, camptothecin treatment was shown to increase the level of both caspases compared to untreated HUVEC. Co-incubation of RBC did not significantly increase the activities of caspases in HUVEC compared to control groups, but interestingly, co-incubation with PRBC significantly increased the levels of caspase activities compared to control groups to levels even higher than the positive control camptothecin.

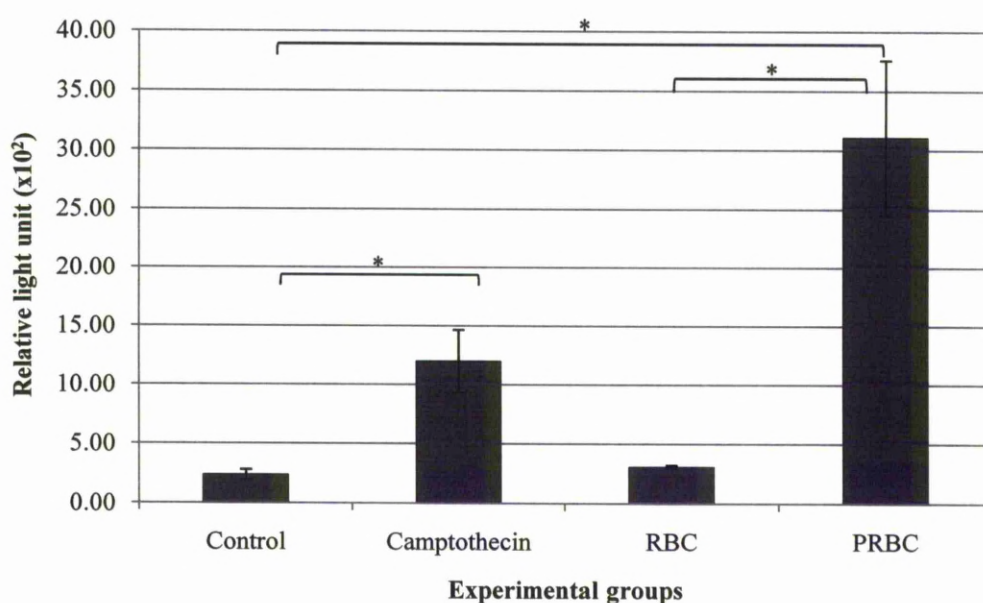


**Figure 3.13<sup>a</sup>** Caspase-8 activity in HUVEC. Data are mean luminescence  $\pm$  SE of at least three experiments. \* denotes statistically significant difference ( $p < 0.05$ ).

<sup>a</sup> In collaboration with Dr. Parnpen Viriyavejakul

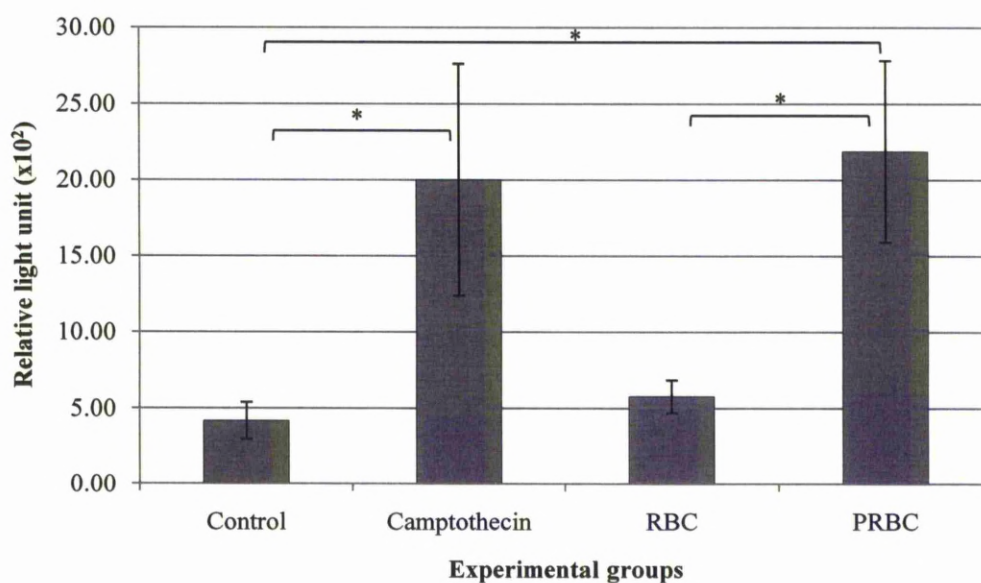


**Figure 3.14<sup>a</sup>** Caspase-9 activity in HUVEC. Data are mean luminescence  $\pm$  SE of at least three experiments. \* denotes statistically significant difference ( $p < 0.05$ ).

	Caspase-8 activity Mean luminescence $\pm$ SE	Caspase-9 activity Mean luminescence $\pm$ SE
<b>Control</b>	$2.37 \times 10^2 \pm 0.44$	$4.18 \times 10^2 \pm 1.22$
<b>Camptothecin</b>	$11.98 \times 10^2 \pm 2.67$	$19.99 \times 10^2 \pm 7.62$
<b>RBC</b>	$3.08 \times 10^2 \pm 0.14$	$5.78 \times 10^2 \pm 1.07$
<b>PRBC</b>	$31.07 \times 10^2 \pm 6.52$	$21.86 \times 10^2 \pm 5.97$

**Table 3.2** Caspase-8 and Caspase-9 activities. Values are expressed as mean luminescence  $\pm$  SE of at least three experiments.

<sup>a</sup> In collaboration with Dr. Parnpen Viriyavejakul



### 3.4 DISCUSSION

Recently, the adhesion of PRBC to endothelial cells has been reported to induce a deleterious effect on endothelial cells, i.e. apoptosis of endothelial cells (Pino *et al.*, 2005). A physical interaction between endothelial cell and PRBC was necessary to induce apoptosis in endothelial cells. This was demonstrated by co-culture of endothelial cells either with poorly adherent parasite clone or with adherent parasite clone in transwell culture plate which provide a porous membrane to allow co-culture of different cell type without physical contact between the cells. Under non-contact or poorly adherent parasites co-culture conditions, there was no induction of apoptosis of endothelial cells (Pino et al., 2003b). We have taken these observations further. Here, our study confirms that the direct binding of PRBC to HUVEC induces apoptosis of HUVEC. HUVEC with attached PRBC showed alterations in their morphology leading to apoptosis. These alterations were not observed in HUVEC co-culture with RBC (Fig 3.2 A). The morphological changes include cell membrane shrinkage, blebbing and/or annexin V staining positive and generating of endothelial microparticles (EMPs) (Fig 3.4 (A-D)).

In contrast to earlier studies, we used the single cell approach to study this phenomenon which is useful in providing a detailed understanding of the cellular events that follow binding of PRBC to HUVEC in co-culture without the complication and contribution to the noise of the HUVEC without bound PRBC. Importantly, our HUVEC were not stimulated with TNF- $\alpha$  as in other studies. In addition, we demonstrate a quantitative correlation between PRBC-HUVEC binding and apoptosis i.e. all HUVEC ( $\geq 90\%$ ) with bound PRBC underwent apoptosis in this *in vitro* model.

To investigate whether apoptosis of HUVEC requires the binding of PRBC to a specific receptor or whether it is just a general effect of PRBC binding to endothelial cells, we used two different parasite isolates, ITG and C24, which have specific binding affinity for different endothelial cell receptors, i.e. ITG has binding preference to ICAM-1 whereas C24 tends to bind more to CD36 (Gray *et al.*, 2003). Although HUVEC (CD36<sup>-</sup>) does not support the binding of C24 parasites to CD36 (Gray *et al.*, 2003), we found that both parasite strains can induce apoptosis in HUVEC to almost the same extent. Both ITG and C24 parasites are genetically identical but differ in their expression of *var* genes resulting in different binding phenotypes (Jenkins *et al.*, 2007). However, switching to alternative *var* genes, which results in expression of distinct PfEMP-1, can occur at a rate up to 2% per generation (Roberts *et al.*, 1992). This means that a subset of C24 and ITG parasite populations used in the co-culture will express PfEMP-1s which are distinct from the original clones and from this pool probably comes PfEMP-1 responsible for binding and inducing apoptosis in HUVEC. This may explain why both parasite isolates can induce HUVEC apoptosis, even though they have nominally different binding preferences.

We assessed the ability of non-viable parasites killed by heat and artesunate to adhere and induce apoptosis of HUVEC. Our data indicated that dead parasites can still bind to HUVEC and induce apoptosis. This observation is consistent with an ultrastructural analysis of brains from patients with cerebral malaria which found that morphologically damaged parasites bound to brain endothelial cells (Pongponratn *et al.*, 2003). There was a difference in the extent of binding resulting from the two procedures with artesunate-killed parasites retaining a greater ability to bind to HUVEC than heat-killed parasites. This may be readily explained by looking at the

morphology of the parasites. Parasites killed by artesunate appeared morphologically unaffected compared to heat-killed parasites (Table 3.1). This finding is in agreement with the recent report showing that artesunate-killed malaria parasites retained the ability to cytoadhere even after 24 h of drug treatment. This is due to the continued and undisrupted presence of PfEMP-1 on the surface of PRBC after loss of parasite viability (Hughes *et al.*, 2010). We concluded that induction of HUVEC apoptosis is not dependent on the viability of parasites and consequent active cell-cell signalling but is dependent only on the host red cell membrane, and presumable PfEMP-1 being intact.

Apoptosis is the tightly regulated form of physiological cell death in which the terminal stage involves activation of a family of proteases, the caspases (Hengartner, 2000). To further establish the role of a caspase-dependent apoptotic pathway, we used the pan-caspase inhibitor (Z-VAD-FMK) to inhibit apoptosis of HUVEC attached to PRBC. The pan-caspase inhibitor had no effect on binding of PRBC to HUVEC but significantly reduce apoptosis of HUVEC. To sort out the cellular pathways involved, we used specific caspase-8 and caspase-9 inhibitors and measured caspase-8 and -9 activities. The results indicated that both death receptor pathways mediated through caspase-8 and the mitochondrial pathway mediated through caspase-9 involve in the apoptosis of HUVEC.

In conclusion, the results in this chapter demonstrate that PRBC adhesion to HUVEC induce caspase-8 and caspase-9 dependent apoptosis in HUVEC. This apoptogenic effect of PRBC on endothelial cell might be one of the factors leading to the BBB dysfunction and lesion in CM. Apoptosis of HUVEC as a consequence of PRBC adhesion also leads to generation of endothelial microparticles (apoptotic bodies)

which are the sub-micron elements produced after membrane remodelling during physiological or pathogenic processes such as apoptosis (Combes *et al.*, 2006). This is consistent with the study conducted in Malawian children which found dramatically higher level of EMPs in plasma of children with acute phase CM than in plasma of children with severe malarial anaemia, uncomplicated malaria or healthy control condition (Combes *et al.*, 2004). Our study also shows that the binding of PRBC to HUVEC is dependent on the host red cell membrane being intact but independent of viability of the parasites.

# **CHAPTER 4: MEASURING THE EFFECT OF MALARIA PARASITE BINDING ON THE MITOCHONDRIAL MEMBRANE POTENTIAL OF HUMAN ENDOTHELIAL CELLS**

---

## **4.1 INTRODUCTION**

In living cells, mitochondria are the site of energy production. This energy production is driven by the electrochemical gradient consisting of a proton gradient and a transmembrane electrical potential ( $\Delta\Psi$ ) built across the inner mitochondrial membrane (Cooper, 2007). In many apoptotic models, the dissipation of the mitochondrial inner membrane potential ( $\Delta\Psi_m$ ) is one of the early events in the mitochondrial apoptotic pathway (intrinsic pathway). This is a result of opening of the mitochondrial permeability transition pore (PTP), a multiprotein complex consisting of both inner and outer membrane proteins, which is presented at the contact sites between the outer and the inner membranes (Antonsson, 2004). The opening of this pore also leads to the release of caspase-activating proteins such as cytochrome *c* and apoptosis-inducing factor (AIF) which locate within the intermembrane space into the cytosol and induce apoptosis (Green & Kroemer, 2004).

The loss of mitochondrial membrane potential can be detected by a unique cationic dye, 5,5',6,6'-tetrachloro-1,1',3,3'-tetraethylbenzimidazolycarbocyanine iodide, commonly known as JC-1. JC-1 is a lipophilic cationic dye that displays potential-dependent accumulation in mitochondria (Cossarizza *et al.*, 1993). This dye can selectively enter into mitochondria and reversibly change colour from green to red as the membrane potential increases. In healthy cells with high mitochondrial membrane potential (180 - 220 mV, negative inside), the dye forms a complex called J-aggregates

with a fluorescence emission in the red region. In contrast, in apoptotic cells with low mitochondrial membrane potential, the dye remains in a monomeric form characterised by emission fluorescence in the green region (Cossarizza *et al.*, 1993). Thus, apoptotic cells showing primarily green fluorescence are easily differentiated from healthy cells.

The data in chapter 3 indicated that apoptosis of HUVEC attached to PRBC involves the mitochondrial apoptotic pathway, as demonstrated by the increased activity of caspase 9 in HUVEC attached to PRBC and decreased numbers of apoptotic HUVEC attached to PRBC when treated with a caspase-9 inhibitor. As described in Chapter 1, apoptosis signalling can involve intrinsic or extrinsic pathways (section 1.2.1 in Chapter 1). In intrinsic pathways, the mitochondrion plays a critical part in signal transduction. In this chapter, the involvement of HUVEC mitochondria in PRBC cytoadherence-induced apoptosis was studied to define the apoptotic pathway in greater detail.

## **4.2 MATERIALS AND METHODS**

### **4.2.1 Preparation of HUVEC for co-culturing**

HUVEC used in the experiments were from passage 4-6. HUVEC were cultured as described in Chapter 2 section 2.2. When HUVEC reached to 80-90% confluence, cells were trypsinised and seeded on 40 mm diameter gelatin coated coverslips (Bioptechs) placed in petri dishes (Nunc). The seeding density was 15,000-20,000 cells/cm<sup>2</sup>. Approximately 500 µl of cell suspension was gently loaded onto the coated coverslips. Cells were allowed to settle for 1 h at 37 °C, 5% CO<sub>2</sub> in a humidified incubator. The medium was then removed and 2 ml of pre-warmed fresh medium was added. Cells were then further cultured until they reached 80-90% confluence.

### **4.2.2 Preparation of malaria parasites for co-culturing**

*P. falciparum* strain ITG was cultured as described in Chapter 2 section 2.1. Parasites were cultured until they reached 5-8% parasitemia (trophozoite or schizont stages). Parasites were then submitted to a magnetic separation technique in order to obtain 80-90% parasitemia. Briefly, the parasite suspension was spun down at 2000 rpm for 5 min. The parasite pellet was re-suspended in 10 ml of binding solution (1X PBS containing 2% BSA (Sigma) and 20 mM glucose (Sigma)). The CS column was placed on a VarioMACS magnet (Miltenyi Biotec) and pre-washed once with binding solution. The column was not allowed to dry at any time during the procedure. The parasite suspension was applied to the top of the column and the column was washed with binding solution until the flow through was clear. The column was removed from the magnet and the concentrated parasites were eluted by adding 10 ml of binding

solution to the top of the column. The eluent was centrifuged at 2000 rpm for 5 min. The pellet was washed three times with parasite culture media.

#### **4.2.3 Co-culture of HUVEC with malaria parasites**

The concentrated parasites were re-suspended in 1% FCS in medium 199 to a parasitemia of 50% in 1% haematocrit. Endothelial medium was removed from HUVEC grown on coverslips at 80-90% confluence and the cells were gently washed once with 1X PBS. Two ml of parasite suspension was then added to the HUVEC monolayer and co-cultured for 3, 8, 18 or 24 h at 37 °C, 5% CO<sub>2</sub> in a humidified incubator. The co-culture dishes were agitated either clockwise or counter clockwise every 10-15 min to allow more cell-to-cell contact until the third hour.

#### **4.2.4 Measurement of endothelial cell mitochondrial membrane potential ( $\Delta\Psi_m$ ) by confocal laser scanning microscope**

After co-incubation, co-culture media were discarded. HUVEC were washed twice with 1X PBS to wash out unbound PRBC and RBC. HUVEC were stained with the cationic dye 5,5',6,6'-tetrachloro-1,1',3,3'-tetraethylbenzimidazolycarbocyanine iodide (JC-1) (Molecular Probes). The dye was prepared in medium 199 plus 1% FCS at a concentration of 5  $\mu$ M. HUVEC were left in the probe solution for 15 min at 37 °C, 5% CO<sub>2</sub> in humidified incubator. The coverslips were then gently washed once with 1X PBS. The coverslips were assembled into a Bioptechs FCS2 perfusion chamber, perfused with medium 199 plus 1% FCS and observed with a Zeiss Pascal confocal laser scanning microscope (CLSM). Cells were viewed through a Plan-Apochromat 63x 1.2 numerical aperture water objective. Fluorescence signals from JC-1 were collected by excitation with argon ions and HeNe laser at 488 and 543 nm and



collection of emitted light through a 505-530 nm band pass filter and a 560 nm long pass filter, respectively. For positive control, the protonophore carbonyl cyanide p-(trifluoromethoxy) phenylhydrazone (FCCP) at a concentration of 10  $\mu$ M was perfused in to the chamber. At least 500 endothelial cells were counted for each replicate and scored according to the appearance of cells, i.e. attached or unattached with PRBC and the red/green fluorescence of cells.

#### **4.2.5 Statistical analysis**

Results were expressed as mean  $\pm$  standard error of individual experimental groups. Statistical analysis was performed with GrapPad InStat version 3.05. Data were analysed by One-way ANOVA with Tukey-Kramer Multiple Comparisons post test. A value of  $p < 0.05$  was considered significant.

## 4.3 RESULTS

### 4.3.1 Binding of PRBC to HUVEC

Apart from observing the mitochondrial membrane potential of HUVEC attached to PRBC, the number of HUVEC adhered to PRBC were also recorded at each co-incubation time point. The mean percentage of HUVEC attached to PRBC were  $4.79\% \pm 0.16$  (SE),  $3.99\% \pm 0.22$  (SE),  $4.29\% \pm 0.34$  (SE) and  $3.83\% \pm 0.28$  (SE) at 3, 8, 18 and 24 h of co-incubation, respectively. There was no statistically significant difference in number of HUVEC attached to PRBC between each time point (Fig 4.1).

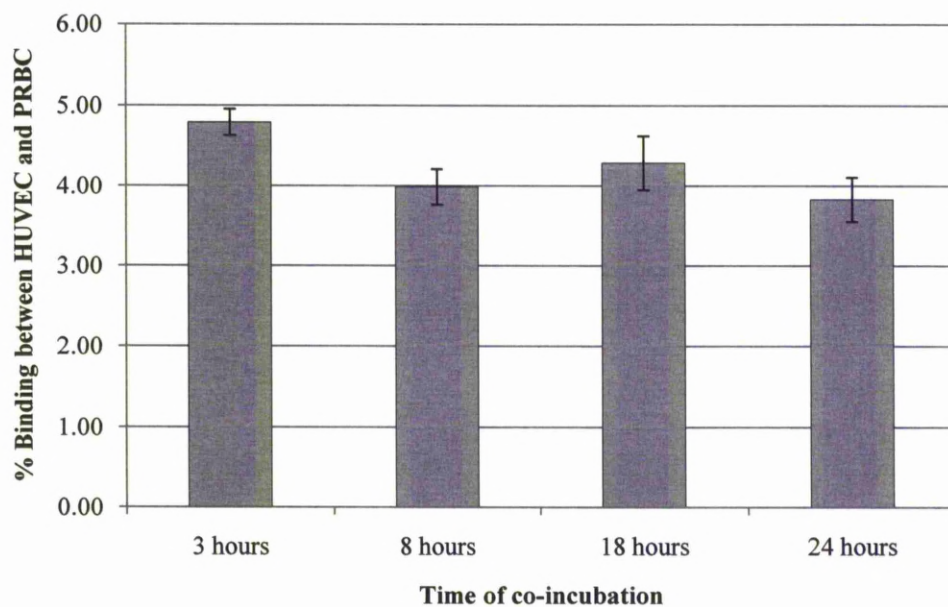


**Figure 4.1** Comparison amount of binding of PRBC to HUVEC at different co-incubation time points. Data are mean  $\pm$  SE of at least five experiments.

### **4.3.2 Mitochondrial membrane potential of HUVEC attached to PRBC**

The dissipation of mitochondrial membrane potential of HUVEC attached to PRBC was detected by staining cells with the mitochondrial-targeted dye, JC-1. Mitochondria of control cells (normal HUVEC) showed either red or green fluorescence. The proportions of green and red mitochondria were not evenly distributed in cells. Instead, the red-fluorescing, highly energized mitochondria were proportionally more prevalent in the periphery of cells (Fig 4.2, panel A). Depolarisation of the mitochondrial membrane potential with the H<sup>+</sup>-uncoupler FCCP resulted in a uniform green fluorescence emission from mitochondria (Fig. 4.2, panel B). Mitochondria of HUVEC with attached PRBC revealed a depolarisation as indicated by the green fluorescence emission (Fig 4.2, Panel C-L).

Cells with green fluorescence, indicating the loss of mitochondrial membrane potential, were counted at each co-incubation time point. The degree of unattached HUVEC which lost their mitochondrial  $\Delta\Psi$  were  $0.45\% \pm 0.09$  (SE),  $0.52\% \pm 0.17$  (SE),  $0.40\% \pm 0.12$  (SE),  $1.19\% \pm 0.31$  (SE) and  $1.64\% \pm 0.22$  (SE) at 0, 3, 8, 18 and 24 h of co-incubation, respectively (Fig 4.3). The percentage of HUVEC with attached PRBC that lost their mitochondrial  $\Delta\Psi$  were  $0.00\% \pm 0.00$  (SE),  $21.71\% \pm 3.64$  (SE),  $56.70\% \pm 1.68$  (SE),  $58.35\% \pm 0.86$  (SE) and  $70.94\% \pm 3.87$  (SE) at 0, 3, 8, 18 and 24 hours of co-incubation, respectively (Fig 4.3). This indicates that the mitochondria are affected by binding of PRBC to HUVEC and confirmed the involvement of a mitochondrial apoptotic pathway in apoptosis of HUVEC with attached PRBC.

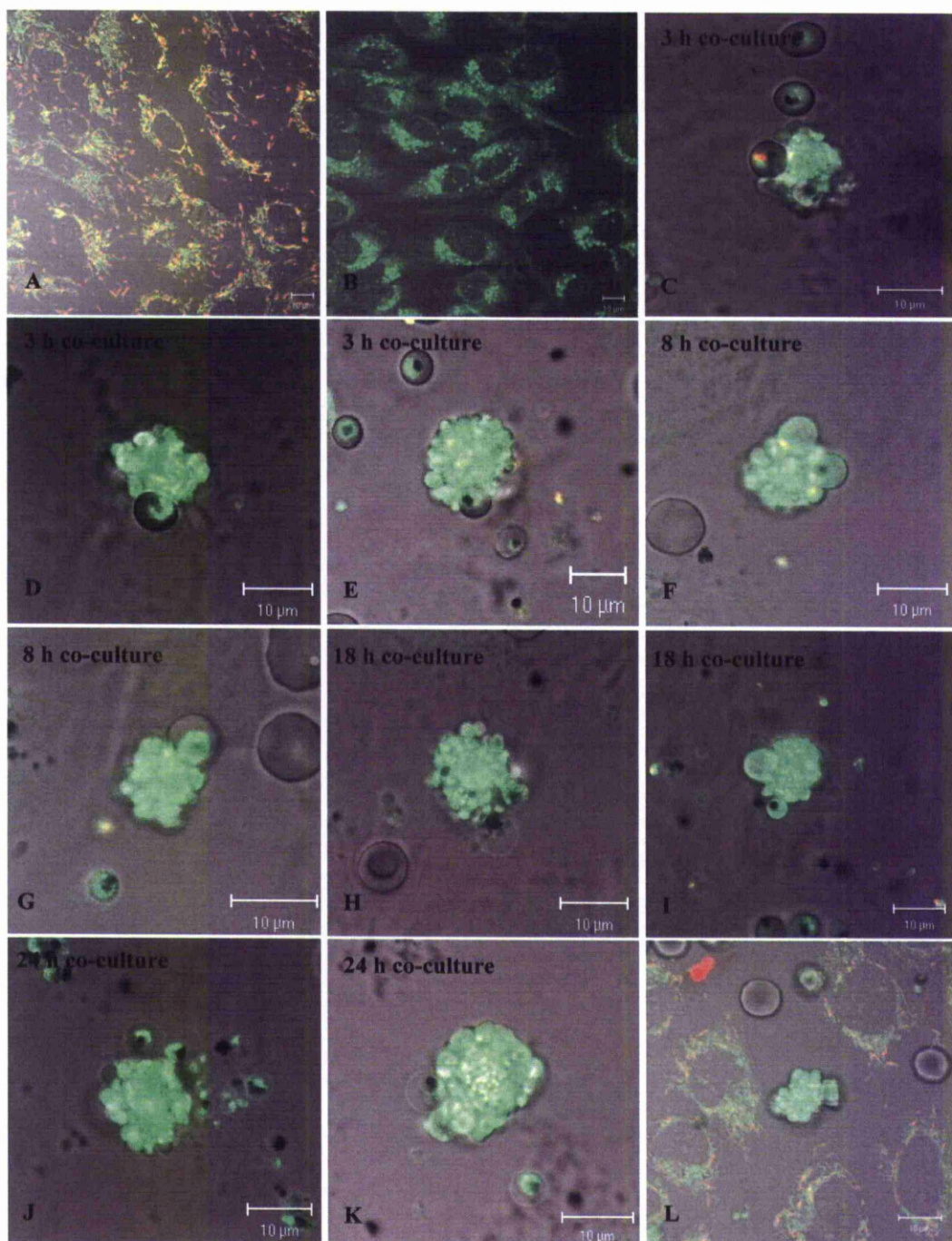


**Figure 4.2** Confocal images of HUVEC stained with JC-1 dye. (A) Healthy normal HUVEC showed both red and green fluorescence, (B) HUVEC treated with FCCP showed shift in fluorescence from red to green, (C-K) PRBC-adhered HUVEC at different time points showed green fluorescence together with membrane blebbing, (L)



Difference in fluorescence staining of PRBC-adhered HUVEC (green fluorescence) compared with surrounding unattached HUVEC (red and green fluorescence).

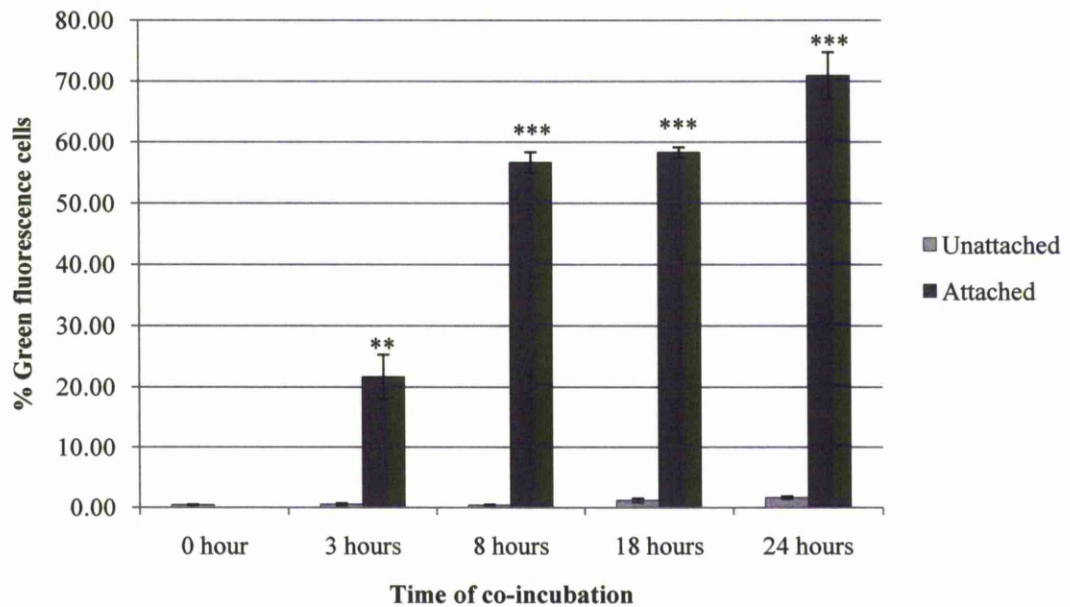


**Figure 4.3** Comparison the percentage green fluorescence cell of HUVEC with and without attached PRBC at different co-incubation time points. Data are mean  $\pm$  SE of at least five experiments. \* denotes statistically significant difference (\*\*  $p < 0.01$ , \*\*\*  $p < 0.001$ ) as analysed by one-way ANOVA with Tukey-Kramer Multiple Comparisons post test.

#### 4.4 DISCUSSION

Energy generated from the mitochondrial respiratory chain is stored as an electrochemical gradient consisting of a proton gradient and a transmembrane electrical potential ( $\Delta\Psi$ ) across the inner mitochondrial membrane (Cooper, 2007). The dissipation of this potential is often observed in apoptosis. Measurement of this event is made possible by the lipophilic cationic dye JC-1 which exists as green fluorescent monomer at low membrane potential and as orange/red fluorescent aggregates at high membrane potential.

By loading with JC-1, a study revealed a distinct heterogeneity of the mitochondrial  $\Delta\Psi$  inside HUVEC. The mitochondria did not show a homogeneous red or green JC-1 fluorescence. They were either green or red with more intensely red-fluorescing, highly energized mitochondria at the periphery of cells (Collins *et al.*, 2002). A similar pattern was observed in our control HUVEC, indicating that mitochondria were heterogeneous with respect to their energetic status. HUVEC showed uniform depolarisation of mitochondrial  $\Delta\Psi$  when treated with a potent mitochondrial uncoupler, FCCP, which can depolarise the mitochondrial membrane potential by dissipating the proton gradient across the inner mitochondrial membrane (Park *et al.*, 2002).

Multiple lines of research demonstrated that collapse of mitochondrial  $\Delta\Psi$  is the early, obligate event in the apoptotic signalling pathway. Apoptosis of rat embryo cells induced by the simian virus 40 large T antigen showed a lowered mitochondrial  $\Delta\Psi$  and a decrease in mitochondrial respiration, which are detectable early in the apoptotic process (Vayssiere *et al.*, 1994). Thymocytes induced to undergo apoptosis with

dexamethasone showed an early decrease in mitochondrial  $\Delta\Psi$  and also alteration in mitochondrial structure (Petit *et al.*, 1995). Loss of mitochondrial  $\Delta\Psi$  indicates the opening of a large channel known as the mitochondrial permeability transition pore (PTP) leading to release of apoptogenic factors into the cytosol such as cytochrome *c*. In the cytosol, cytochrome *c* can form complex with the apoptosis activating factor 1 (Apaf-1) and activate caspase-9 (Vermeulen *et al.*, 2005).

The data from the previous chapter suggested that the mitochondria are implicated in apoptosis of HUVEC induced by PRBC, as shown by activation of caspase-9. Thus the status of the mitochondrial  $\Delta\Psi$  in PRBC-adhered HUVEC was observed to confirm the involvement of mitochondrial pathway in apoptosis of HUVEC. We found that loss of mitochondrial  $\Delta\Psi$  in the apoptotic HUVEC occurred together with cell membrane blebbing. This is in agreement with published data illustrating that malaria parasites can reduce mitochondrial  $\Delta\Psi$  and lead to apoptosis of host cells (Guha *et al.*, 2006). Furthermore, the significant amount of PRBC-adhered HUVEC losing their mitochondrial  $\Delta\Psi$  could be detected immediately after 3 hours of co-culture indicating that the dissipation of mitochondrial  $\Delta\Psi$  is the early event occurring in apoptosis of PRBC-adhered HUVEC. Again, we observed a quantitative relationship between cytoadherence, the early collapse of the mitochondrial membrane potential and apoptosis.

Taken together, we assume that the adhesion of PRBC to HUVEC induces the opening of the mitochondrial transition pore. This leads to a decrease in the mitochondrial  $\Delta\Psi$  and release of apoptotic inducing factors from mitochondria such as cytochrome *c* which induces the activation of caspase-9.

## **CHAPTER 5: MALARIA PARASITE CYTOADHERENCE INDUCES OXIDATIVE STRESS IN HUMAN ENDOTHELIAL CELLS**

---

### **5.1 INTRODUCTION**

In aerobic organisms, reactive oxygen species (ROS), including  $O_2^-$ ,  $H_2O_2$ , hydroxyl radical ( $\cdot OH$ ), and nitric oxide/peroxynitrate ( $NO/ONOO^-$ ), are generated in cells through various endogenous and exogenous sources. These include the mitochondrial electron transport chain, biotransformation of various xenobiotics and drugs, inflammation, UV and ionic irradiation, and nitric oxide synthetase (Yang *et al.*, 2003). As ROS are toxic to the cell, mammalian cells have developed a number of antioxidant defence mechanisms to detoxify ROS. An imbalance between the pro-oxidant/antioxidant systems causes oxidative stress in the cells. Oxidative stress causes peroxidation of cell membrane lipids as well as damage to DNA or protein, culminating in cell death (Catala, 2009). During the process of lipid peroxidation, a great diversity of aldehydes such as malonaldehyde, alkaneals, and hydroxyalkenals are formed when polyunsaturated fatty acids (PUFAs) in biomembranes are degraded (Catala, 2006). The most prominent aldehydes generated during lipid peroxidation are 4-hydroxy-2-alkenals. The main representative of these aldehydes, 4-hydroxy-2-noneal (4-HNE), is the major product formed during lipid peroxidation of n-6 polyunsaturated fatty acid, such as linoleic acid and arachidonic acid. 4-HNE is considered to be a sensitive marker of oxidative damage and lipid peroxidation and can be detected by immunocytochemical staining (Catala, 2009).



The association of oxidative stress in malaria-induced apoptosis of host cells has been proposed (Pino *et al.*, 2005). The oxidative stress developed during malarial infection induced liver apoptosis in mice through activation of the mitochondrial pathway. Apoptosis in the liver of infected animals was prevented by administration of hydroxyl radical scavengers and free radical scavengers such as melatonin to the infected animals (Guha *et al.*, 2006, Guha *et al.*, 2007). A study by Pino and co-workers proposed that apoptosis in human endothelial cells co-cultured with malaria parasites was mediated through an oxidative stress pathway. In this study, it was demonstrated that inhibition of nitric oxide (NO), which in turn reduces peroxynitrite (ONOO<sup>-</sup>) synthesis, and addition of the superoxide dismutase mimetic protected the endothelial cells from malaria parasite-induced apoptosis (Pino *et al.*, 2003a). However, there was no direct evidence of ROS generation in this study.

During the maturation from ring stage to trophozoite stage, malaria parasites digest up to 75% of erythrocyte haemoglobin and polymerize the undigested heme moiety to hemozoin (Schwarzer *et al.*, 2003). Hemozoin is a likely generator of oxidative stress because it contains redox active iron which can peroxidise PUFAs present in membranes (Schwarzer *et al.*, 2003, Skorokhod *et al.*, 2010). It has been found that the membrane lipoperoxides and 4-HNE significantly increased in isolated hemozoin-fed human monocytes (Schwarzer *et al.*, 1996). In PRBC, the onset of hemozoin formation in the parasites was accompanied by the appearance of 4-HNE on the cell surface which decreased the deformability of the erythrocytes (Skorokhod *et al.*, 2007). Furthermore, the oxidative stress generated by hemozoin has been reported to play a role in apoptosis of erythroid precursors (Lamikanra *et al.*, 2009).

In chapter 3, it was shown that HUVEC with attached malaria parasites have the propensity to undergo apoptosis. Previously published data (Lamikanra et al., 2009, Pino et al., 2003a) have referred to the importance of oxidative stress in apoptosis induced by malaria parasites and malarial pigment. In this chapter, we have performed an immunocytochemical study using anti-4HNE antibodies to reveal the spatio-temporal manifestation of the apoptosis-associated cellular oxidative stress in PRBC-adhered HUVEC.

## **5.2 MATERIALS AND METHODS**

### **5.2.1 Preparation of HUVEC for co-culturing**

HUVEC used in the experiments were from passage 4-6. HUVEC culture methodologies have been described in detail in Chapter 2 section 2.2. When HUVEC reached to 80-90% confluence, cells were trypsinised and seeded on the gelatin coated 13 mm round sterile coverslip (Nunc) which were placed in the 24 multiwell plate (Nunc). Cells were seeded at a density of 40,000 cells/well. After seeded, cells were allowed to settle for 1 h at 37 °C, 5% CO<sub>2</sub> in a humidified incubator. The medium was then removed and 500 µl of pre-warmed fresh medium was added. Cells were then allowed to grow until reach about 90% confluence before used in the experiments.

### **5.2.2 Preparation of malaria parasites for co-culturing**

Malaria parasite used in this experiment was the ITG parasites selected to have potential to bind and induce apoptosis of HUVEC as describe in detail in Chapter 7. Parasites were cultured, as described in Chapter 2 section 2.1, until they reached 5-8% parasitemia (trophozoite or schizont stages). Then, parasites were submitted to magnetic separation technique in order to get 80-90% parasitemia. The parasite suspension was spun down at 2000 rpm for 5 min. The parasite pellet was re-suspended in 10 ml of binding solution (1X PBS containing 2% BSA (Sigma) and 20 mM glucose (Sigma)). The CS column was placed on a VarioMACS magnet (Miltenyi Biotec) and pre-washed once with binding solution. The column was not allowed to dry at any time during the procedure. The parasite suspension was applied to the top of the column and the column was washed with binding solution until the flow through was totally clear. The column was removed from the magnet and the effluent

containing concentrated parasites was eluted by adding 10 ml of binding solution to the top of the column. The effluent was spun down at 2000 rpm for 5 min. The pellet was washed three times with parasite culture media.

### **5.2.3 Co-culture of HUVEC with malaria parasites**

The concentrated parasites were re-suspended in 1% FCS in medium 199 to get a parasitemia of 20% in 1% haematocrit per well. Endothelial medium was removed from HUVEC grown on coverslip and the cells were gently washed once with 1X PBS. Then, the 500  $\mu$ l/well of parasite suspension were added onto the HUVEC monolayer and co-cultured for 3 h at 37 °C, 5% CO<sub>2</sub> in a humidified incubator. In the control group, uninfected red blood cells were re-suspended in 500  $\mu$ l of 1% FCS in medium 199 to get 1% haematocrit and applied onto HUVEC monolayer washed with 1X PBS. The co-culture were agitated either clockwise or counter clockwise every 10-15 min to allow more cell-to-cell contact, until the third hour.

For the positive control, the HUVEC cultured on coverslip were induced to apoptosis with camptothecin (Sigma) at the concentration of 5  $\mu$ M for 24 h at 37 °C, 5% CO<sub>2</sub> in a humidified incubator. To define the role of hemozoin from ruptured PRBC on the induction of oxidative stress in HUVEC, desferrioxamine (DFO) (Sigma), an iron chelator (van Zyl *et al.*, 1993), was added to the co-culture of HUVEC and PRBC at concentrations of 20, 50 and 100  $\mu$ M.

### **5.2.4 Immunocytochemistry for the detection of 4-HNE formation**

To evaluate the formation of 4-hydroxynonenal (4-HNE), a marker of oxidative stress, co-culture medium was removed from each well after 3 h of co-culture. The coverslip in each well was removed using forceps. The coverslip was then held vertically and

dipped gently into a universal containing 25 ml 1X PBS to remove excess red blood cells. This process was repeated twice more. Then, the coverslip was placed upside down on 500  $\mu$ l medium 199 supplemented with 1% FCS in an angled 24 multiwell plate for 30 min. The coverslip was transferred to fresh gravity wash in a clean 24 multiwell plate for a further 15 min before transferring to clean 24 multiwell plate containing 500  $\mu$ l/well of 4% paraformaldehyde (Gibco). Cells were fixed for 30 min at 4 °C. Cells were then washed twice with 1 ml of 1X PBS before permeabilising with 0.5% Triton X-100 in PBS for 15 min at room temperature. Cells were washed twice with 1 ml 1X PBS and then incubated with PBS containing 3% goat serum for 1 h at 4 °C. Cells were then washed with 1 ml PBS twice. Thereafter, cells were incubated with 500  $\mu$ l of anti-4-hydroxynoneal antibody (Alexis biochemicals) at 1:500 dilution overnight at 4 °C. The primary antibody was removed and cells were washed with PBS. The secondary antibody, goat anti-rabbit IgG antibody conjugated with Alexa Fluor 488 (Molecular Probes), was applied in a dilution of 1:500 and incubated for 1 h at room temperature. Washed cells were embedded in Vectashield (Vector laboratories), and fluorescence distribution was examined by confocal laser scanning microscopy.

#### **5.2.5 Determination of 4-HNE formation using confocal laser scanning microscope**

Cells embedded in Vectashield on a glass slide were observed using a Zeiss Pascal confocal laser scanning microscope (CLSM). Cells were viewed through a Plan-Apochromat 63x 1.2 numerical aperture (N.A.) water objective. Fluorescence signals were collected by single excitation with an argon ion laser at 488 nm and collection of emitted light through a 505-530 nm band pass filter.

## **5.3 RESULTS**

### **5.3.1 Malaria parasites induced the formation of 4-HNE in HUVEC**

To evaluate the implication of oxidative stress in the malaria parasite-induced apoptosis of HUVEC, we used immunocytochemical staining to detect the formation of 4-HNE, the marker of oxidative stress. In the control group, HUVEC were co-cultured with uninfected red blood cells for 3 h. HUVEC in this group showed some 4-HNE formation (Fig 5.1 panel D-F) but the degree of adduct formation was not different from control HUVEC (Fig 5.1 panel A-C). Significantly, most of HUVEC that were co-cultured with PRBC showed a marked increase in 4-HNE formation when compare to HUVEC co-cultured with uninfected red blood cell or normal HUVEC (Fig 5.1 panel G-I) as well as surrounding HUVEC which unattached to PRBC (Fig 5.2).

As a positive control, HUVEC were treated with camptothecin, a known inducer of oxidative stress in many cell types (Brea-Calvo *et al.*, 2009). Treatment HUVEC with camptothecin caused a profound change in HUVEC morphology. As expected, cells showed membrane blebbing and the formation of 4-HNE increased (Fig 5.1 panel J-L).

### **5.3.2 Effect of iron chelator on the formation of 4-HNE in HUVEC co-cultured with malaria parasites**

As hemozoin composes of large quantities of ferric heme and small amount of free iron, it is a likely generator of oxidative radicals that can cause lipid peroxidation of polyunsaturated fatty acids in the biomembrane which results in the formation of 4-HNE (Schwarzer *et al.*, 1996). To identify whether oxidative stress in HUVEC

induced by PRBC is due to hemozoin released from the ruptured PRBC or due to the binding of PRBC to HUVEC, we co-cultured HUVEC together with PRBC in the presence of DFO, the iron chelator. However, we found that the cells treated with DFO at different concentration varying from 20 to 100  $\mu$ M still showed the same pattern of 4-HNE formation when compared with cells co-cultured with PRBC in absence of DFO (Fig 5.3).

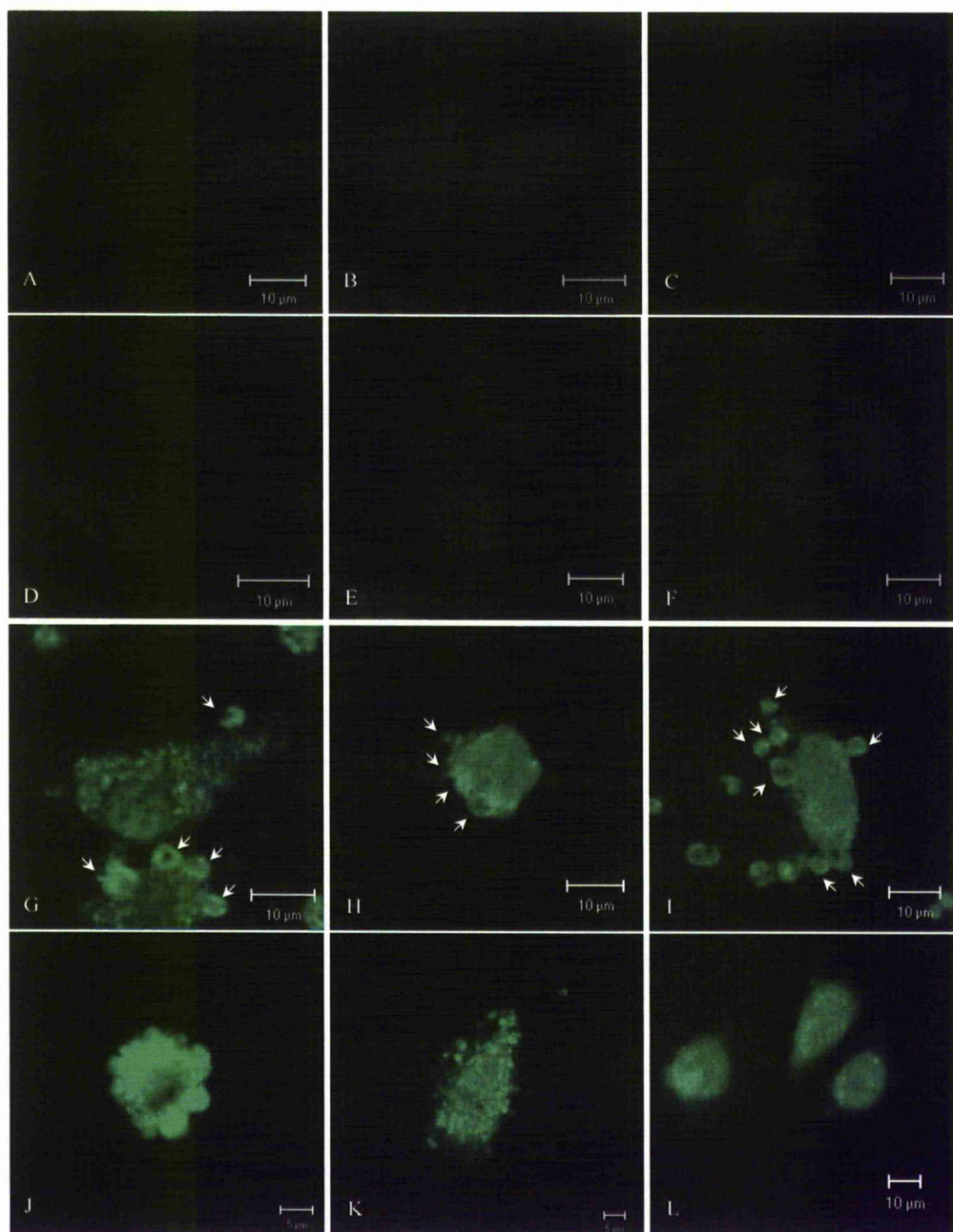


**Figure 5.1** Confocal images of HUVEC stained with anti-4-hydroxynoneal antibody. (A-C) control HUVEC, (D-F) HUVEC co-cultured with uninfected red blood cells, (G-I) HUVEC co-cultured with PRBC, (J-L) HUVEC treated with camptothecin. The arrows indicate PRBC which attached to HUVEC.



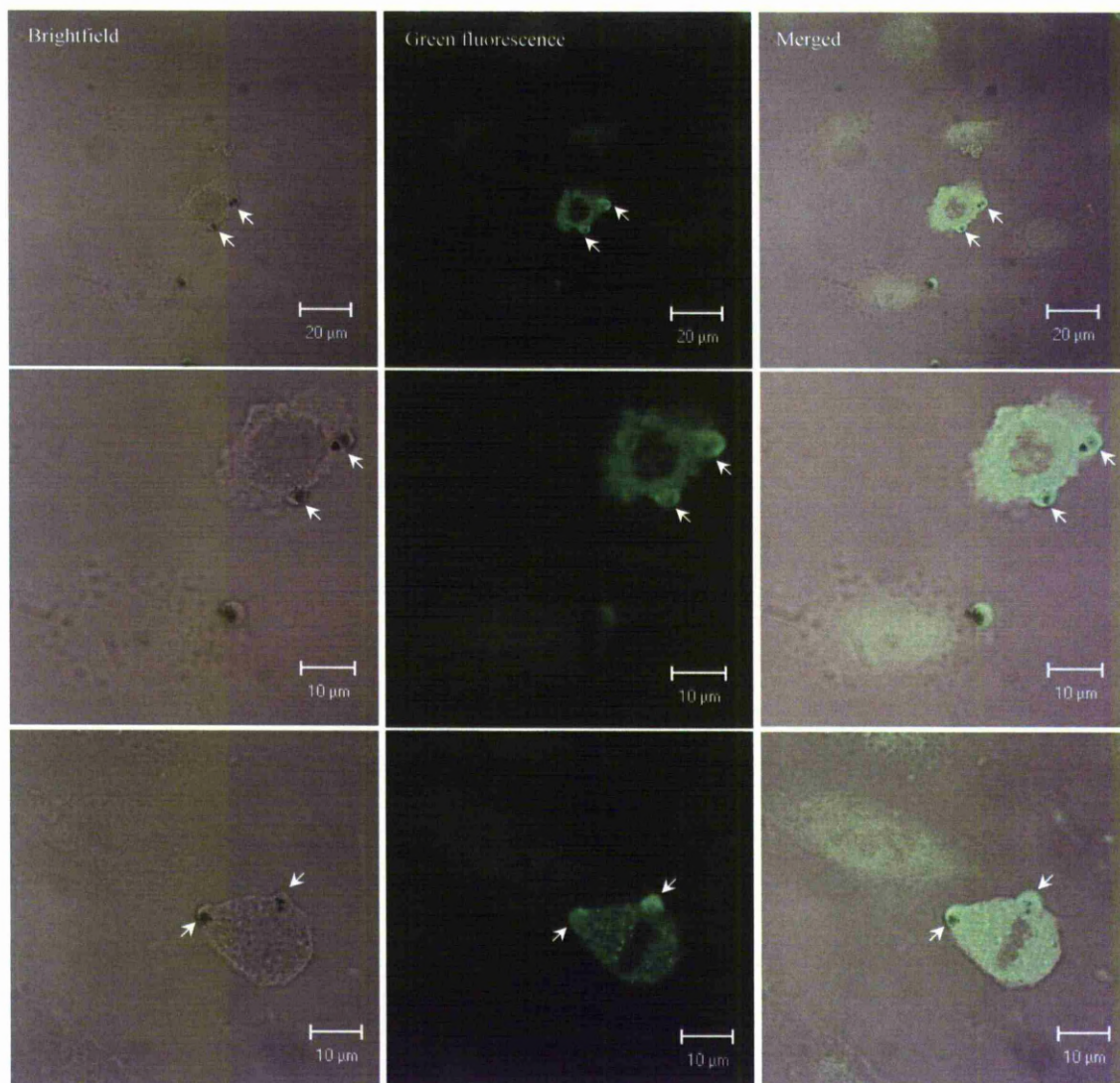


**Figure 5.2** Confocal images of PRBC-adhered HUVEC stained with anti-4-hydroxynoneal antibody. Amount of 4-HNE adducts on PRBC-adhered HUVEC increased when compared with surrounding HUVEC which unattached to PRBC. The arrows indicate PRBC which attached to HUVEC.

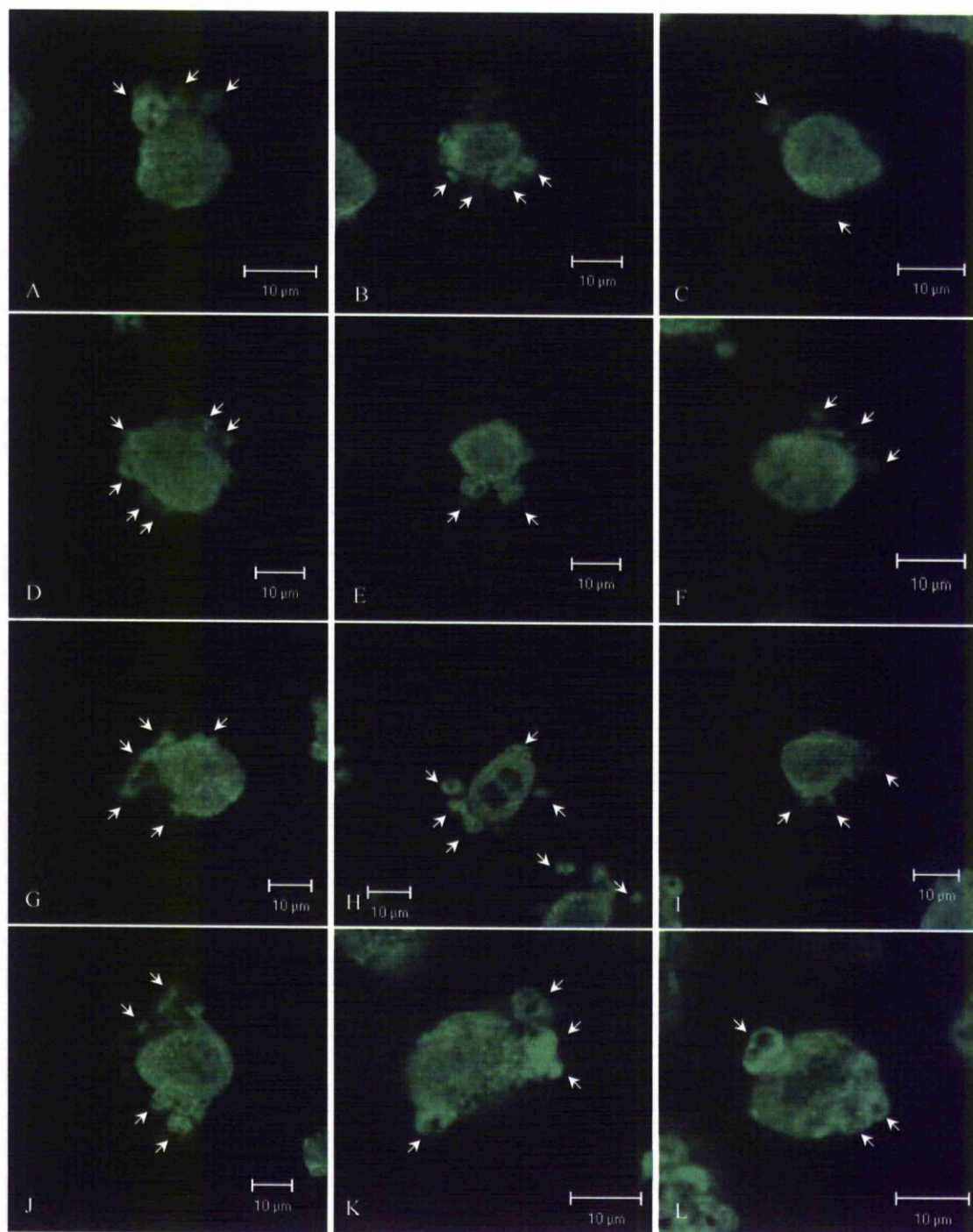


**Figure 5.3** Confocal images of PRBC-adhered HUVEC stained with anti-4-hydroxynoneal antibody in the presence and absence of DFO. (A-C) HUVEC co-culture with PRBC in absence of the iron chelator DFO, (D-F) HUVEC co-cultured with PRBC in the presence of 20  $\mu$ M DFO, (G-I) HUVEC co-cultured with PRBC in

the presence of 50  $\mu\text{M}$  DFO, (J-L) HUVEC co-cultured with PRBC in the presence of 100  $\mu\text{M}$  DFO. The arrows indicate PRBC which attached to HUVEC.

## 5.4 DISCUSSION

Previously published data implicates a role for oxidative stress in apoptosis of endothelial cells following cytoadherence by malaria parasites. The study conducted by Pino and co-workers showed that malaria parasite-induced apoptosis of endothelial cells can be prevented by addition of MnTBAP, a permeable chemical superoxide dismutase mimetic, and inhibition of nitric oxide synthesis (which in turn, reduces peroxynitrite ( $\text{ONOO}^-$ ) formation, (Pino et al., 2003a)). The authors suggested that the apoptotic process induced by PRBC is mediated by  $\text{O}_2^-$  and nitric oxide ( $\text{NO}\bullet$ ). Transfection of endothelial cells with the antioxidant enzyme superoxide dismutase (SOD1), an antioxidative enzyme that dismutates superoxide anion ( $\text{O}_2^-$ ), also provided the protective effect against *P. falciparum*-induced oxidative stress and apoptosis in endothelial cells (Taoufiq et al., 2006). In this chapter, we again confirm the implication of oxidative stress in apoptosis of endothelial cell induced by malaria parasites. We found a significant increase in formation of 4-HNE in HUVEC co-cultured with PRBC compared to normal HUVEC and HUVEC co-cultured with uninfected red blood cells.

During asexual development of malaria parasites, parasites ingest host cell cytoplasm, including haemoglobin to obtain nutrients. However, parasites cannot digest heme liberated from haemoglobin which is toxic to parasites. Free heme is polymerised to form hemozoin (Mabeza *et al.*, 1999) which has been found to cause oxidative stress in host cells, sometimes leading to apoptosis (Lamikanra et al., 2009, Schwarzer et al., 2003, Schwarzer et al., 1996, Skorokhod et al., 2007). We assessed whether the oxidative stress observed in HUVEC co-cultured with PRBC was due to the heme/hemozoin release from the rupture of PRBC by adding DFO, which has been

widely used as an effective iron chelator (Loyevsky *et al.*, 1999, Lytton *et al.*, 1994, van Zyl *et al.*, 1993).

Addition of DFO to the HUVEC-PRBC co-culture had no effect on 4-HNE formation when compared to HUVEC-PRBC co-culture in absence of DFO. These data would suggest that DFO-chelatable substances such as heme are not responsible for the formation of the 4-HNE adducts, and that the lipid peroxidation is caused by the HUVEC undergoing apoptosis. These data are consistent with data shown in chapter 3, that PRBC-cytoadherence is required for the initiation of apoptosis.

Due to the nature of apoptotic cells which detach themselves from coverslips and the long fixation and staining processes, many cells were lost, making it difficult to assess the quantity of cells with 4-HNE formation. Future work to quantify the 4-HNE adducts in positive cells by other techniques such as flow cytometry (Skorokhod *et al.*, 2010) or ELISA (Borovic *et al.*, 2006) could be performed.



## **CHAPTER 6: EFFECT OF CELL SIGNALLING INHIBITORS ON MALARIA PARASITE-INDUCED HUMAN ENDOTHELIAL CELL APOPTOSIS**

---

### **6.1 INTRODUCTION**

Apoptosis or programmed cell death is a process that plays an important role in development and maintenance of tissue homeostasis. The apoptotic process of cells is characterized by many morphological changes, for example, cell shrinkage, loss of adhesion and rounding (in adherent cells), plasma membrane blebbing, chromatin condensation and fragmentation (Zimmermann & Green, 2001). This process has been reported to be implicated in the pathogenesis of a number of human diseases including cancer, viral infection, autoimmune diseases, and neurodegenerative disorders (Thompson, 1995). Recently, apoptosis has also been proposed to be one of the factors which might involve in the severe disease of *Plasmodium falciparum* infection (Hemmer *et al.*, 2005, Toure *et al.*, 2008, Wilson *et al.*, 2008).

As described in Chapter 1, apoptosis occurs through two major pathways. The first pathway is the extrinsic pathway. Activation of this pathway is initiated by binding of a specific protein ligand to cell surface transmembrane receptor which finally leads to the activation of caspase-8. The transmembrane receptors that trigger external apoptosis signalling belong to the tumor necrosis factor (TNF)-receptor superfamily such as TNF receptor-1 (TNF-R1) and FAS receptor (Schultz & Harrington, 2003). The second pathway is the intrinsic pathway which mediates the triggering of caspase-9. The main regulator of intrinsic pathway is the mitochondria. An important event in the mitochondria mediated apoptosis is mitochondrial outer membrane

permeabilization (MOMP) which is controlled by Bcl-2 family members (Jin & El-Deiry, 2005).

Besides those two main pathways of apoptosis, other signalling pathways leading to cell apoptosis are also present. The endoplasmic reticulum (ER) is one of the organelle that participates in apoptotic process of cells which is referred to as ER stress-induced pathways. ER regulated apoptosis by sensitizing mitochondria to a variety of death stimuli and by initiating death signals of its own (Breckenridge *et al.*, 2003). Stress-activated protein kinase pathways, the c-Jun N-terminal kinase and p38 MAPK pathways, also implicate in apoptosis of cells (Grethe *et al.*, 2004, Karahashi *et al.*, 2009). However, the role of these two pathways in apoptosis depends on cell type and the nature of the death stimuli (Wagner & Nebreda, 2009). The nuclear transcription factor NF- $\kappa$ B and transcription factor p53 also play an important role in the regulation of apoptosis (Aoki *et al.*, 2001, Kuhnel *et al.*, 2000). Furthermore, important sensors of innate immune system, Toll-like receptors (TLR), are capable of controlling the survival of microbial challenged cells by governing the induction of pro- or antiapoptotic signalling pathways (Ruckdeschel *et al.*, 2004).

It has been shown by Pamplona and colleagues that administration of carbon monoxide (CO), which is one of the products from catabolism heme by heme oxygenase (HO)-1, provides the protective effects to mice induced to have cerebral malaria by *Plasmodium berghei* ANKA (Pamplona *et al.*, 2007). The authors suggest that the protective effects of CO are associated with inhibition of the blood-brain barrier disruption, brain microvascular congestion and hemorrhage, suppression of neuroinflammation, inhibition of adhesion molecule expression in the brain

microvasculature and suppression of activated CD8<sup>+</sup> T cell sequestration in the brain (Pamplona *et al.*, 2007).

It is clear from the results in previous chapter (chapter 3) that cytoadhesion of PRBC causes apoptosis of HUVEC. However, the subtle signalling pathways which underlie apoptosis of HUVEC are not known. As described above that apoptosis can occur through several pathways, in this chapter, we used various inhibitors against molecules implicated in apoptotic pathway to unveil the mechanism of apoptosis in HUVEC. In addition, it was also possible in this chapter of CO on apoptosis of endothelial cell by using carbon monoxide releasing molecules (CORMs) which were gifts from ALFAMA, Portugal.



## **6.2 MATERIALS AND METHODS**

### **6.2.1 Preparation of HUVEC for co-culturing**

HUVEC used in the experiments were from passage 4-6. HUVEC were cultured as described in detail in Chapter 2 section 2.2. When HUVEC reached to 80-90% confluence, cells were trypsinised and seeded on 40 mm diameter gelatin coated coverslip (Bioptechs) placed in petri dish (Nunc). The seeding density was 15,000-20,000 cells/cm<sup>2</sup>. Approximately, 500 µl of cell suspension was gently loaded onto the coated coverslips. Cells were allowed to settle for 1 h at 37 °C, 5% CO<sub>2</sub> in a humidified incubator. The medium was then removed and 2 ml of pre-warmed fresh medium was added. Cells were then further cultured until they reached 80-90% confluence before used in the experiments.

### **6.2.2 Preparation of malaria parasites for co-culturing**

Malaria parasites used in this experiment were ITG parasites and the ITG parasites selected to have potential to bind and induce apoptosis of HUVEC as describe in detail in Chapter 7. Both parasites were cultured as described in Chapter 2 section 2.1. Parasites were cultured until they reached 5-8% parasitemia (trophozoite or schizont stages). Then, parasites were submitted to magnetic separation technique in order to get 80-90% parasitemia. The parasite suspension was spun down at 2000 rpm for 5 min. The parasite pellet was re-suspended in 10 ml of binding solution (1X PBS containing 2% BSA (Sigma) and 20 mM glucose (Sigma)). The CS column was placed on a VarioMACS magnet (Miltenyi Biotec) and pre-washed once with binding solution. The column was not allowed to dry at any time during the procedure. The parasite suspension was applied to the top of the column and the column was washed

with binding solution until the flow through was totally clear. The column was removed from the magnet and the effluent containing concentrated parasites was eluted by adding 10 ml of binding solution to the top of the column. The effluent was spun down at 2000 rpm for 5 min. The pellet was washed three times with parasite culture media.

### **6.2.3 Co-culture of HUVEC with malaria parasites**

ITG parasites were used in all experiments except the experiments which treated HUVEC with MyD88 inhibitor, NF- $\kappa$ B inhibitors and carbon monoxide releasing molecules (CORMs) received from ALFAMA (Portugal) where the enriched parasites were used instead. The concentrated parasites were re-suspended in 1% FCS in medium 199 to get a parasitemia of 50% in 1% haematocrit for ITG parasites and a parasitemia of 20% in 1 % haematocrit for the enriched parasites. Endothelial medium was removed from HUVEC grown on coverslip at 80-90% confluence and the cells were gently washed once with 1X PBS. Then, the 2 ml of parasite suspension were added onto HUVEC monolayer and co-cultured for 3 h at 37 °C, 5% CO<sub>2</sub> in humidified incubator. The co-culture dishes were agitated either clockwise or counter clockwise every 10-15 min to allow more cell-to-cell contact until the third hour.

### **6.2.4 Inhibitor treatment**

In order to define the signalling pathways underlying apoptosis of HUVEC induced by malaria parasites, various apoptotic inhibitors were selected to use in the experiments. Inhibitors included c-Jun N-terminal kinase (JNK) inhibitor, p38 MAP kinase inhibitor, endoplasmic reticulum stress inhibitor, p53 inhibitor, Bax inhibitor, caspase-8 inhibitor, caspase-9 inhibitor, pan-caspase inhibitor, intracellular calcium chelator,

toll-like receptor pathway inhibitor, NF- $\kappa$ B signalling pathway inhibitors and carbon monoxide releasing molecules (CORMs). List of inhibitors and their targets were summarised in Table 6.1.

In the apoptosis inhibition experiments, HUVEC were treated with the inhibitors as described here. HUVEC were pretreated with 10  $\mu$ M of c-Jun N-terminal kinase inhibitor (SP600125) (Sigma) or 10  $\mu$ M p38 MAP kinase inhibitor (SB202190) (Sigma) for 30 min, and HUVEC were co-cultured with PRBC in the presence of these inhibitors. Salubrinal (ER stress inhibitor) (Tocris bioscience), Bax inhibiting peptide (Calbiochem) and Pifithrin- $\alpha$  (p53 inhibitor) (Calbiochem) were used to pretreat HUVEC at the concentration of 50  $\mu$ M, 200  $\mu$ M and 30  $\mu$ M, respectively, for 60 min. These inhibitors were also presented in the co-culture medium of HUVEC to PRBC. BAPTA-AM (intracellular calcium chelator) (Molecular probes) was used to pretreat HUVEC at 100  $\mu$ M for 45 min. MyD88 homodimerization inhibitor peptide (Imgenex) were used to pretreat HUVEC at 200  $\mu$ M for 24 h and presented in the co-culture. Z-IETD-FMK (caspase-8 inhibitor) (R&D system), Z-LEHD-FMK (caspase-9 inhibitor) (R&D system) and Z-VAD-FMK (pan-caspase inhibitor) (Promega) were added at the beginning of the co-culture at concentration of 100  $\mu$ M, 100  $\mu$ M and 20  $\mu$ M, respectively. MG132 and BAY11-7082 (NF- $\kappa$ B inhibitors) (Calbiochem) were used to pretreat HUVEC at 10  $\mu$ M and 4  $\mu$ M, respectively, for 60 min, and also added the co-culture medium. The carbon monoxide releasing molecules which are ALF186 and ALF466 (gifted from ALFAMA) were added to HUVEC at 100  $\mu$ M together with the co-culture medium.

Inhibitors	Target(s) of inhibitors
SP600125	c-Jun N-terminal kinase (JNK)
SB202190	p38 MAP kinase
Salubrinal	Cellular phosphatase complexes that dephosphorylate eukaryotic translation initiation factor 2 subunit $\alpha$ (eIF2 $\alpha$ ) (protect cell from ER stress apoptosis)
Bax inhibiting peptide	<i>Bax</i> mediated apoptosis
Pifithrin- $\alpha$	p53-mediated apoptosis
Z-IETD-FMK	Caspase-8
Z-LEHD-FMK	Caspase-9
Z-VAD-FMK	General caspase inhibitor
BAPTA-AM	Chelator of intracellular Ca <sup>2+</sup> stores
MyD88 homodimerization inhibitor peptide	MyD88 dependent TLR/IL-1R signalling
MG132	NF- $\kappa$ B
BAY11-7082	NF- $\kappa$ B

**Table 6.1** Summary apoptotic pathway inhibitors used in the experiments and their targets

### **6.2.5 Determination of apoptotic cells using confocal laser scanning microscope**

After 3 h of co-cultivation, the co-culture medium was discarded. HUVEC in all groups of experiments were washed twice with 1X PBS to remove unbound uninfected red blood cells or parasites. HUVEC were double stained with annexin V and propidium iodide (8  $\mu$ l of annexin V and 2  $\mu$ l of 2.5  $\mu$ g/ml PI into 2 ml of annexin-binding buffer). Cells were incubated within this mixture at 37 °C, 5% CO<sub>2</sub> in humidified incubator for 20 min. The coverslips were gently washed once with annexin-binding buffer. The coverslips were assembled into a Biopetechs FCS2 perfusion chamber (Biopetechs), perfused with annexin-binding buffer and observed with Zeiss Pascal confocal laser scanning microscope (CLSM). Cells were viewed through a Plan-Apochromat 63x 1.2 numerical aperture (N.A.) water objective. Fluorescence signals from annexin V and PI were collected by single excitation with argon ion laser at 488 nm and collection of emitted light through a 505-530 nm band pass filter and a 650 nm long pass filter, respectively. At least 500 cells were counted for each replicate and scored according to the appearance of cells, i.e. attached/unattached to PRBC, blebbing and/or annexin V/PI staining.

### **6.2.6 Statistical analysis**

Results were expressed as mean  $\pm$  standard error of individual experimental groups. Statistical analysis was performed with GrapPad InStat version 3.05. Data were analysed by Mann-Whitney U test. A value of  $p < 0.05$  was considered significant.

## 6.3 RESULTS

### 6.3.1 Cytoadherence of PRBC and to HUVEC

The percentages of attachment between HUVEC and PRBC in control and inhibitor treated groups for all experiment are tabulated in Table 6.2.

Name of inhibitors	Attachment (%)	
	Control group	Inhibitor treated group
SP600125	4.71 $\pm$ 0.78	3.97 $\pm$ 0.30
SB202190	5.62 $\pm$ 0.25	5.58 $\pm$ 0.32
Salubrinal	3.26 $\pm$ 0.28	3.39 $\pm$ 0.36
Bax inhibitor	3.67 $\pm$ 0.35	3.65 $\pm$ 0.19
Pifithrin- $\alpha$	5.14 $\pm$ 0.25	6.40 $\pm$ 0.65
Z-IETD-FMK	5.74 $\pm$ 0.34	6.09 $\pm$ 0.33
Z-LEHD-FMK	5.23 $\pm$ 0.39	5.59 $\pm$ 0.55
Z-VAD-FMK	6.31 $\pm$ 0.67	5.55 $\pm$ 0.71
BAPTA-AM	5.65 $\pm$ 0.32	5.76 $\pm$ 0.72
MyD88 inhibitor	8.27 $\pm$ 0.03	8.25 $\pm$ 0.07
MG132	9.07 $\pm$ 0.42	9.12 $\pm$ 0.78
BAY11-7082	8.79 $\pm$ 0.25	9.64 $\pm$ 0.37
ALF186	8.30 $\pm$ 0.18	8.17 $\pm$ 0.26
ALF466	8.03 $\pm$ 0.22	7.71 $\pm$ 0.08

**Table 6.2** Comparison the percentage attachment of PRBC to HUVEC in control and inhibitor treated groups. Data are mean  $\pm$  SE of at least three experiments.

As shown in Table 6.2 and Fig 6.1, the addition of the following inhibitors: c-Jun N-terminal kinase inhibitor (SP600125), p38 MAP kinase inhibitor (SB202190), ER stress inhibitor (salubrinal), Bax inhibitor, p53 inhibitor (pifithrin- $\alpha$ ), caspase-8 inhibitor (Z-IETD-FMK), caspase-9 inhibitor (Z-LEHD-FMK), pan-caspase inhibitor (Z-VAD-FMK), intracellular calcium chelator (BAPTA-AM), Toll-like receptor signalling pathway inhibitor (MyD88 homodimerization inhibitor peptide), NF- $\kappa$ B inhibitors (MG132 and BAY11-7082) or carbon monoxide releasing molecules (ALF186 and ALF466) to the HUVEC-PRBC co-culture had no effect on PRBC binding to HUVEC. There was no statistically significant difference among the quantity of binding between control and inhibitor treated groups in all cases.

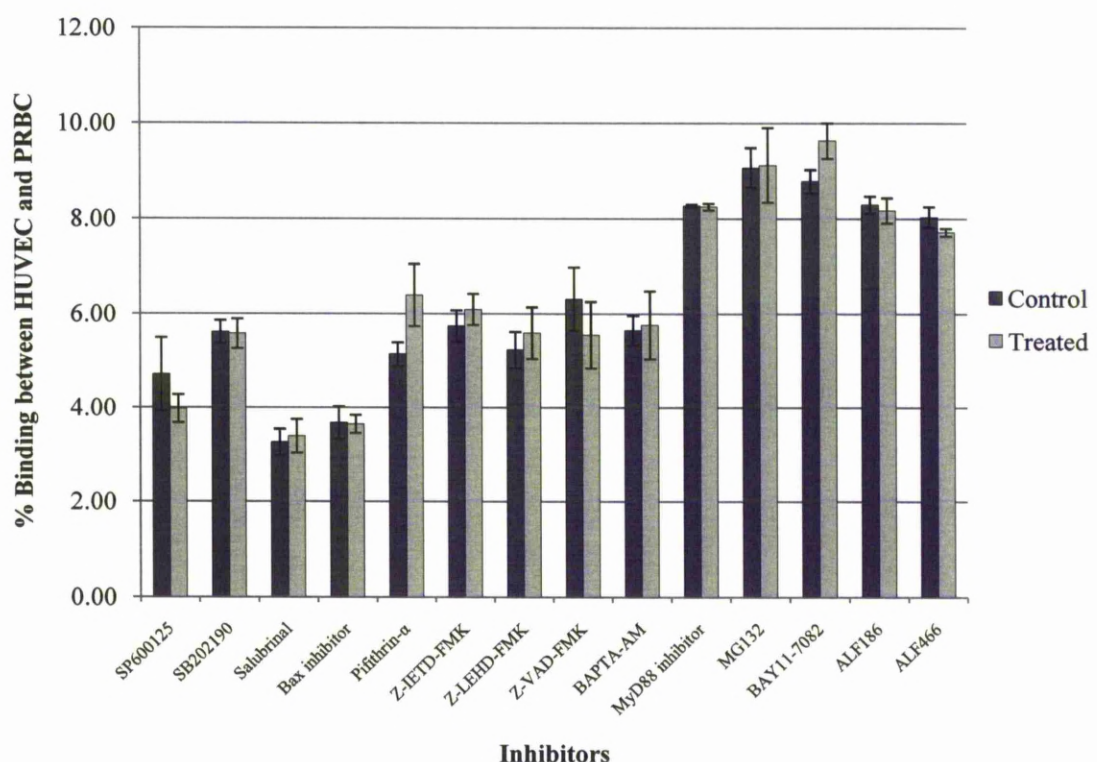


**Figure 6.1** Comparison amount of binding between PRBC and HUVEC in control group and inhibitors treated groups. Data are mean  $\pm$  SE of at least three experiments.

### **6.3.2 Effect of various apoptotic inhibitors on apoptosis of HUVEC attached to PRBC**

The capacity of various apoptotic signalling pathway inhibitors to inhibit apoptotic effect of PRBC on HUVEC was determined by comparing the degree of apoptosis of HUVEC attached to PRBC in control group to inhibitor treated group. The percentages of HUVEC undergoing apoptosis when attached to PRBC in control and inhibitor treated groups for all experiments are summarised in Table 6.3.

As shown in Table 6.3 and Fig 6.2, among the inhibitors used in our experiments, only caspase-8 (Z-IETD-FMK), caspase-9 (Z-LEHD-FMK), pan-caspase inhibitors (Z-VAD-FMK), intracellular calcium chelator (BAPTA-AM) and NF- $\kappa$ B inhibitors (MG132 and BAY11-7082) had ability to significantly decrease the amount of apoptosis of HUVEC attached to PRBC.

The quantity of apoptosis was decreased from  $84.98\% \pm 0.58$  (SE) in control group to  $52.52\% \pm 1.42$  (SE) in Z-IETD-FMK treated group, from  $87.98\% \pm 3.10$  (SE) in control group to  $40.27\% \pm 2.76$  (SE) in Z-LEHD-FMK treated group, from  $91.06\% \pm 2.14$  (SE) in control group to  $27.02\% \pm 3.65$  (SE) in Z-VAD-FMK treated group, from  $94.26\% \pm 1.14$  (SE) in control group to  $40.27\% \pm 4.28$  (SE) in BAPTA-AM treated group, from  $98.31\% \pm 1.11$  (SE) in control group to  $35.55\% \pm 3.09$  (SE) in MG132 treated group, and from  $96.15\% \pm 0.86$  (SE) to  $58.57\% \pm 1.25$  (SE) in BAY11-7082 treated group. The confocal images of apoptotic HUVEC induced by PRBC and HUVEC attached to PRBC in the presence of caspase-8 inhibitor, caspase-9 inhibitor, pan-caspase inhibitor, NF- $\kappa$ B inhibitors and intracellular calcium chelator are shown in Fig 6.3.



Name of inhibitors	Apoptosis among attached cells (%)	
	Control	Inhibitor treated
SP600125	95.01 ± 2.00	96.10 ± 1.26
SB202190	92.96 ± 3.55	91.28 ± 2.85
Salubrinal	93.05 ± 2.30	90.76 ± 0.72
Bax inhibitor	85.32 ± 4.85	87.97 ± 3.26
Pifithrin-α	86.45 ± 1.23	88.57 ± 3.02
Z-IETD-FMK	84.98 ± 0.58	52.52 ± 1.42*
Z-LEHD-FMK	87.98 ± 3.10	40.27 ± 2.76*
Z-VAD-FMK	91.06 ± 2.14	27.20 ± 3.65*
BAPTA-AM	94.26 ± 1.14	40.27 ± 4.28*
MyD88 inhibitor	99.19 ± 0.81	98.79 ± 0.82
MG132	98.31 ± 1.11	35.55 ± 3.09*
BAY11-7082	96.15 ± 0.86	58.57 ± 1.25*
ALF186	95.95 ± 2.12	94.88 ± 2.95
ALF466	95.95 ± 2.12	96.12 ± 0.76

**Table 6.3** Comparison the percentage apoptosis of HUVEC attached to PRBC in control and inhibitor treated groups. Data are mean ± SE of at least three experiments.

\* denotes statistically significant difference (p < 0.05).

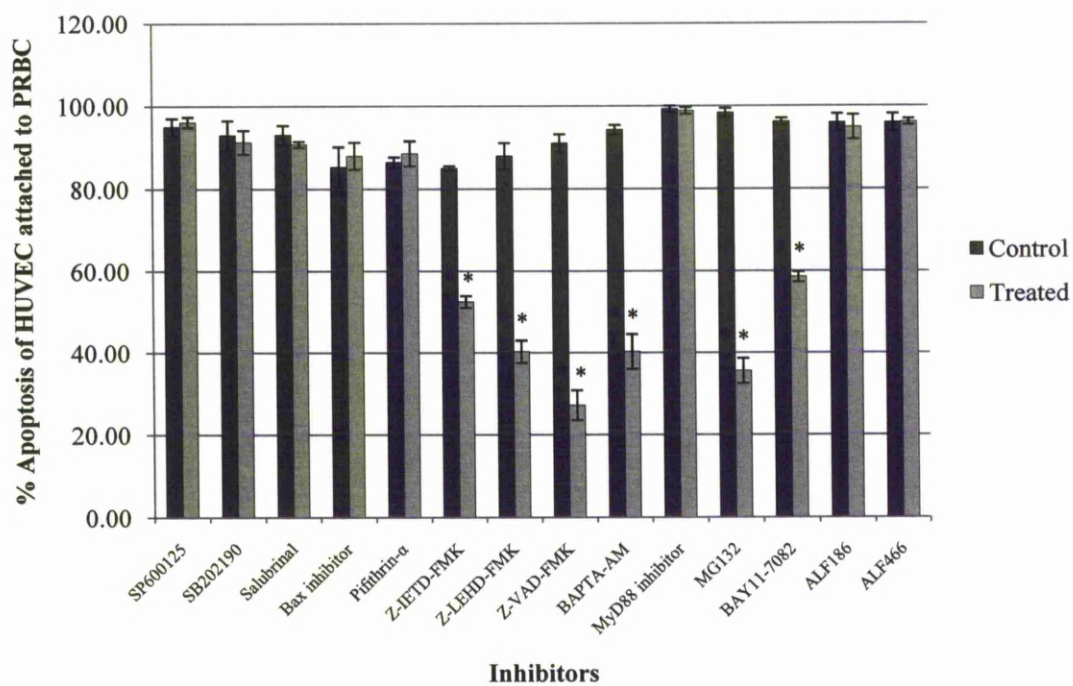


**Figure 6.2** Apoptosis of HUVEC attached to PRBC in control groups and apoptotic inhibitors treated groups. Data are mean  $\pm$  SE of at least three experiments. \* denotes statistically significant difference ( $p < 0.05$ ).

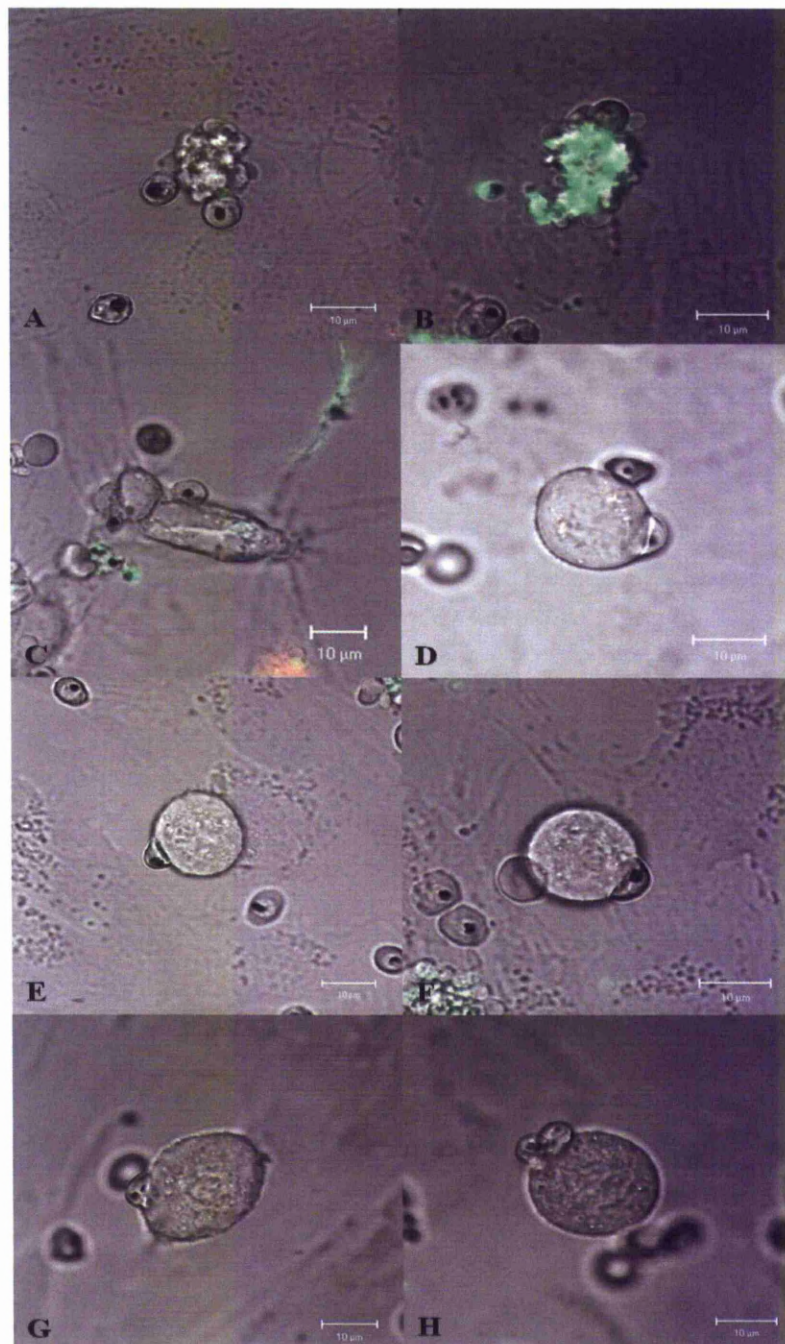


**Figure 6.3** Confocal images of HUVEC attached to PRBC in control group and in presence of inhibitors. (A-B) HUVEC attached to PRBC in control group illustrated cell membrane blebbing and/or annexin V positive; (C) HUVEC attached to PRBC in the presence of BAPTA-AM (intracellular calcium chelator); (D-H) HUVEC attached

to PRBC in the presence of MG132 and BAY11-7082 (NF- $\kappa$ B inhibitors), caspase-8 inhibitor (Z-IETD-FMK), caspase-9 inhibitor (Z-LEHD-FMK) and pan-caspase inhibitor (Z-VAD-FMK), respectively.

## 6.4 DISCUSSION

Apoptosis of cells can occur through several pathways, for example, extrinsic pathway, intrinsic pathway, stress-activated protein kinase pathways and endoplasmic reticulum pathway. In order to define the pathway which mediates apoptosis of HUVEC induced by attachment of PRBC, various inhibitors against molecules in the apoptotic pathway were selected for use in these experiments. Among the inhibitors tested in our experiments, only caspase-8 (Z-IETD-FMK), caspase-9 (Z-LEHD-FMK), pan-caspase inhibitors (Z-VAD-FMK), intracellular calcium chelator (BAPTA-AM) and NF- $\kappa$ B inhibitors (MG132 and BAY11-7082) had the potential to reduce the apoptotic effect of PRBC to HUVEC.

The results showed that the pan-caspase inhibitor (Z-VAD-FMK) significantly reduced apoptosis of HUVEC which indicates the role of a caspase dependent apoptotic pathway. To sort out the implication of extrinsic and intrinsic apoptotic pathways, which mediate through caspase-8 and caspase-9 respectively, specific caspase-8 and caspase-9 inhibitors were added to the HUVEC-PRBC co-culture. Both caspase-8 and caspase-9 inhibitors were capable of protecting HUVEC from apoptosis induced by PRBC. These results are consistent with the finding in Chapter 3 of PhD thesis of Dr. Parnpen Viriyavejakul (2007) which showed high activities of caspase-8 and caspase-9 in HUVEC co-culture with PRBC. Furthermore, the findings are in agreement with the work of Pino and colleagues (Pino et al., 2003b). The conclusion for the data would be that apoptosis of HUVEC induced by PRBC involves both extrinsic (caspase-8) and intrinsic (caspase-9) apoptotic pathways.

It is well established that calcium plays an important role in the events leading to cell apoptosis (Orrenius *et al.*, 2003, Pinton *et al.*, 2002). The calcium dependence of apoptosis in endothelial cells after PRBC cytoadherence has not been reported previously. However, the implication of a role for  $\text{Ca}^{2+}$  in apoptosis of host cells after the interaction with other pathogens has been describes in some studies (Buommino *et al.*, 1999, Chaibi *et al.*, 2005, Muller *et al.*, 1999). We investigated the involvement of intracellular calcium in the apoptosis of HUVEC by using the intracellular calcium ion chelator, BAPTA-AM. We found that treatment HUVEC with BAPTA-AM caused dramatic decrease in the amount of apoptosis. These results imply that  $\text{Ca}^{2+}$  is required for the development of apoptosis in HUVEC attached to PRBC.

NF- $\kappa$ B is a nuclear transcription factor which regulates expression of many genes involved in the regulation of cell proliferation, inflammation, immune response and apoptosis (Kleinberg & Davidson, 2009). In its inactive form, NF- $\kappa$ B is sequestered in the cytoplasm, bound to inhibitor proteins of the I $\kappa$ B family. The phosphorylation of I $\kappa$ B which is followed by its degradation occurs when NF- $\kappa$ B is activated by various stimuli. This results in translocation of NF- $\kappa$ B from the cytoplasm to the nucleus where NF- $\kappa$ B regulates expression of various genes (Neumann & Naumann, 2007). NF- $\kappa$ B has been shown to have both anti- and pro-apoptotic functions which might depend on the nature of the death stimulus (Dehio *et al.*, 2005, Grimm *et al.*, 1996, Hansberger *et al.*, 2007, Keller *et al.*, 2006). Recently, the activation of NF- $\kappa$ B in human brain endothelial in response to PRBC has been reported (Tripathi *et al.*, 2009, Tripathi *et al.*, 2006). To investigate the role of NF- $\kappa$ B in malaria parasites induced HUVEC apoptosis further, the inhibitor of NF- $\kappa$ B, MG132 and BAY11-7082, were added to the co-cultures. Both inhibitors significantly reduce the number of apoptotic

cells confirming that NF- $\kappa$ B plays a proapoptotic role in the apoptosis of HUVEC induced by PRBC.

Carbon monoxide (CO), the product from catabolism of heme by heme oxygenase (HO)-1, has been shown to have protective effects in rodent disease models including murine cerebral malaria (Pamplona et al., 2007, Sato *et al.*, 2001, Soares *et al.*, 1998). The pathogenesis of cerebral malaria in mice infected with *P. berghei* can be suppressed by administration of exogenous CO via inhalation (Pamplona et al., 2007). CO has also been reported to possess the ability to inhibit apoptosis of cells (Bainbridge *et al.*, 2006, Liu *et al.*, 2002). Recently, the work of Wei and colleagues showed that infusion of carbon monoxide releasing molecules to rats reduced the levels of hepatocyte apoptosis after hepatic ischemia-reperfusion injury (Wei *et al.*). To determine the effect of CO in apoptosis of HUVEC induced by PRBC, carbon monoxide releasing molecules (ALF186 and ALF466) were added to the co-culture medium. Unfortunately, in our experiment, these molecules did not protect HUVEC interacted with PRBC from undergoing apoptosis. This may be, in part, due to the type of apoptotic stimuli. This has been shown by a study on Jurkat cells, which when stimulated with a variety of apoptosis-inducing agents elicited different responses to CO (Song *et al.*, 2004). In our model, PRBC might trigger an apoptotic signalling pathway in HUVEC which is beyond the protective ability of CO.

The initiation of the intrinsic apoptotic pathway is mediated and controlled by Bcl-2 family members which can be divided according to their function and structure into three categories: antiapoptotic members, such as Bcl-2, Bcl-XL and Bcl-w; proapoptotic molecules, such as Bax, Bak and Bok; and the BH3-only proteins such as Bid and Bim (Jin & El-Deiry, 2005). The current widely accept model of the intrinsic

pathway suggests an important role for Bax and Bak insertion into the outer mitochondrial membrane leading to the release of apoptogenic factors. Our results, however, demonstrated that inhibition of Bax cannot protect HUVEC from the apoptotic effects of PRBC, although we did find the association of the intrinsic apoptotic pathways in apoptosis of HUVEC attached to PRBC. The induction of Bax-independent intrinsic apoptotic pathways has been described in which Bax deficient cells showed evidence of the intrinsic pathway activation including the release of apoptogenic factors including cytochrome *c* and apoptosis inducing factor (AIF) and loss of mitochondrial transmembrane potential ( $\Delta\Psi_m$ ). Apoptosis in those cells was suggested to be mediated through the activation and accumulation of multiple BH3-only proteins in mitochondria, leading to the release of apoptogenic factors and loss of  $\Delta\Psi_m$  (Lomonosova *et al.*, 2009). In addition, the intrinsic apoptotic pathway can also be mediated by  $\text{Ca}^{2+}$  (Orrenius *et al.*, 2003), and our data already demonstrated the involvement of  $\text{Ca}^{2+}$  in the apoptosis of HUVEC. It is plausible that apoptosis of HUVEC attached to PRBC occurs through the calcium- or other Bcl-2 family member dependent intrinsic apoptotic pathway.

Stress-activated protein kinase pathways, the c-Jun N-terminal kinase and p38 MAPK pathways, can be activated in response to various cellular and environmental stresses including changes in osmolarity or metabolism, DNA damage, heat shock, ischemia, inflammatory cytokines, UV irradiation and oxidative stress (Wada & Penninger, 2004). These pathways have been reported to play role in both pro-apoptosis (Grethe *et al.*, 2004, Karahashi *et al.*, 2009) and anti-apoptosis (Matusali *et al.*, 2009, Yu *et al.*, 2004) depending on the type of cell and stimuli (Wada & Penninger, 2004). However, in our experiment, neither c-Jun N-terminal kinase (JNK) inhibitor nor p38 MAP



kinase inhibition protected HUVEC from apoptosis induced by PRBC. The conclusion must be that apoptosis of PRBC-adhered HUVEC occurs through JNK/p38 MAPK-independent pathways.

p53 is a transcription factor which plays a role in the response of cells to stress such as DNA damaging agents, hypoxia or oncogene activation (Amaral *et al.*, 2009). Activation of this transcription factor can lead to cell cycle arrest, DNA repair, cellular senescence or apoptosis depend on cell type or stress signal (Haupt *et al.*, 2003, Vousden & Lu, 2002). p53 can trigger apoptosis by activating the transcription of genes known to promote apoptosis such as Fas, Bid, NOXA and PUMA (Haupt *et al.*, 2003, Pietsch *et al.*, 2008). On the other hand, translocation of p53 to the mitochondria also leads to the release of apoptotic-inducing factors (Marchenko *et al.*, 2000, Nemajero *et al.*, 2005). Despite inhibiting the function of p53 in HUVEC with pifithrin- $\alpha$ , HUVEC still underwent apoptosis after co-culture with PRBC. We must assume that apoptosis of PRBC-adhered HUVEC occurs through a p53-independent pathway.

One of the main functions of the ER in mammalian cells is for  $\text{Ca}^{2+}$  storage and signalling as well as the folding, modifying and sorting of newly synthesized proteins. The ER stress can occur when any of these functions are disturbed (Breckenridge *et al.*, 2003). The ER stress inhibitor, salubrinal, used in our experiment functions on the unfolded protein response (UPR) signalling pathway, which is activated in response to changes in the capacity of the ER to fold proteins properly (Boyce *et al.*, 2005). Our data showed that this inhibitor had no effect on inhibition of HUVEC apoptosis. We presume that the UPR signalling pathway in ER is not involved in apoptosis of HUVEC attached to PRBC. Nevertheless, the implication of ER stress pathways in

apoptosis of HUVEC cannot be excluded because, as mentioned above, the ER also functions as an intracellular  $\text{Ca}^{2+}$  storage organelle, which in turn can play a role in apoptosis of HUVEC induced by PRBC.

Toll-like receptors (TLR), the components of the innate immune response, have been reported to be involved in apoptosis (Aravalli *et al.*, 2007, Hsu *et al.*, 2004). The signalling of TLR is mediated by the myeloid differentiation factor 88 (MyD88)-dependent and MyD88-independent pathways (Salaun *et al.*, 2007). The potential role of this receptor in malaria infection has been established and involves malarial components such as hemozoin complexed to DNA and glycosylphosphatidylinositol (GPI) which have been shown to activate MyD88-dependent TLR signalling (Krishnegowda *et al.*, 2005, Parroche *et al.*, 2007). In addition, HUVEC has been reported to express TLR1, TLR2, TLR3, TLR4 and TLR6 (Faure *et al.*, 2000, Livengood *et al.*, 2007) all of which, except TLR3, mediate signalling through the MyD88-dependent pathway (Kawai & Akira, 2006). Therefore, to reveal whether the MyD88-dependent TLR signalling pathway was involved in apoptosis of HUVEC induced by PRBC, a peptide which blocks MyD88 homodimerization was added to HUVEC-PRBC co-culture medium. The results showed that inhibition of MyD88 was unable to suppress the apoptotic effect of PRBC on HUVEC. These data imply that the MyD88-dependent TLR signalling pathway is not implicated in PRBC-induced HUVEC apoptosis. However, as TLR signalling can also be mediated through a MyD88-independent pathway, i.e. TLR3 and TLR4 which are also presented on HUVEC (Faure *et al.*, 2000, Livengood *et al.*, 2007), the role of this pathway cannot be completely ignored.

In conclusion, the results in this chapter suggest the role of the extrinsic and intrinsic apoptotic pathways as well as calcium and NF- $\kappa$ B signalling pathways in PRBC-induced HUVEC apoptosis. We were unable to implicate other well characterised pathways despite the use of widely used inhibitor probes at concentrations shown to be effective in other mammalian cell systems. Other techniques such as RNA interference (Borrallho *et al.*, 2007, Liang *et al.*, 2007) could be conducted to further examine the signalling pathways involved in the malaria-specific apoptotic phenotype.

## **CHAPTER 7: CHARACTERISATION OF HUMAN ENDOTHELIAL CELL SURFACE MEMBRANE RECEPTORS ELICITING CYTOADHERENCE-INDUCED APOPTOSIS**

---

### **7.1 INTRODUCTION**

The pathogenesis of severe malaria is thought to be due to the ability of infected red blood cells to sequester in the small blood vessels of various organs. The high level of infected red blood cells bound to microvasculature has been shown in post-mortem study of patients with severe malaria (Taylor *et al.*, 2004). The adhesion of infected red blood cells to endothelial cells lining blood vessels could result in obstruction of blood vessels, metabolic disturbances, and release of damaging inflammatory mediators (Rowe *et al.*, 2009).

Endothelial cells express several receptors on their surfaces. Some of these molecules are constitutively expressed such as CD31/PECAM-1, CD34, and CD105/endoglin. Other molecules are expressed only after activation by growth factors or inflammatory cytokines, for example, CD54/ICAM-1, CD106/VCAM-1, CD62E/E-selectin, and CD62P/P-selectin (Garlanda & Dejana, 1997). The adhesion of infected red blood cells to endothelial cells is also mediated through cell surface molecules on endothelial cells. As described in Chapter 1 (section 1.1.2), several cell adhesion molecules have been proposed to be involved in cytoadherence of infected red blood cells, including intercellular adhesion molecule-1 (ICAM-1) (Berendt *et al.*, 1989), CD36 (Oquendo *et al.*, 1989), and CD31/PECAM-1 (Treutiger *et al.*, 1997).

Apart from being the mediator of cell-cell interactions, the adhesive cell surface can also mediate intracellular signalling in endothelial cells. Cytoadherence of infected red blood cells is known to induce signalling events in endothelial cells (Jenkins *et al.*, 2007, Medana & Turner, 2007). Some of these signalling responses have deleterious effect to host cells. The interaction between brain endothelial cells and infected red blood cells resulted in increase expression of ICAM-1 which could lead to further sequestration of parasites (Tripathi *et al.*, 2006). Parasite cytoadherence also leads to apoptosis and leakage in endothelial cells (Pino *et al.*, 2003b, Tripathi *et al.*, 2007).

In our study, we found that adhesion of malaria parasites to HUVEC induces apoptosis in the absence of TNF- $\alpha$  activation. However, the endothelial cell surface receptor involved in mediating the observed binding and subsequent apoptosis in our system has not been characterised. In this final chapter, an attempt has been made to describe the HUVEC membrane receptor involved in mediating cytoadherence-dependent apoptosis. To aid this work, PRBC were panned on unstimulated HUVEC for their ability to cytoadhere and induce apoptosis in unstimulated HUVEC. These enriched parasites were subsequently tested in TNF- $\alpha$  unstimulated and stimulated HUVEC in the presence of specific cell surface receptor antibodies.

## **7.2 MATERIAL AND METHODS**

### **7.2.1 HUVEC-bound malaria parasites selection**

As described in the previous sections, the level of binding of PRBC to unstimulated HUVEC is low (typically < 4%). In this part of the study, it was therefore decided to attempt to enrich the binding phenotype by sub-culturing only bound parasites (see below for methodology).

#### **7.2.1.1 Preparation of HUVEC for parasites selection**

HUVEC used in the experiment were from passage 4-6. HUVEC were grown in gelatin coated T25 cm<sup>2</sup> vented cap flasks until 80-90% confluence as described in Chapter 2 section 2.2.

#### **7.2.1.2 Preparation of malaria parasites for parasites selection**

*P. falciparum* strain ITG were cultured as described in Chapter 2 section 2.1. Parasites were cultured until reached 5-8% parasitemia of trophozoite or schizont stage. Then, parasites were submitted to magnetic separation technique in order to get 80-90% parasitemia of trophozoite or schizont stage. The parasite suspension was centrifuged at 2000 rpm for 5 min. The parasite pellet was re-suspended in 10 ml of binding solution (1X PBS containing 2% BSA (Sigma) and 20 mM glucose (Sigma)). The CS column was placed on a VarioMACS magnet (Miltenyi Biotec) and pre-washed once with binding solution. The column was not allowed to dry at any time during the procedure. The parasite suspension was applied to the top of the column and the column was washed with binding solution until the flow through was totally clear. The column was removed from the magnet and the concentrated parasites were eluted by

adding 10 ml of binding solution to the top of the column. The eluent was spun down at 2000 rpm for 5 min. The pellet was washed three times with parasite culture media.

#### **7.2.1.3 HUVEC-bound malaria parasites selection**

The concentrated trophozoite or schizont stage parasites were re-suspended in 1% FCS in medium 199 to obtain a parasitemia of 50% in 1% haematocrit. Endothelial medium was removed from HUVEC grown in T25 cm<sup>2</sup> vented cap flasks at 80-90% confluence and cells were gently washed once with 1X PBS. Then, 4 ml of parasite suspension were added onto HUVEC monolayer and co-cultured for 3 h at 37 °C, 5% CO<sub>2</sub> in humidified incubator. After 3 h of co-cultured, the binding medium were removed and HUVEC were gently washed several times with warm RPMI 1640 medium to removed as many unattached PRBC and RBC as possible. Then, HUVEC-bound PRBC which remained within the flask were cultured by standard parasite culture techniques as described in Chapter 2 section 2.1. These selected parasites (the first enriched parasites) were continuously cultured and the selection was repeated to get the second enriched parasites.

#### **7.2.1.4 Determination of percentage binding between HUVEC and enriched parasites and percentage apoptosis of HUVEC attached to enriched parasites**

In order to determine percentage attachment between HUVEC and the selected parasites, and also percentage apoptosis of HUVEC attached to the selected parasites, the first and second enriched malaria parasites were cultured until reached 5-8% parasitemia of trophozoite or schizont stage. Then, the selected parasites were submitted to magnetic separation technique in order to achieve 80-90% parasitemia of trophozoite or schizont stage as described in section 7.2.1.2. Malaria parasites were

prepared at 20% parasitemia in 1% haematocrit in medium 199 supplemented with 1% FCS. The parasite suspension was added to HUVEC grown on 40 mm coverslips to 80-90% confluence. HUVEC and malaria parasites were co-cultured for 3 h at 37 °C, 5% CO<sub>2</sub> in humidified incubator. In the control group, unselected ITG parasites were enriched for trophozoite or schizont stage by magnetic separation as described in section 7.2.1.2. Then, the unselected parasites were prepared at 20% parasitemia in 1% haematocrit in medium 199 supplemented with 1% FCS and co-cultured with HUVEC for 3 h at 37 °C, 5% CO<sub>2</sub> in humidified incubator. The co-culture dishes were agitated either clockwise or counter clockwise every 10-15 min to allow more cell-to-cell contact until the third hour.

After 3 h of co-cultivation, the co-culture medium was discarded. HUVEC in all groups of experiment were washed twice with 1X PBS to remove unbound uninfected red blood cells or parasites. HUVEC were double stained with annexin V and propidium iodide which were prepared by adding 8 µl of annexin V and 2 µl of 2.5 µg/ml PI into 2 ml of annexin-binding buffer. Cells were incubated in this mixture at 37 °C, 5% CO<sub>2</sub> in humidified incubator for 20 min. The coverslips were gently washed once with annexin-binding buffer. The coverslips were assembled into a Biopetechs FCS2 perfusion chamber (Biopetechs), perfused with annexin-binding buffer and observed with Zeiss Pascal confocal laser scanning microscope (CLSM). Cells were viewed through a Plan-Apochromat 63x 1.2 numerical aperture (N.A.) water objective. Fluorescence signals from annexin V and PI were collected by single excitation with argon ion laser at 488 nm and collection of emitted light through a 505-530 nm band pass filter and a 650 nm long pass filter, respectively. At least 500 cells were counted



for each replicate and scored according to the appearance of cells, i.e. attached/unattached to PRBC, blebbing and/or annexin V/PI staining.

### **7.2.2 Determination the effect of TNF- $\alpha$ on apoptosis of HUVEC**

The prolonged exposure of endothelial cells to TNF- $\alpha$  is known to induce apoptosis (Polunovsky *et al.*, 1994). To avoid apoptotic induction effect of TNF- $\alpha$  in our experiment, we tested whether the concentration of TNF- $\alpha$  used to stimulate the expression of ICAM-1 leads to apoptosis of HUVEC.

HUVEC grown on 40 mm coverslip to 80-89% confluence were stimulated with 1 ng/ml TNF- $\alpha$  (Gibco) for 18 h. Unstimulated HUVEC were used as the control. After 18 h of stimulation, HUVEC in all groups were washed once with 1X PBS and stained with annexin V and propidium iodide. The number of apoptotic cells were measured in each experimental group by counting at least 500 cells/replicate under confocal laser scanning microscope as described in section 7.2.1.4.

### **7.2.3 HUVEC immunofluorescence staining for ICAM-1 expression analysis by FACS**

HUVEC grown to 80-90% confluence in T25 cm<sup>2</sup> vented cap flasks were treated with 1 ng/ml TNF- $\alpha$  for 18 h. Untreated HUVEC were used as a control group. Cells in both groups were washed with endothelial cell culture medium followed by sera free endothelial cell culture medium. Cells were washed again with PBS. Cells were incubated with accutase (Sigma) to detach cells at 37 °C for 5-10 min. Cells were observed to rounded up and detached. Equal volume of PBS containing 1% BSA was then added to neutralise the enzyme. Cell solution was centrifuged at 1500 rpm and washed with PBS containing 1% BSA. Cells in each group were re-suspended in PBS

containing 1% BSA and split into two Eppendorf tubes in the volume of 80 µl for each Eppendorf tube. One tube of each group was incubated with 20 µl APC mouse anti-human ICAM-1 (BD biosciences) for 30 min in the dark at room temperature. Another tube left in each group was incubated with 20 µl APC mouse IgG isotype control (BD biosciences) for 30 min in the dark at room temperature. All Eppendorf tubes were centrifuged at 3000 rpm and the pellets were washed with PBS containing 1% BSA. Cells were centrifuged again and the pellets were resuspended in 500 µl PBS. ICAM-1 expression of cells in each tube was measured by FACS.

#### **7.2.4 ICAM-1 inhibition**

Malaria parasite ITG strain used in our experiment is known to selectively bind to ICAM-1 (Ockenhouse *et al.*, 1991). In this experiment, we aimed to reveal whether ICAM-1 is the receptor that parasites bind to and mediate the death of endothelial cells.

HUVEC were grown on 40 mm coverslip to 80-90% confluence. HUVEC were stimulated with 1 ng/ml TNF- $\alpha$  for 18 h to induce expression of ICAM-1 or left as unstimulated cells in the control group. The enriched parasites and parasites which selected to bind to ICAM-1 were submitted to magnetic separation to obtain concentrated trophozoite or schizont stage as described in section 7.2.1.2. Malaria parasites were prepared at 20% parasitemia in 1% haematocrit in medium 199 supplemented with 1% FCS. The parasite suspension was added to both unstimulated and stimulated HUVEC grown on coverslips. To inhibit binding of parasite to ICAM-1 on endothelial cells, HUVEC were pre-treated with 10 µg/ml anti-ICAM-1 monoclonal antibody [15.2] (Abcam) for 30 min at 37°C. HUVEC were incubated

with malaria parasites for 3 h at 37 °C, 5% CO<sub>2</sub> in humidified incubator. After that, unattached PRBC and uninfected red blood cells were washed out with 1X PBS. HUVEC were stained with annexin V and propidium iodide, and observed under confocal scanning microscopes described in section 7.2.1.4. At least 500 cells were counted for each replicate and scored according to the appearance of cells, i.e. attached/unattached to PRBC, blebbing and/or annexin V/PI staining.

#### **7.2.5 CD31, CD36 and CD105 inhibition**

To inhibit binding of PRBC to CD31, CD36 and CD105, 10 µg/ml of anti-CD31 monoclonal antibody [JC/70A] (Abcam), 10µg/ml of anti-CD36 monoclonal antibody [FA6-152] (Abcam), and 50 µg/ml of anti-CD105 polyclonal antibody (Abcam) were added to HUVEC grown on 40 mm coverslip. HUVEC were pre-treated with the antibodies for 30 min at 37 °C. The enriched malaria parasites were submitted to magnetic separation technique in order to achieve 80-90% parasitemia of trophozoite or schizont stage as described in section 7.2.1.2. Malaria parasites were prepared at 20% parasitemia in 1% haematocrit in medium 199 supplemented with 1% FCS. The parasite suspension was added to HUVEC grown on 40 mm coverslips to 80-90% confluence. HUVEC and malaria parasites were co-cultured for 3 h at 37 °C, 5% CO<sub>2</sub> in humidified incubator. After 3 h of co-culture, HUVEC were washed with 1X PBS and stained with annexin V and propidium iodide. Then, HUVEC were observed under confocal scanning microscope as described in section 7.2.1.4. At least 500 cells were counted for each replicate and scored according to the appearance of cells, i.e. attached/unattached to PRBC, blebbing and/or annexin V/PI staining.

### **7.2.6 Statistical analysis**

Results were expressed as mean  $\pm$  standard error of individual experimental groups. Statistical analysis was performed using GrapPad InStat version 3.05. Data were analysed by Mann-Whitney U test or one-way ANOVA with Tukey-Kramer Multiple Comparisons post test. A value of  $p < 0.05$  was considered significant.

## 7.3 RESULTS

### 7.3.1 Attachment between HUVEC and PRBC

After selection, parasites have more ability to bind to HUVEC when compared to parasites in control group. The amount of binding between HUVEC and PRBC were  $7.99\% \pm 0.47$  (SE) and  $7.05\% \pm 0.45$  (SE) for the first and the second parasite enrichment, respectively, whereas the amount of binding between non-enriched control PRBC and HUVEC was  $1.67\% \pm 0.13$  (SE) (the difference following enrichment was shown to be statistically significant, Fig 7.1).

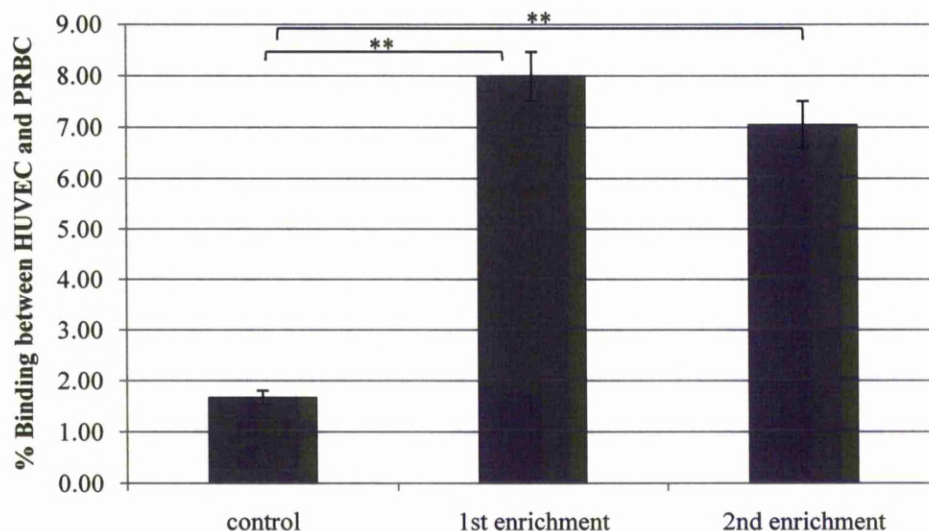


**Figure 7.1** Comparison amount of binding of PRBC to HUVEC in the control parasites, the first and the second enriched parasites. Data are mean  $\pm$  SE of at least five experiments. \*\* denotes statistical difference ( $p < 0.01$ ) as analysed by one-way ANOVA with Tukey-Kramer Multiple Comparisons post test.

### 7.3.2 Apoptosis of HUVEC attached to PRBC

Besides the increase in amount of binding, the selected parasites also have the potential to induce apoptosis of HUVEC (Fig 7.2). The amount of apoptosis among attached HUVEC were  $90.18\% \pm 6.08$  (SE) in the control group, and  $91.90\% \pm 2.58$  (SE) and  $94.19\% \pm 1.61$  (SE) in the first enriched and second enriched parasite groups, respectively. There was no statistically significant difference in the amount of apoptosis among attached HUVEC in the control group, the first enriched parasite group and the second enriched parasite group (Fig 7.3).

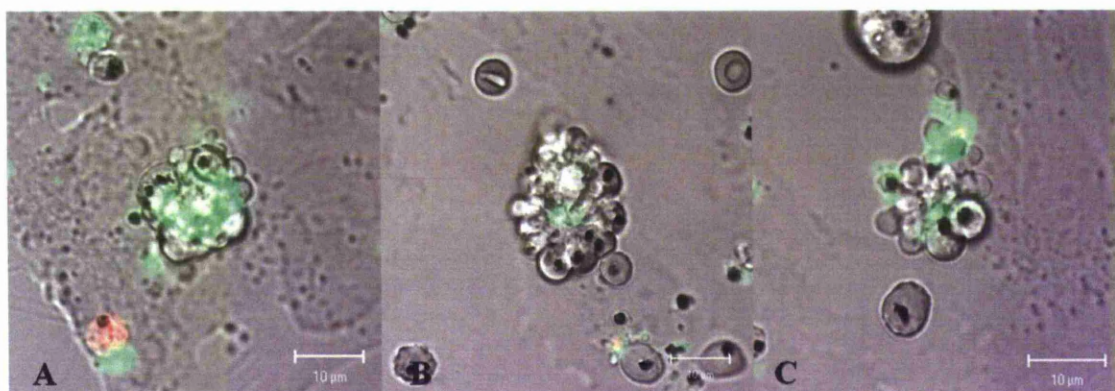


**Figure 7.2** Apoptosis of HUVEC induced by cytoadherence of (A) control (non-enriched), (B) the first enriched and (C) the second enriched parasites. Apoptotic cells displayed cell membrane blebbing and annexin V positivity.

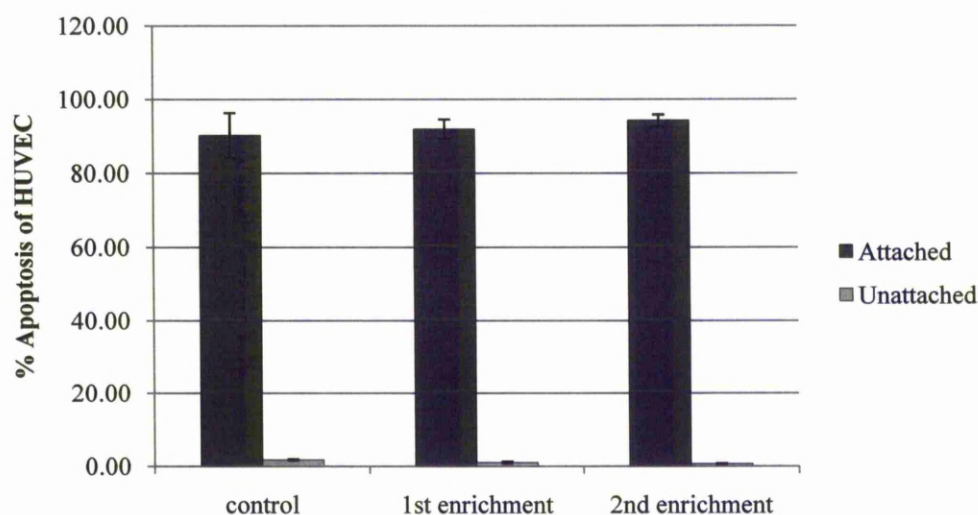


**Figure 7.3** Comparison of apoptosis (%) of HUVEC attached and unattached to PRBC in control, the first enriched parasite and the second enriched parasite group. Data are mean  $\pm$  SE of at least five experiments.

### 7.3.3 Effect of TNF- $\alpha$ on apoptosis of HUVEC

It is known that TNF- $\alpha$  can promote apoptosis of endothelial cell when exposed for prolonged periods (Polunovsky et al., 1994). TNF- $\alpha$  is also used to stimulate ICAM-1 expression on endothelial cells. To avoid the effect of apoptosis induction by TNF- $\alpha$  in our experiments, we also tested the concentration of TNF- $\alpha$  used to stimulate ICAM-1 expression of HUVEC in our experiments.

The morphology of HUVEC in unstimulated and TNF- $\alpha$  stimulated group looked similar. HUVEC appeared in attached monolayer cells. Some apoptotic cells can be seen in both groups. The apoptotic cells found in both groups appear as detached, membrane blebbing and/or annexin V positive cells. Fig 7.4 shows the images of



HUVEC in unstimulated and TNF- $\alpha$  stimulated groups taken with an inverted microscope and a confocal laser scanning microscope.

After treating HUVEC with 1 ng/ml TNF- $\alpha$  for 18 h, the quantity of apoptotic HUVEC was slightly increased when compare with control group. The percentage of apoptotic HUVEC were  $1.73\% \pm 0.41$  (SE) and  $2.23\% \pm 0.20$  (SE) in unstimulated and TNF- $\alpha$  stimulated groups, respectively (Fig 7.5). However, there was no statistically significant difference in the number of HUVEC showing signs of apoptosis in the unstimulated and TNF- $\alpha$  stimulated groups.

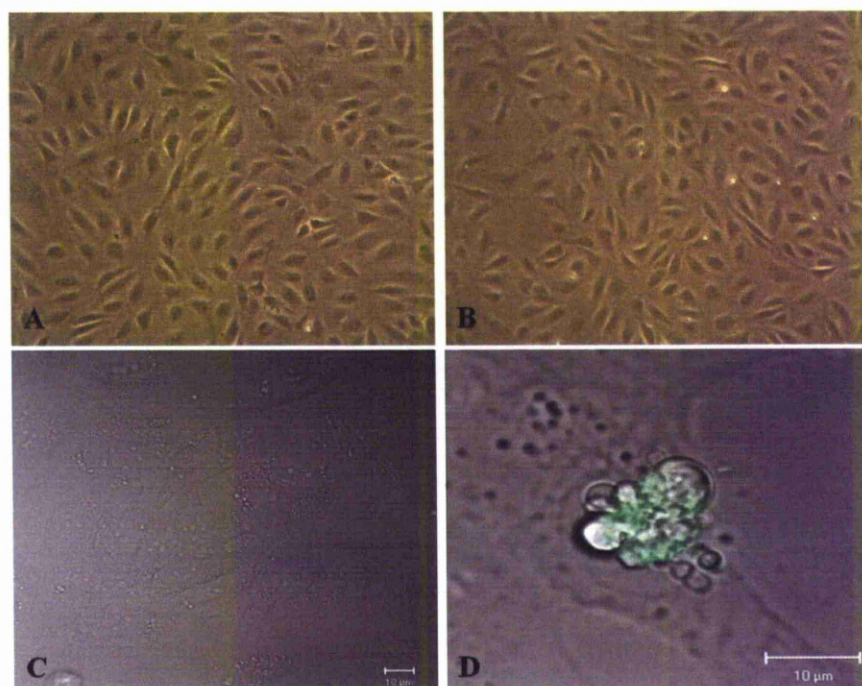


**Figure 7.4** HUVEC morphology. (A) image of unstimulated HUVEC under inverted microscope, (B) image of TNF- $\alpha$  stimulated HUVEC under inverted microscope, (C) confocal image of monolayer cells in the unstimulated group, (D) confocal image of apoptotic HUVEC in 1 ng/ml TNF- $\alpha$  stimulated group. Apoptotic cell shows membrane blebbing together with annexin V positivity.



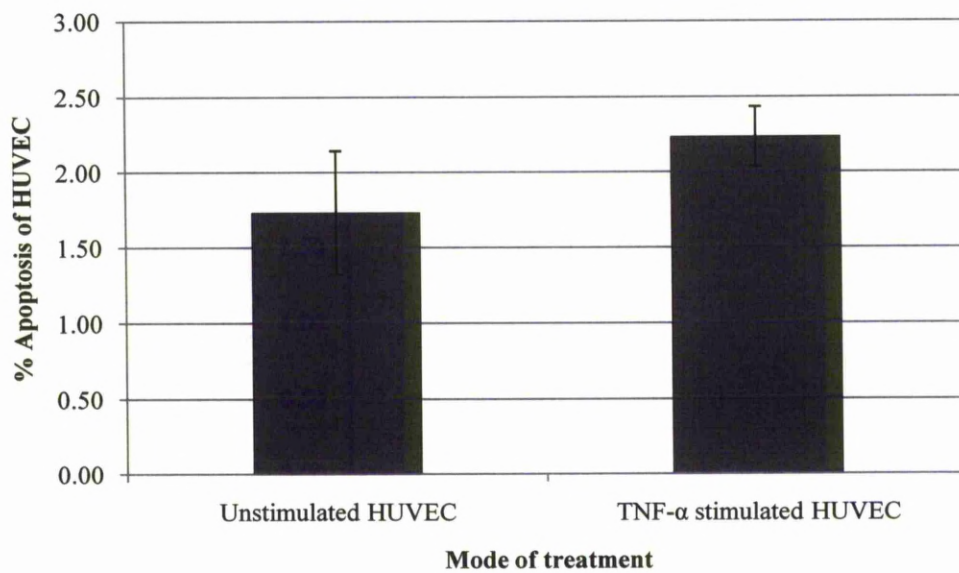
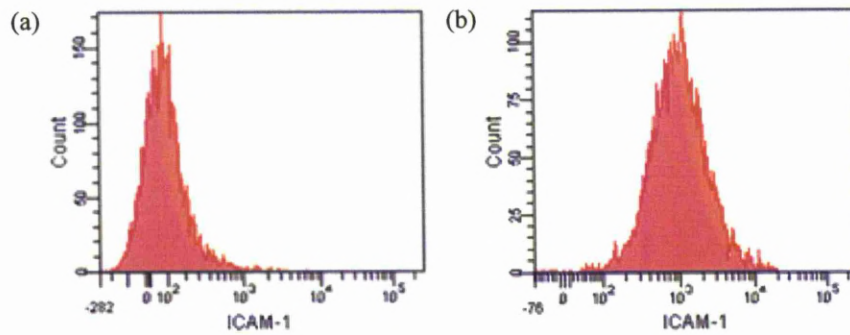


**Figure 7.5** The degree of apoptosis in unstimulated and TNF- $\alpha$  stimulated HUVEC groups. Data are mean  $\pm$  SE of at least three experiments.

#### 7.3.4 Quantitative measurement of ICAM-1 expression

To confirm the expression of ICAM-1 on HUVEC after stimulation with TNF- $\alpha$ , we measured the expression of ICAM-1 on HUVEC using FACS. Following stimulation of HUVEC with TNF- $\alpha$ , the mean fluorescence intensity (MFI) of ICAM-1 was shown to increase by approximately ten-fold ( $1,345.50 \text{ MFI} \pm 16.91 \text{ (SE)}$ ) compared to unstimulated HUVEC ( $100.17 \text{ MFI} \pm 2.77 \text{ (SE)}$ ) (Fig 7.6).

**A**



**B**

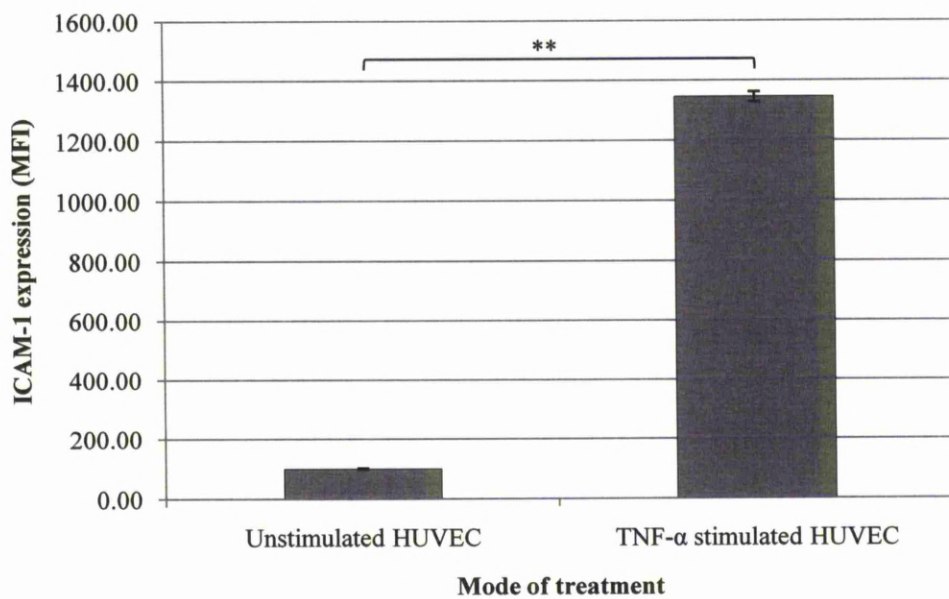


**Figure 7.6** ICAM-1 expression on HUVEC measured by FACS. (A) Representative histogram of mean fluorescence intensity of (a) control (unstimulated HUVEC) and (b) 1ng/ml TNF- $\alpha$  stimulated HUVEC. (B) Mean fluorescence intensity of ICAM-1 positive population of control and 1ng/ml TNF- $\alpha$  stimulated HUVEC. Data are mean  $\pm$  SE. \*\* denotes statistical difference ( $p < 0.01$ ) as analysed by Mann-Whitney U test.

### **7.3.5 Inhibition of binding of PRBC to ICAM-1 on HUVEC**

To reveal whether ICAM-1 is an important receptor for the observed cytoadherence-mediated apoptosis of HUVEC, unstimulated and TNF- $\alpha$  stimulated HUVEC were treated with an anti-ICAM-1 monoclonal antibody to block the binding of PRBC to ICAM-1 on HUVEC. The degree of PRBC binding for both ITG and enriched parasites to unstimulated and TNF- $\alpha$  stimulated HUVEC in the presence and absence of anti-ICAM, is given in Table 7.1 and Fig 7.7.

The amount of binding between HUVEC and the enriched parasites were almost the same quantity in all groups of the experiment. In contrast, the amount of binding between HUVEC and ICAM-1 selected parasites was increased when HUVEC were stimulated with TNF- $\alpha$ , then decreased to almost the same amount as control group when ICAM-1 mAb was added to TNF- $\alpha$  stimulated HUVEC. Furthermore, blocking of ICAM-1 in unstimulated HUVEC had no effect on binding between the ICAM-1 selected parasites and HUVEC.

There was no statistically significant difference in the percentage binding of the enriched parasites among experimental groups. However, there were statistically significant differences in the percentage binding of the ICAM-1 selected parasites among experimental groups ( $p < 0.0001$ ). The post-test showed that there were statistically significant differences in the degree of binding between the following groups; unstimulated HUVEC and TNF- $\alpha$  stimulated HUVEC, TNF- $\alpha$  stimulated HUVEC and TNF- $\alpha$  stimulated HUVEC + ICAM-1 mAb, and TNF- $\alpha$  stimulated HUVEC and unstimulated HUVEC + ICAM-1 mAb ( $p < 0.001$ ) (Fig 7.7).

	HUVEC			
	Unstimulated	TNF- $\alpha$ stimulated	Unstimulated +ICAM-1 mAb	TNF- $\alpha$ stimulated +ICAM-1 mAb
<b>Enriched ITG</b>	9.65% $\pm$ 0.20	11.53% $\pm$ 0.47	9.07% $\pm$ 0.04	10.13% $\pm$ 0.69
<b>ICAM-1 selected ITG</b>	4.09% $\pm$ 0.26	9.27% $\pm$ 0.47	3.64% $\pm$ 0.13	4.62% $\pm$ 0.19

**Table 7.1** The percentage of adhesion of the enriched parasites and the ICAM-1 selected parasites to unstimulated HUVEC and TNF- $\alpha$  stimulated HUVEC in the presence or absence of anti-ICAM-1 mAb. Data are mean  $\pm$  SE of at least five experiments.

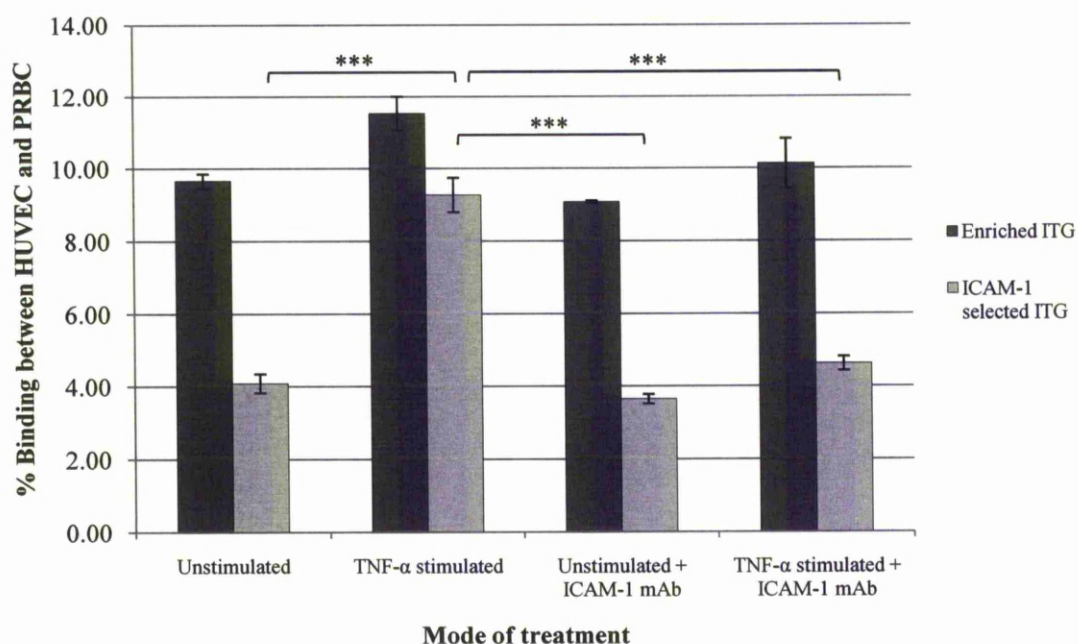


**Figure 7.7** Cytoadherence of the enriched parasite and the ICAM-1 selected parasites to unstimulated HUVEC and TNF- $\alpha$  stimulated HUVEC in the presence or absence of anti-ICAM-1 mAb. Data are mean  $\pm$  SE. \*\*\* denotes statistical difference ( $p < 0.001$ ) as analysed by one-way ANOVA with Tukey-Kramer Multiple Comparisons post test.

The degree of apoptosis of HUVEC attached to both parasite lines is shown in Table 7.2 and Fig 7.8. The amount of apoptosis in almost all experimental groups when attached to both parasite lines were approximately 90%, however, in TNF- $\alpha$  stimulated HUVEC the amount of apoptosis when HUVEC attached to both parasite lines decreased. This can be explained by the increase in the amount of binding of both parasite lines to stimulated HUVEC but some parasites failed to induce apoptosis of attached HUVEC. The morphology of apoptotic and non-apoptotic HUVEC in TNF- $\alpha$  stimulated group which attached to both parasite lines was shown in Fig 7.9.

There were statistically significant differences in percentage apoptosis of HUVEC attached to both parasite lines among experimental groups ( $p < 0.0001$ ). The post-test showed that there were statistically significant differences in percentage apoptosis of HUVEC attached to both parasite lines between the following groups; unstimulated HUVEC and TNF- $\alpha$  stimulated HUVEC, TNF- $\alpha$  stimulated HUVEC and TNF- $\alpha$  stimulated HUVEC + ICAM-1 mAb, and TNF- $\alpha$  stimulated HUVEC and unstimulated HUVEC + ICAM-1 mAb ( $p < 0.001$ ) (Fig 7.8).

	HUVEC			
	Unstimulated	TNF- $\alpha$ stimulated	Unstimulated +ICAM-1 mAb	TNF- $\alpha$ stimulated +ICAM-1 mAb
<b>Enriched ITG</b>	94.06% $\pm$ 0.72	78.84% $\pm$ 2.48	95.51% $\pm$ 1.27	93.80% $\pm$ 0.83
<b>ICAM-1 selected ITG</b>	89.69% $\pm$ 2.17	67.90% $\pm$ 2.38	92.78% $\pm$ 1.66	92.09% $\pm$ 1.23

**Table 7.2** The percentage apoptosis of unstimulated HUVEC and TNF- $\alpha$  stimulated HUVEC attached to the enriched parasites and the ICAM-1 selected parasites in the presence or absence of anti-ICAM-1 mAb. Data are mean  $\pm$  SE of at least five experiments.

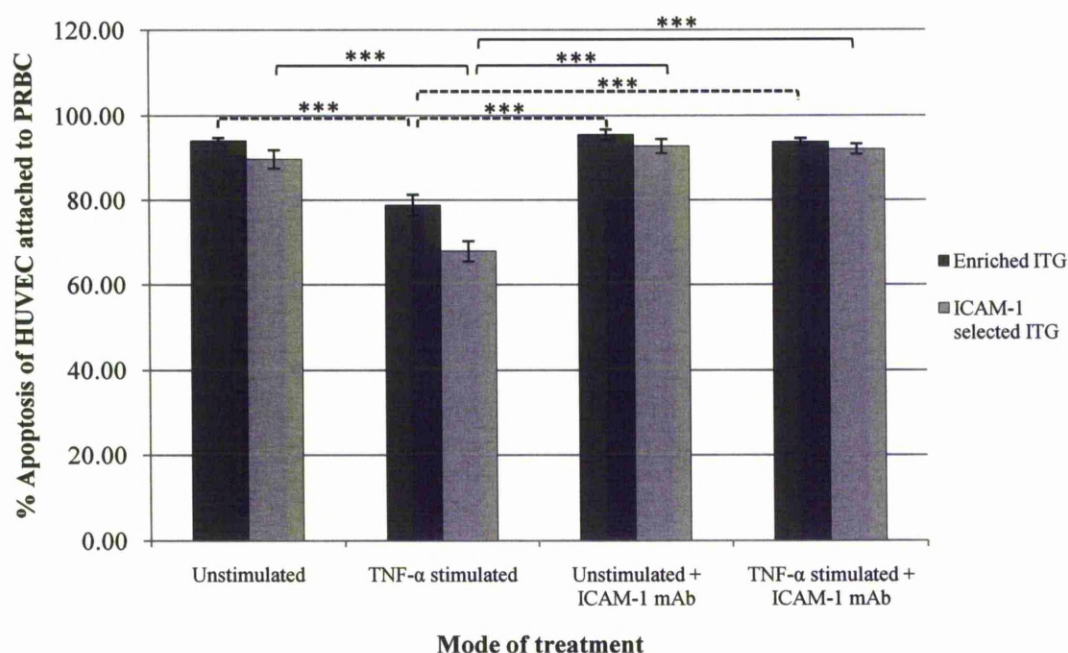


**Figure 7.8** Apoptosis of unstimulated HUVEC and TNF- $\alpha$  stimulated HUVEC attached to the enriched parasites or the ICAM-1 selected parasites in the presence or absence of anti-ICAM-1 mAb. Data are mean  $\pm$  SE. \*\*\* denotes statistical difference ( $p < 0.001$ ) as analysed by one-way ANOVA with Tukey-Kramer Multiple Comparisons post test.



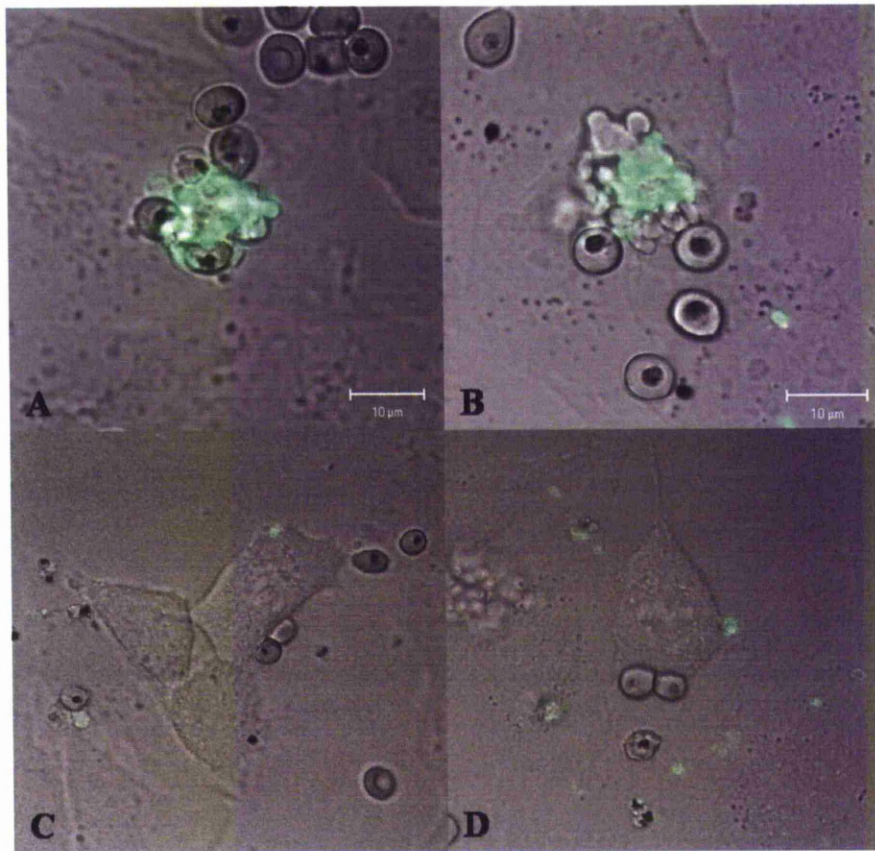


**Figure 7.9** The morphology of HUVEC in TNF- $\alpha$  stimulated group attached to enriched parasites or ICAM-1 selected parasites. (A-B) Apoptosis of TNF- $\alpha$  stimulated HUVEC induced by enriched and ICAM-1 selected parasites, respectively. Apoptotic cells shows cell membrane blebbing together with annexin V positive. (C-D) Attachment of enriched and ICAM-1 selected parasites, respectively, to TNF- $\alpha$  stimulated HUVEC failed to induce HUVEC apoptosis.



### **7.3.6 Inhibition of binding of PRBC to CD31, CD36 and CD105 on HUVEC**

According to the results from the previous experiment (section 7.3.5), the inducible receptor ICAM-1 might not be the receptor that mediates cytoadherence-induced apoptosis of HUVEC, as there was no difference in the amount of binding of the enriched parasites to HUVEC in unstimulated and TNF- $\alpha$  stimulated HUVEC. We assume that the enriched parasites do not bind to an inducible cell receptor, but that they bind to a cell surface receptor which is constitutively expressed on HUVEC. In the next experiment, we tried to block binding of parasites to HUVEC by using antibodies raised against constitutively expressed endothelial cell receptors; CD31, CD36 and CD105.

The quantity of binding of the enriched parasites to HUVEC in the presence or absence of antibodies was shown in Table 7.3. The antibodies used in our experiments had no effect on blocking the binding between parasites and HUVEC as the amount of binding after HUVEC was treated with the antibodies remained the same as in the control group. There was no statistically significant difference in percentage binding between control HUVEC and HUVEC blocked with the antibody in all experiments.

	Cell surface receptor		
	CD31	CD36	CD105
<b>Control</b>	8.23% $\pm$ 0.35	8.67% $\pm$ 0.19	8.22% $\pm$ 0.20
<b>Ab treatment</b>	8.46% $\pm$ 0.12	8.66% $\pm$ 0.10	8.35% $\pm$ 0.27

**Table 7.3** The percentage of binding between the enriched parasites and HUVEC in the presence or absence of anti-CD31 mAb, anti-CD36 mAb, and anti-CD105 pAb. Data are mean  $\pm$  SE of at least three experiments.

The quantity of apoptosis of HUVEC attached to parasites is illustrated in Table 7.4. Up to 90% of HUVEC with attached parasites in all experimental groups were observed to be undergoing apoptosis. There was no statistically significant difference in percentage apoptosis between control HUVEC and HUVEC blocked with the antibody in all experiments. Fig 7.10 shows PRBC cytoadherence-induced apoptosis of HUVEC in the presence or absence of antibodies against CD31, CD36 and CD105.

	Cell surface receptors		
	CD31	CD36	CD105
<b>Control</b>	93.28% $\pm$ 1.35	97.67% $\pm$ 0.77	95.53% $\pm$ 0.45
<b>Ab treatment</b>	93.01% $\pm$ 0.89	98.15% $\pm$ 0.46	95.92% $\pm$ 0.90

**Table 7.4** The percentage of apoptosis of the HUVEC attached to the enriched parasites in the presence or absence of CD31 mAb, CD36 mAb, and CD105 pAb. Data are mean  $\pm$  SE of at least three experiments.

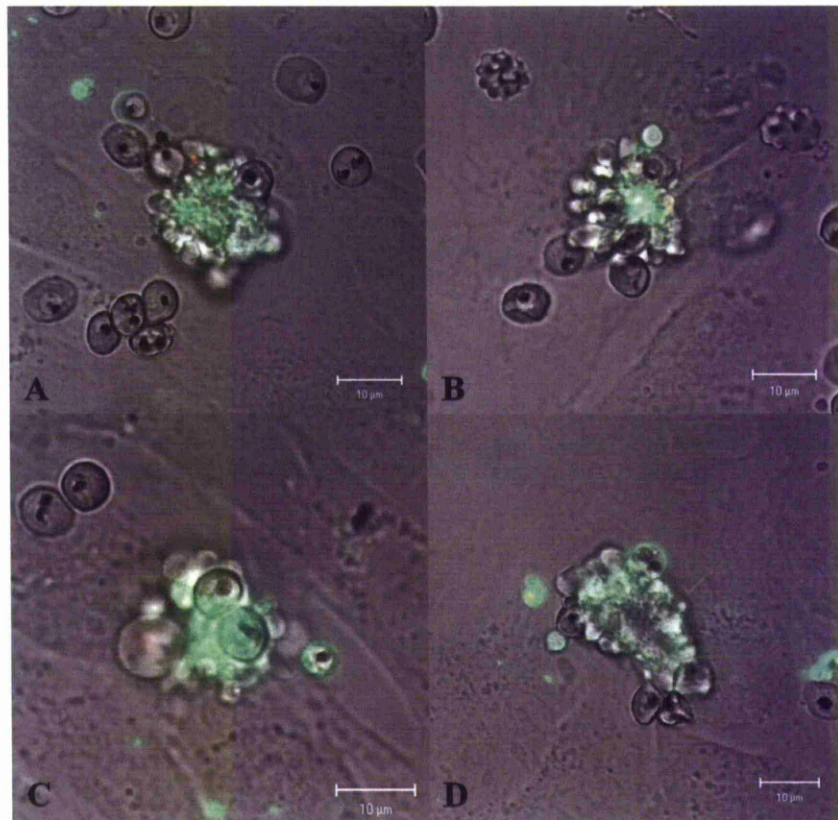


**Figure 7.10** Cytoadherence of enriched parasites induced apoptosis of HUVEC in presence or absence of cell receptors specific antibodies. (A) control group (absence of any antibodies), (B) presence of anti-CD-31 mAb, (C) presence of anti-CD36 mAb, and (D) presence of anti-CD105 pAb.

## 7.4 DISCUSSION

The enrichment of adhesive phenotype malaria parasites can be achieved by a panning procedure, where PRBC are incubated either on isolated receptor molecules coated on plates (Ockenhouse et al., 1991, Salanti *et al.*, 2003) or on receptor-expressing cells such as Saimiri brain endothelial cells (SBEC) expressing CSA and/or CD36 and ICAM-1 (Gay *et al.*, 1995), human lung endothelial cells (HLEC) expressing CD36 and ICAM-1 (Muanza *et al.*, 1996), human choriocarcinoma cells expressing CSA and CD36 (Viebig *et al.*, 2006) or Chinese hamster ovary cells (CHO) transfected with the respective receptors (Hasler *et al.*, 1993). In this final chapter, by panning ITG parasites on unstimulated HUVEC, PRBC with the cytoadherence-mediated apoptosis phenotype were successfully enriched (Fig. 7.1 and 7.3). After selection, parasites not only retained the potential to induce apoptosis of HUVEC but also displayed a greater ability to attach to HUVEC. With these improved properties, the enriched PRBC provide a better experimental strain to study the cytoadherence-induced apoptosis phenomenon.

Generally, TNF- $\alpha$  is used to activated expression of inducible adhesion molecules, including ICAM-1, on endothelial cells (Viebig *et al.*, 2005). As expected, when we treated HUVEC with TNF- $\alpha$ , we also observed increased ICAM-1 dependent PRBC binding (Table 7.1, Fig 7.7). However, TNF- $\alpha$  has been reported to induce apoptosis of endothelial cells in a concentration- and time-dependent fashion (Polunovsky et al., 1994, Robaye *et al.*, 1991). To avoid this potential effect in our experiments, we assessed the effect of TNF- $\alpha$  on our HUVEC. After stimulation of HUVEC with TNF- $\alpha$ , the degree of apoptosis (described by cell membrane blebbing and/or annexin V positivity) was only slightly higher compared to HUVEC in the control group (Fig

7.5), however, this was not statistically significant. We therefore considered that under our experimental conditions, our experiments were not affected by the duration and concentration of TNF- $\alpha$  used to activate ICAM-1 expression.

The unique ability of infected red blood cells to sequester in the microvasculature is associated with severe malaria. This process is thought to be mediated by the *Plasmodium* derived protein and modified erythrocyte protein on infected red blood cells and ligands on endothelial cells (Newton *et al.*, 2000). Several adhesion molecules on endothelial cells have been identified, including ICAM-1 (Berendt *et al.*, 1989), CD36 (Oquendo *et al.*, 1989), and CD31/PECAM-1 (Treutiger *et al.*, 1997). It is known that cytoadherence of infected red blood cells induces signalling in endothelial cells, for example, apoptosis of endothelial cells (Medana & Turner, 2007). Therefore, it is important to identify the adhesion molecules on endothelial cells mediating the cytoadhesion of infected red blood cells. In this chapter, we tried to block some molecules on HUVEC to reveal the receptors that parasites bound in order to induce apoptosis of HUVEC.

We first investigated the role of ICAM-1 in cytoadherence of infected red blood cells as our experiment involved HUVEC, which constitutively express small amounts of ICAM-1 on their surface, and the ITG parasite line, which is a strong ICAM-1 binder (Gray *et al.*, 2003, Phiri *et al.*, 2009). When HUVEC were activated to express ICAM-1, the binding of our enriched parasites was only slightly increased, whereas binding was highly increased for ICAM-1 selected parasites (Table 7.1, Fig 7.7). Although the ICAM-1 selected parasites showed a considerable increase in amount of binding to HUVEC, the majority of attached parasites failed to induce apoptosis of HUVEC. Furthermore, the anti-ICAM-1 antibody failed to inhibit the cytoadhesion, which

induced apoptosis of HUVEC, of both parasite lines. Taken together, these data suggest that ICAM-1 is unlikely to be the target of cytoadhesion and furthermore that the cytoadherence-induced apoptotic phenotype is ICAM-1-independent.

TNF- $\alpha$  activation of HUVEC was unable to increase the degree of cytoadhesion which induce apoptosis of HUVEC. Therefore, it can be hypothesised that the adhesive receptor on HUVEC mediated apoptosis is not a TNF- $\alpha$  inducible molecule(s).

As inducible receptors seems unlikely to be the target of binding of our enriched parasites, the constitutively expressed receptors on endothelial cells, including PECAM-1/CD31, CD36 and CD105, were investigated. PECAM-1/CD31 is a member of the immunoglobulin gene superfamily which is widely expressed on endothelial cells, granulocytes, monocytes and platelet (Treutiger et al., 1997). The monoclonal antibody which has been reported to be able to block the cytoadhesion of PRBC was used in our experiment (Treutiger et al., 1997, Vogt *et al.*, 2003). Unfortunately, this antibody failed to inhibit binding. Another main cytoadherence receptor CD36 which is expressed on several endothelial cells was also blocked with the monoclonal antibody. The antibody was also unable to inhibit binding of PRBC to HUVEC. The failure of anti-CD36 antibody to block binding might due to the lack of CD36 on HUVEC (Swerlick *et al.*, 1992). Although, the binding of malaria parasites to CD105 on endothelial cell has never been reported, this molecule is predominantly expressed on endothelial cells (Fonsatti & Maio, 2004). It is possible that parasites bound to this receptor and induce apoptosis of HUVEC. However, the selected antibody failed to inhibit cytoadhesion of parasites.

From all the evidence presented here, it can be concluded that cytoadhesion of enriched parasites did not involve ICAM-1, CD36, CD31 or CD105 based on our antibody inhibition studies. However, as a note of caution, it should be considered that receptors have a very large structure (approximately 90 kDa on average). Antibodies are likely only to inhibit part of the receptor and therefore more work will be required to conclusively rule out the involvement of any receptors. This notwithstanding, the data presented here suggest that the cytoadherence-mediated apoptotic phenotype of the enriched parasites probably operates via a hitherto unknown or poorly studied cell-membrane receptor and signalling pathway.

## CHAPTER 8: GENERAL DISCUSSION

---

Cerebral malaria is a complex syndrome and it is reasoned that no one single process is responsible for all of its pathogenesis. It has been proposed that the pathogenesis of cerebral malaria can be better explained by the integration of three processes, i.e. hemostasis, inflammation and PRBC sequestration. This unifying hypothesis suggests that parasite antigens activate the host inflammatory response leading to increased levels of endothelial cell adhesion molecules. This, in turn, results in a further increase in level of PRBC sequestration in the brain microvasculature (van der Heyde *et al.*, 2006). It has been shown that the interaction between PRBC and endothelial cells lining blood vessels can result in activation of intracellular signalling pathways in endothelial cells (Jenkins *et al.*, 2007, Taoufiq *et al.*, 2008) including apoptotic pathways which could be directly involved in the disruption of the blood-brain barrier (Pino *et al.*, 2003b). The work described in this thesis aims to understand the signalling events that follow the cytoadherence of PRBC to endothelial cells in order to provide a better understanding of the pathogenesis of CM.

In chapter 3, we addressed the question of what happens after cytoadherence of PRBC to endothelial cells. We demonstrated that PRBC adhesion induced apoptosis in HUVEC. This event occurred rapidly within a few hours of co-culture in the absence of any TNF- $\alpha$  activation. The morphological changes observed in the apoptotic cells included annexin V binding, cell membrane blebbing and the shedding of microparticles (MP). We found that the ability of parasites to induce endothelial apoptosis is dependent on the PRBC membrane remaining intact but independent of viability of the parasites. The level of apoptosis was markedly reduced when a pan-



caspase inhibitor (Z-VAD-FMK) was added to the co-culture. This suggested that apoptosis induced by PRBC is mediated by a caspase-dependent pathway. By measuring caspase-8 and -9 activities and using Z-IETD-FMK and Z-LEHD-FMK, which are specific inhibitors of caspase-8 and -9, respectively, we found that PRBC-induced apoptosis involves both receptor-mediated (caspase-8) and mitochondrial-mediated (caspase-9) pathways. These findings are in agreement with the published data of Pino and colleagues (Pino et al., 2003b). However, in contrast to their studies, we used the co-culture model of PRBC and HUVEC coupled with confocal microscopy to observe the apoptosis process happening in HUVEC after the adhesion of PRBC. This technique allows us to study this phenomenon at the single cell level without the interfering effect from normal HUVEC without attached PRBC. This advantage makes the single cell approach a powerful tool for the study of this process where only a variable proportion of the population of cells is undergoing change.

In the mitochondrial apoptotic pathway, there is the formation of the mitochondrial permeability transition pore which leads to a loss of mitochondrial  $\Delta\Psi$  and the releases of many apoptotic inducing factors from the mitochondria including cytochrome *c* which forms a complex with other proteins in the cytosol and activates caspase-9 (Vermeulen *et al.*, 2005). In chapter 4, we demonstrated a rapid collapse of the mitochondrial  $\Delta\Psi$  within 3 hours of co-culture in those HUVEC with adhered PRBC and which go on to demonstrate apoptosis. This observation is further confirmation of the role of the mitochondrial pathway in apoptosis of HUVEC attached to PRBC supporting the conclusions of Chapter 3.

Oxidative stress can cause peroxidation of cell membrane lipids which generates various products including 4-hydroxy-2-noneal (4-HNE). The formation of 4-HNE is

considered to be a sensitive marker of this oxidative damage (Catala, 2009). The role of oxidative stress has been implicated in PRBC-induced host cell apoptosis (Guha *et al.*, 2006, Guha *et al.*, 2007, Pino *et al.*, 2003a, Taoufiq *et al.*, 2006). In chapter 5, we used immunocytochemical staining of 4-HNE to reveal the involvement of oxidative stress in the apoptosis of HUVEC induced by PRBC. We found that the adhesion of PRBC to HUVEC led to the prominent increase of 4-HNE formation. Furthermore, DFO-chelatable substances such as heme are not responsible for this event. This data suggest that cytoadherence of PRBC induces oxidative stress in HUVEC that leads to HUVEC apoptosis.

Besides receptor-mediated and mitochondrial-mediated pathways, apoptosis can occur through several pathways, for example, ER stress-induced pathways, stress-activated protein kinase pathways and a p53-mediated pathway. In chapter 6, we tried to unveil other potential pathways which might be involved in HUVEC apoptosis induced by PRBC. To do this, we deployed various known inhibitors of these specific pathways into our co-culture system at pharmacologically relevant concentrations. The results from this chapter indicated a role for calcium signalling and NF- $\kappa$ B signalling pathways in the apoptotic phenomenon we were studying.

The results in previous chapters showed that cytoadherence of PRBC to HUVEC can trigger apoptosis signalling pathways in HUVEC. However, the endothelial cell receptor mediating PRBC binding and triggering apoptosis in our system has not been verified yet. In the final chapter, we attempted to identify the HUVEC membrane receptor involving in cytoadherence-dependent apoptosis. To aid this work, PRBC were enriched for their ability to bind and induce apoptosis in TNF- $\alpha$  unstimulated HUVEC. The enriched parasites displayed a greater ability to attach to HUVEC and

still retained the potential to induce apoptosis, as measured by the proportion of HUVEC with bound PRBC. Because the parasites used for enrichment originated from the ITG isolate which is a strong ICAM-1 binder (Gray *et al.*, 2003), it was possible that the enriched parasites were more efficient ICAM-1 binders and as such binding of PRBC onto the ICAM-1 expressed on the HUVEC was sufficient to trigger apoptosis and explain the data. To reveal the role of ICAM-1 in the apoptosis of PRBC-adhered HUVEC, the enriched parasites were co-cultured with TNF- $\alpha$  un-stimulated and TNF- $\alpha$  stimulated HUVEC in the presence or absence of anti-ICAM-1 monoclonal antibodies. The results showed that ICAM-1 and other inducible receptors are unlikely to mediate this apoptotic event. We then tried to block other constitutively expressed endothelial cell receptors which have been reported to play role in binding of PRBC, i.e. CD31 (Treutiger *et al.*, 1997) and CD 36 (Oquendo *et al.*, 1989). Unfortunately, the antibodies which successfully inhibited PRBC binding in other studies (Treutiger *et al.*, 1997, Vogt *et al.*, 2003) failed to inhibit PRBC binding in our system. The antibody against CD105, which is another constitutively expressed receptor on endothelial cells, was also used even though it has never been reported to mediate binding of PRBC to endothelial cells. However, this antibody also failed to block PRBC binding to HUVEC. From all the results found in this final chapter, we concluded that the receptor responsible for apoptosis of HUVEC induced by PRBC is unlikely to be the inducible receptors. One limitation is that as these receptors are large (approximately 90 kDa), the antibodies may only bind to small regions of the receptor. Therefore, more work is required to conclusively rule out the involvement of any receptors. However, we should remember the fact that at least for the antibodies to

CD31, CD36 and ICAM-1, literature data indicates they can functionally block binding.

The cytoadherence of PRBC to endothelial cells lining brain microvessel is an important process leading to the pathology of cerebral malaria. Our *in vitro* model demonstrated that the binding of PRBC to a receptor on endothelial cells triggers apoptosis of endothelial cells. This involved receptor-mediated and mitochondrial-mediated pathways as well as calcium signalling, oxidative stress and the activation of NF- $\kappa$ B. This deleterious effect of PRBC on endothelial cells could be directly involved in the breakdown of the blood-brain barrier, which results in the microvascular bleeding seen in brain autopsy (Halder *et al.*, 2007). Although the fine mechanisms and signalling pathways implicating in this process remain to be further defined, the data presented here could provide a better understanding of cerebral malaria, which in turn might lead to the new therapeutic intervention for the disease.

### **The proposed mechanism of PRBC-induced endothelial apoptosis**

Based on the results generated from this thesis, the proposed mechanism of endothelial apoptosis induced by PRBC was developed and illustrated in Fig 8.1. The cytoadherence of PRBC to HUVEC might occur through the interaction between parasite ligand (probably PfEMP-1) and endothelial receptor (perhaps ICAM-1 independent). This interaction leads to the activation of caspase-8 which can cleave Bid. The truncated Bid induces the translocation and insertion of other Bcl-2 family members to the mitochondrial membrane leading to the leakage of pro-apoptotic proteins from mitochondria. Reactive oxygen species (ROS) and calcium can also

induce the formation of mitochondrial permeability transition pore (PTP) resulting in the dissipation of the mitochondrial transmembrane potential ( $\Delta\Psi_m$ ) and releasing pro-apoptotic proteins such as cytochrome *c*, which can activate caspase-9. Furthermore, the activation of NF- $\kappa$ B up-regulates the pro-apoptotic genes that can aggravate apoptosis of endothelial cell.

As we have shown in Fig 8.1, there are many the missing links among the pathways. For example, the endothelial receptor and parasite ligand responsible for endothelial apoptosis still need to be defined. The source of calcium is not known, whether it is from intracellular store (endoplasmic reticulum) or extracellular source. Thus future work proposed in the next section could be performed in order to better describe the mechanism of PRBC-induced endothelial apoptosis.

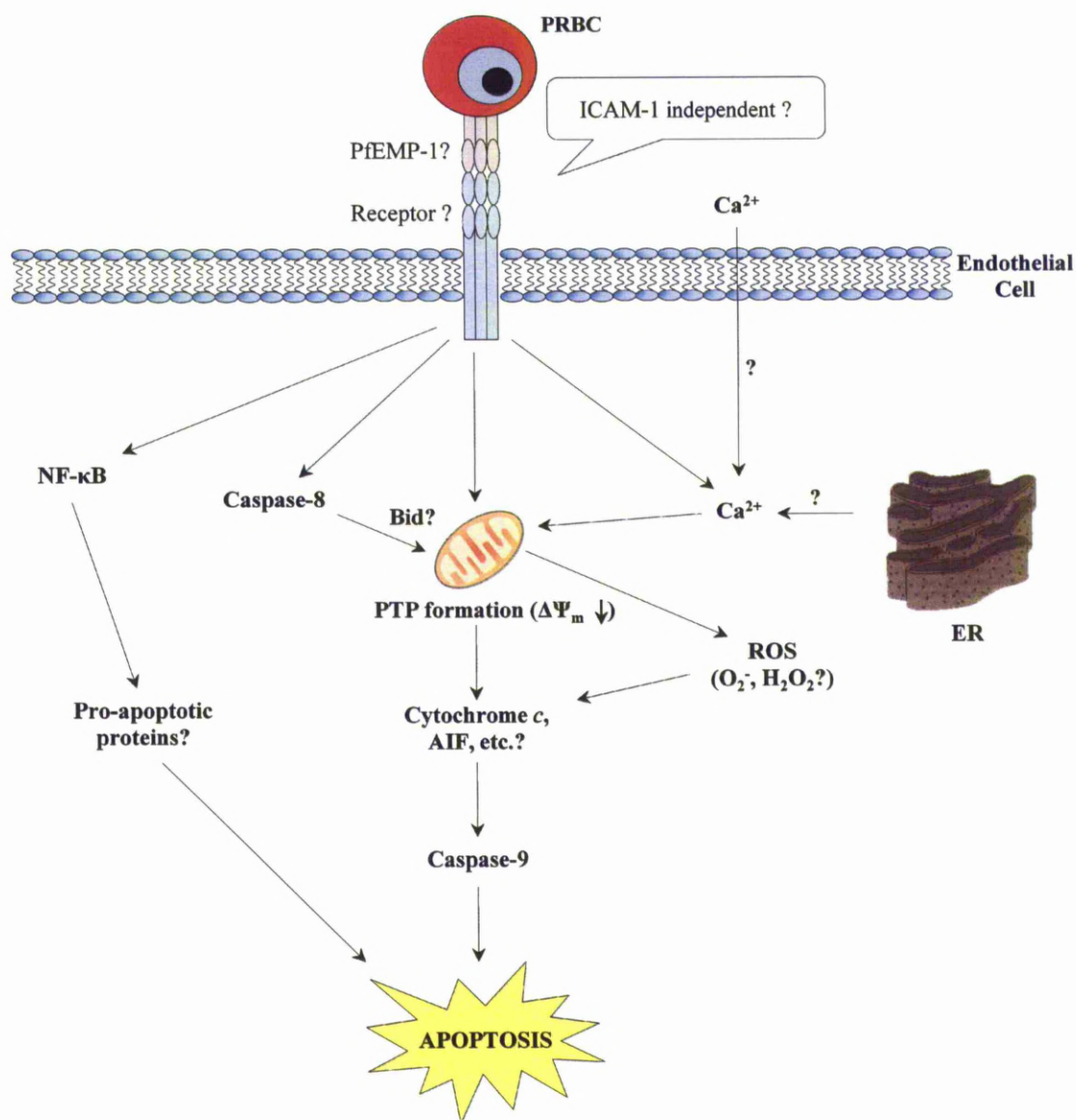


**Figure 8.1** The proposed mechanism of PRBC-induced endothelial apoptosis.

### Potential future work derived from this thesis

The BBB is the specialized interface between the vascular space and the brain parenchyma playing role in regulating solute and cellular transport into the brain (Hawkins & Davis, 2005). This barrier is the results of the tight junctions forming

between endothelial cells lining brain microvessels (Kniesel & Wolburg, 2000). It has been reported that a unique model of the BBB can be established by co-culturing endothelial cells together with astrocytes (Gaillard *et al.*, 2001, Garcia *et al.*, 2004, Jeliaskova-Mecheva & Bobilya, 2003). The contact between astrocytes and endothelial cells induced the BBB properties in endothelial cells. Endothelial cells showed significant increase in transendothelial electrical resistance (TEER), decrease in paracellular transport as well as increase in levels of occludin which is an integral membrane protein localized to tight junctions and contributing the barrier properties of endothelial cells (Gaillard *et al.*, 2001, Garcia *et al.*, 2004, Jeliaskova-Mecheva & Bobilya, 2003). In addition, the co-culture of astrocyte with endothelial cells also resulted in an increase in the activity of endothelial cell  $\gamma$ -glutamyl-transferase (GGT), a characteristic of the differentiated BBB (Garcia *et al.*, 2004). For future work, it would be interesting to use this endothelial cells-astrocytes model to study the interaction of PRBC to the BBB, as it could provide the results which reflect the physiological situation occurring *in vivo*.

In a previous study, apoptosis of endothelial cells induced by PRBC was reported after 4 hours of co-culture (Pino *et al.*, 2003b), but this process was found after 3 hours post co-culture in our study. Therefore, real-time experiments could be done to determine more precisely the time in which apoptosis occurs after HUVEC-PRBC binding.

The results presented in this thesis were performed under static conditions using HUVEC grown on coverslips co-cultured with PRBC. In a future study, endothelial grown on microslides or parallel plate chambers and the cytoadherence assay carried out under laminar flow conditions could be done to mimic physiologically relevant wall shear stresses in the microvasculature (Chakravorty *et al.*, 2008).

Cytoadherence of PRBC to HUVEC resulted in apoptosis of HUVEC which implicated both receptor-mediated and mitochondrial-mediated pathways. As described in Chapter1 (section 1.2.1), these pathways are complicated and consist of several components. By the aid of RNA silencing technology, we can selectively suppress the specific components in the apoptosis pathway (Liang *et al.*, 2007, Wilson *et al.*, 2005). Thus this technique could be used in a future study to define the fine signalling events of the pathways involving in apoptosis induced by PRBC. Our results also showed the involvement of calcium and NF- $\kappa$ B in HUVEC apoptosis induced by PRBC. The next phase of study could be done to determine the source of calcium, whether it derived from intracellular stores or extracellular source. This could be done by treating HUVEC with EGTA (an extracellular calcium chelator) (Arimoto *et al.*, 2006) or Thapsigargin (depleting intracellular calcium store) (Treiman *et al.*, 1998). The direct visualisation of NF- $\kappa$ B translocation from the cytoplasm to the nucleus using GFP fusion protein could help confirm our finding and determine the timing when the activation of NF- $\kappa$ B occurs after binding of PRBC to HUVEC (Bartfeld *et al.*, 2010).

In our final chapter, we failed in an attempt to define the endothelial cell surface receptor responsible for PRBC cytoadherence and apoptosis by using specific antibodies. As discussed in the chapter, this might be because the antibody can only block part of the large and complex molecule of the receptor. Many investigators have reported that the expression of cell surface receptors can be successfully suppressed by RNA silencing techniques (Nishiwaki *et al.*, 2003, Walker *et al.*, 2005, Walker *et al.*, 2007). This technique could be used in our further works to describe the endothelial



cell adhesion receptor which plays a role in PRBC attachment and inducing HUVEC apoptosis.

In conclusion, we have taken a single cell imaging approach to help understand the interaction between endothelial cells (in our case HUVEC) and the PRBC. We can confirm adhesion depended cell death which has elements of the well accepted apoptotic pathways. Adhesion and apoptosis requires intact PRBC but does not require living viable parasites, suggesting a simple receptor-ligand trigger rather than a cell-cell signalling event. We were able to selectively enhance binding by panning suggesting that the extent of adhesion is derived from the expression of parasite expressed ligands but we could not identify the binding receptor on the HUVEC.

## REFERENCES

---

- Akira, S. & K. Takeda, (2004) Toll-like receptor signalling. *Nat Rev Immunol* **4**: 499-511.
- Amaral, J. D., R. E. Castro, C. J. Steer & C. M. Rodrigues, (2009) p53 and the regulation of hepatocyte apoptosis: implications for disease pathogenesis. *Trends Mol Med* **15**: 531-541.
- Antonsson, B., (2004) Mitochondria and the Bcl-2 family proteins in apoptosis signaling pathways. *Mol Cell Biochem* **256-257**: 141-155.
- Aoki, M., T. Nata, R. Morishita, H. Matsushita, H. Nakagami, K. Yamamoto, K. Yamazaki, M. Nakabayashi, T. Ogihara & Y. Kaneda, (2001) Endothelial apoptosis induced by oxidative stress through activation of NF-kappaB: antiapoptotic effect of antioxidant agents on endothelial cells. *Hypertension* **38**: 48-55.
- Aravalli, R. N., S. Hu & J. R. Lokensgard, (2007) Toll-like receptor 2 signaling is a mediator of apoptosis in herpes simplex virus-infected microglia. *J Neuroinflammation* **4**: 11.
- Arimoto, E., S. Iwai, T. Sumi, Y. Ogawa & Y. Yura, (2006) Involvement of intracellular free Ca<sup>2+</sup> in enhanced release of herpes simplex virus by hydrogen peroxide. *Virol J* **3**: 62.
- Armah, H. B., N. O. Wilson, B. Y. Sarfo, M. D. Powell, V. C. Bond, W. Anderson, A. A. Adjei, R. K. Gyasi, Y. Tettey, E. K. Wiredu, J. E. Tongren, V. Udhayakumar & J. K. Stiles, (2007) Cerebrospinal fluid and serum biomarkers of cerebral malaria mortality in Ghanaian children. *Malar J* **6**: 147.
- Bainbridge, S. A., L. Belkacemi, M. Dickinson, C. H. Graham & G. N. Smith, (2006) Carbon monoxide inhibits hypoxia/reoxygenation-induced apoptosis and secondary necrosis in syncytiotrophoblast. *Am J Pathol* **169**: 774-783.
- Bartfeld, S., S. Hess, B. Bauer, N. Machuy, L. A. Ogilvie, J. Schuchhardt & T. F. Meyer, (2010) High-throughput and single-cell imaging of NF-kappaB oscillations using monoclonal cell lines. *BMC Cell Biol* **11**: 21.
- Baruch, D. I., J. A. Gormely, C. Ma, R. J. Howard & B. L. Pasloske, (1996) Plasmodium falciparum erythrocyte membrane protein 1 is a parasitized erythrocyte receptor for adherence to CD36, thrombospondin, and intercellular adhesion molecule 1. *Proc Natl Acad Sci U S A* **93**: 3497-3502.

- Beare, N. A., T. E. Taylor, S. P. Harding, S. Lewallen & M. E. Molyneux, (2006) Malarial retinopathy: a newly established diagnostic sign in severe malaria. *Am J Trop Med Hyg* **75**: 790-797.
- Berendt, A. R., A. McDowall, A. G. Craig, P. A. Bates, M. J. Sternberg, K. Marsh, C. I. Newbold & N. Hogg, (1992) The binding site on ICAM-1 for *Plasmodium falciparum*-infected erythrocytes overlaps, but is distinct from, the LFA-1-binding site. *Cell* **68**: 71-81.
- Berendt, A. R., D. L. Simmons, J. Tansey, C. I. Newbold & K. Marsh, (1989) Intercellular adhesion molecule-1 is an endothelial cell adhesion receptor for *Plasmodium falciparum*. *Nature* **341**: 57-59.
- Berendt, A. R., G. D. Tumer & C. I. Newbold, (1994) Cerebral malaria: the sequestration hypothesis. *Parasitol Today* **10**: 412-414.
- Berridge, M. J., M. D. Bootman & H. L. Roderick, (2003) Calcium signalling: dynamics, homeostasis and remodelling. *Nat Rev Mol Cell Biol* **4**: 517-529.
- Berridge, M. J., P. Lipp & M. D. Bootman, (2000) The versatility and universality of calcium signalling. *Nat Rev Mol Cell Biol* **1**: 11-21.
- Biswas, A. K., A. Hafiz, B. Banerjee, K. S. Kim, K. Datta & C. E. Chitnis, (2007) *Plasmodium falciparum* uses gC1qR/HABP1/p32 as a receptor to bind to vascular endothelium and for platelet-mediated clumping. *PLoS Pathog* **3**: 1271-1280.
- Bootman, M. D., T. J. Collins, C. M. Peppiatt, L. S. Prothero, L. MacKenzie, P. De Smet, M. Travers, S. C. Tovey, J. T. Seo, M. J. Berridge, F. Ciccolini & P. Lipp, (2001) Calcium signalling--an overview. *Semin Cell Dev Biol* **12**: 3-10.
- Borovic, S., F. Rabuzin, G. Waeg & N. Zarkovic, (2006) Enzyme-linked immunosorbent assay for 4-hydroxynonenal-histidine conjugates. *Free Radic Res* **40**: 809-820.
- Borrhalho, P. M., I. B. Moreira da Silva, M. M. Aranha, C. Albuquerque, C. Nobre Leitao, C. J. Steer & C. M. Rodrigues, (2007) Inhibition of Fas expression by RNAi modulates 5-fluorouracil-induced apoptosis in HCT116 cells expressing wild-type p53. *Biochim Biophys Acta* **1772**: 40-47.
- Bortner, C. D., N. B. Oldenburg & J. A. Cidlowski, (1995) The role of DNA fragmentation in apoptosis. *Trends Cell Biol* **5**: 21-26.
- Boyce, M., K. F. Bryant, C. Jousse, K. Long, H. P. Harding, D. Scheuner, R. J. Kaufman, D. Ma, D. M. Coen, D. Ron & J. Yuan, (2005) A selective inhibitor

- of eIF2 $\alpha$  dephosphorylation protects cells from ER stress. *Science* **307**: 935-939.
- Bratton, D. L., V. A. Fadok, D. A. Richter, J. M. Kailey, L. A. Guthrie & P. M. Henson, (1997) Appearance of phosphatidylserine on apoptotic cells requires calcium-mediated nonspecific flip-flop and is enhanced by loss of the aminophospholipid translocase. *J Biol Chem* **272**: 26159-26165.
- Brea-Calvo, G., E. Siendones, J. A. Sanchez-Alcazar, R. de Cabo & P. Navas, (2009) Cell survival from chemotherapy depends on NF-kappaB transcriptional up-regulation of coenzyme Q biosynthesis. *PLoS One* **4**: e5301.
- Breckenridge, D. G., M. Germain, J. P. Mathai, M. Nguyen & G. C. Shore, (2003) Regulation of apoptosis by endoplasmic reticulum pathways. *Oncogene* **22**: 8608-8618.
- Brown, H., S. Rogerson, T. Taylor, M. Tembo, J. Mwenechanya, M. Molyneux & G. Turner, (2001) Blood-brain barrier function in cerebral malaria in Malawian children. *Am J Trop Med Hyg* **64**: 207-213.
- Brown, H., T. T. Hien, N. Day, N. T. Mai, L. V. Chuong, T. T. Chau, P. P. Loc, N. H. Phu, D. Bethell, J. Farrar, K. Gatter, N. White & G. Turner, (1999) Evidence of blood-brain barrier dysfunction in human cerebral malaria. *Neuropathol Appl Neurobiol* **25**: 331-340.
- Buommino, E., F. Morelli, S. Metafora, F. Rossano, B. Perfetto, A. Baroni & M. A. Tufano, (1999) Porin from *Pseudomonas aeruginosa* induces apoptosis in an epithelial cell line derived from rat seminal vesicles. *Infect Immun* **67**: 4794-4800.
- Catala, A., (2006) An overview of lipid peroxidation with emphasis in outer segments of photoreceptors and the chemiluminescence assay. *Int J Biochem Cell Biol* **38**: 1482-1495.
- Catala, A., (2009) Lipid peroxidation of membrane phospholipids generates hydroxy-alkenals and oxidized phospholipids active in physiological and/or pathological conditions. *Chem Phys Lipids* **157**: 1-11.
- Chaibi, C., J. Cotte-Laffitte, C. Sandre, A. Esclatine, A. L. Servin, A. M. Quero & M. Geniteau-Legendre, (2005) Rotavirus induces apoptosis in fully differentiated human intestinal Caco-2 cells. *Virology* **332**: 480-490.
- Chakravorty, S. J., K. R. Hughes & A. G. Craig, (2008) Host response to cytoadherence in *Plasmodium falciparum*. *Biochem Soc Trans* **36**: 221-228.

- Chang-Ling, T., A. L. Neill & N. H. Hunt, (1992) Early microvascular changes in murine cerebral malaria detected in retinal wholemounts. *Am J Pathol* **140**: 1121-1130.
- Cirimotich, C. M., Y. Dong, L. S. Garver, S. Sim & G. Dimopoulos, (2010) Mosquito immune defenses against Plasmodium infection. *Dev Comp Immunol* **34**: 387-395.
- Clark, I. A. & K. A. Rockett, (1994) The cytokine theory of human cerebral malaria. *Parasitol Today* **10**: 410-412.
- Clutton, S., (1997) The importance of oxidative stress in apoptosis. *Br Med Bull* **53**: 662-668.
- Coban, C., K. J. Ishii, T. Kawai, H. Hemmi, S. Sato, S. Uematsu, M. Yamamoto, O. Takeuchi, S. Itagaki, N. Kumar, T. Horii & S. Akira, (2005) Toll-like receptor 9 mediates innate immune activation by the malaria pigment hemozoin. *J Exp Med* **201**: 19-25.
- Coban, C., Y. Igari, M. Yagi, T. Reimer, S. Koyama, T. Aoshi, K. Ohata, T. Tsukui, F. Takeshita, K. Sakurai, T. Ikegami, A. Nakagawa, T. Horii, G. Nunez, K. J. Ishii & S. Akira, (2010) Immunogenicity of whole-parasite vaccines against Plasmodium falciparum involves malarial hemozoin and host TLR9. *Cell Host Microbe* **7**: 50-61.
- Collins, T. J., M. J. Berridge, P. Lipp & M. D. Bootman, (2002) Mitochondria are morphologically and functionally heterogeneous within cells. *EMBO J* **21**: 1616-1627.
- Coltel, N., V. Combes, S. C. Wassmer, G. Chimini & G. E. Grau, (2006) Cell vesiculation and immunopathology: implications in cerebral malaria. *Microbes Infect* **8**: 2305-2316.
- Combes, V., N. Coltel, D. Faille, S. C. Wassmer & G. E. Grau, (2006) Cerebral malaria: role of microparticles and platelets in alterations of the blood-brain barrier. *Int J Parasitol* **36**: 541-546.
- Combes, V., T. E. Taylor, I. Juhan-Vague, J. L. Mege, J. Mwenechanya, M. Tembo, G. E. Grau & M. E. Molyneux, (2004) Circulating endothelial microparticles in malawian children with severe falciparum malaria complicated with coma. *JAMA* **291**: 2542-2544.
- Connolly, J. L., S. E. Rodgers, P. Clarke, D. W. Ballard, L. D. Kerr, K. L. Tyler & T. S. Dermody, (2000) Reovirus-induced apoptosis requires activation of transcription factor NF-kappaB. *J Virol* **74**: 2981-2989.

- Cooper, G. M., (2007) *The cell A molecular approach* **4th edition**: 434-451.
- Cory, S. & J. M. Adams, (2002) The Bcl2 family: regulators of the cellular life-or-death switch. *Nat Rev Cancer* **2**: 647-656.
- Cossarizza, A., M. Baccarani-Contri, G. Kalashnikova & C. Franceschi, (1993) A new method for the cytofluorimetric analysis of mitochondrial membrane potential using the J-aggregate forming lipophilic cation 5,5',6,6'-tetrachloro-1,1',3,3'-tetraethylbenzimidazolcarbocyanine iodide (JC-1). *Biochem Biophys Res Commun* **197**: 40-45.
- Cowan, K. J. & K. B. Storey, (2003) Mitogen-activated protein kinases: new signaling pathways functioning in cellular responses to environmental stress. *J Exp Biol* **206**: 1107-1115.
- Cox-Singh, J., J. Hiu, S. B. Lucas, P. C. Divis, M. Zulkarnaen, P. Chandran, K. T. Wong, P. Adem, S. R. Zaki, B. Singh & S. Krishna, (2010) Severe malaria - a case of fatal *Plasmodium knowlesi* infection with post-mortem findings: a case report. *Malar J* **9**: 10.
- Cox-Singh, J., T. M. Davis, K. S. Lee, S. S. Shamsul, A. Matusop, S. Ratnam, H. A. Rahman, D. J. Conway & B. Singh, (2008) *Plasmodium knowlesi* malaria in humans is widely distributed and potentially life threatening. *Clin Infect Dis* **46**: 165-171.
- de Souza, J. B. & E. M. Riley, (2002) Cerebral malaria: the contribution of studies in animal models to our understanding of immunopathogenesis. *Microbes Infect* **4**: 291-300.
- Dehio, M., M. Quebatte, S. Foser & U. Certa, (2005) The transcriptional response of human endothelial cells to infection with *Bartonella henselae* is dominated by genes controlling innate immune responses, cell cycle, and vascular remodelling. *Thromb Haemost* **94**: 347-361.
- Deng, Y., X. Ren, L. Yang, Y. Lin & X. Wu, (2003) A JNK-dependent pathway is required for TNF $\alpha$ -induced apoptosis. *Cell* **115**: 61-70.
- Eda, S. & I. W. Sherman, (2002) Cytoadherence of malaria-infected red blood cells involves exposure of phosphatidylserine. *Cell Physiol Biochem* **12**: 373-384.
- Eda, S. & I. W. Sherman, (2004) *Plasmodium falciparum*-infected erythrocytes bind to the RGD motif of fibronectin via the band 3-related adhesin. *Exp Parasitol* **107**: 157-162.

- Eda, S., J. Lawler & I. W. Sherman, (1999) Plasmodium falciparum-infected erythrocyte adhesion to the type 3 repeat domain of thrombospondin-1 is mediated by a modified band 3 protein. *Mol Biochem Parasitol* **100**: 195-205.
- Elmore, S., (2007) Apoptosis: a review of programmed cell death. *Toxicol Pathol* **35**: 495-516.
- Equils, O., D. Lu, M. Gatter, S. S. Witkin, C. Bertolotto, M. Arditi, J. A. McGregor, C. F. Simmons & C. J. Hobel, (2006) Chlamydia heat shock protein 60 induces trophoblast apoptosis through TLR4. *J Immunol* **177**: 1257-1263.
- Fadok, V. A., D. R. Voelker, P. A. Campbell, J. J. Cohen, D. L. Bratton & P. M. Henson, (1992) Exposure of phosphatidylserine on the surface of apoptotic lymphocytes triggers specific recognition and removal by macrophages. *J Immunol* **148**: 2207-2216.
- Faure, E., O. Equils, P. A. Sieling, L. Thomas, F. X. Zhang, C. J. Kirschning, N. Polentarutti, M. Muzio & M. Arditi, (2000) Bacterial lipopolysaccharide activates NF-kappaB through toll-like receptor 4 (TLR-4) in cultured human dermal endothelial cells. Differential expression of TLR-4 and TLR-2 in endothelial cells. *J Biol Chem* **275**: 11058-11063.
- Fischer, S. F., M. Rehm, A. Bauer, F. Hofling, S. Kirschnek, M. Rutz, S. Bauer, H. Wagner & G. Hacker, (2005) Toll-like receptor 9 signaling can sensitize fibroblasts for apoptosis. *Immunol Lett* **97**: 115-122.
- Fonsatti, E. & M. Maio, (2004) Highlights on endoglin (CD105): from basic findings towards clinical applications in human cancer. *J Transl Med* **2**: 18.
- Gaillard, P. J., L. H. Voorwinden, J. L. Nielsen, A. Ivanov, R. Atsumi, H. Engman, C. Ringbom, A. G. de Boer & D. D. Breimer, (2001) Establishment and functional characterization of an in vitro model of the blood-brain barrier, comprising a co-culture of brain capillary endothelial cells and astrocytes. *Eur J Pharm Sci* **12**: 215-222.
- Garcia, C. M., D. C. Darland, L. J. Massingham & P. A. D'Amore, (2004) Endothelial cell-astrocyte interactions and TGF beta are required for induction of blood-neural barrier properties. *Brain Res Dev Brain Res* **152**: 25-38.
- Garlanda, C. & E. Dejana, (1997) Heterogeneity of endothelial cells. Specific markers. *Arterioscler Thromb Vasc Biol* **17**: 1193-1202.
- Gaur, D., D. C. Mayer & L. H. Miller, (2004) Parasite ligand-host receptor interactions during invasion of erythrocytes by Plasmodium merozoites. *Int J Parasitol* **34**: 1413-1429.

- Gay, F., C. Robert, B. Pouvelle, S. Peyrol, A. Scherf & J. Gysin, (1995) Isolation and characterization of brain microvascular endothelial cells from Saimiri monkeys. An in vitro model for sequestration of Plasmodium falciparum-infected erythrocytes. *J Immunol Methods* **184**: 15-28.
- Glover, S. J., R. J. Maude, T. E. Taylor, M. E. Molyneux & N. A. Beare, (2010) Malarial retinopathy and fluorescein angiography findings in a Malawian child with cerebral malaria. *Lancet Infect Dis* **10**: 440.
- Gowda, D. C., (2007) TLR-mediated cell signaling by malaria GPIs. *Trends Parasitol* **23**: 596-604.
- Grau, G. E., C. D. Mackenzie, R. A. Carr, M. Redard, G. Pizzolato, C. Allasia, C. Cataldo, T. E. Taylor & M. E. Molyneux, (2003) Platelet accumulation in brain microvessels in fatal pediatric cerebral malaria. *J Infect Dis* **187**: 461-466.
- Gray, C., C. McCormick, G. Turner & A. Craig, (2003) ICAM-1 can play a major role in mediating P. falciparum adhesion to endothelium under flow. *Mol Biochem Parasitol* **128**: 187-193.
- Green, D. R. & G. Kroemer, (2004) The pathophysiology of mitochondrial cell death. *Science* **305**: 626-629.
- Greenwalt, D. E., R. H. Lipsky, C. F. Ockenhouse, H. Ikeda, N. N. Tandon & G. A. Jamieson, (1992) Membrane glycoprotein CD36: a review of its roles in adherence, signal transduction, and transfusion medicine. *Blood* **80**: 1105-1115.
- Grethe, S., M. P. Ares, T. Andersson & M. I. Porn-Ares, (2004) p38 MAPK mediates TNF-induced apoptosis in endothelial cells via phosphorylation and downregulation of Bcl-x(L). *Exp Cell Res* **298**: 632-642.
- Grimm, S., M. K. Bauer, P. A. Baeuerle & K. Schulze-Osthoff, (1996) Bcl-2 down-regulates the activity of transcription factor NF-kappaB induced upon apoptosis. *J Cell Biol* **134**: 13-23.
- Guha, M., P. Maity, V. Choubey, K. Mitra, R. J. Reiter & U. Bandyopadhyay, (2007) Melatonin inhibits free radical-mediated mitochondrial-dependent hepatocyte apoptosis and liver damage induced during malarial infection. *J Pineal Res* **43**: 372-381.
- Guha, M., S. Kumar, V. Choubey, P. Maity & U. Bandyopadhyay, (2006) Apoptosis in liver during malaria: role of oxidative stress and implication of mitochondrial pathway. *FASEB J* **20**: 1224-1226.



- Haldar, K., S. C. Murphy, D. A. Milner & T. E. Taylor, (2007) Malaria: mechanisms of erythrocytic infection and pathological correlates of severe disease. *Annu Rev Pathol* **2**: 217-249.
- Hansberger, M. W., J. A. Campbell, P. Danthi, P. Arrate, K. N. Pennington, K. B. Marcu, D. W. Ballard & T. S. Dermody, (2007) IkappaB kinase subunits alpha and gamma are required for activation of NF-kappaB and induction of apoptosis by mammalian reovirus. *J Virol* **81**: 1360-1371.
- Hasler, T., G. R. Albrecht, M. R. Van Schravendijk, J. C. Aguiar, K. E. Morehead, B. L. Pasloske, C. Ma, J. W. Barnwell, B. Greenwood & R. J. Howard, (1993) An improved microassay for Plasmodium falciparum cytoadherence using stable transformants of Chinese hamster ovary cells expressing CD36 or intercellular adhesion molecule-1. *Am J Trop Med Hyg* **48**: 332-347.
- Haupt, S., M. Berger, Z. Goldberg & Y. Haupt, (2003) Apoptosis - the p53 network. *J Cell Sci* **116**: 4077-4085.
- Hawkins, B. T. & T. P. Davis, (2005) The blood-brain barrier/neurovascular unit in health and disease. *Pharmacol Rev* **57**: 173-185.
- Hayden, M. S. & S. Ghosh, (2008) Shared principles in NF-kappaB signaling. *Cell* **132**: 344-362.
- Hemmer, C. J., A. Vogt, M. Unverricht, R. Krause, M. Lademann & E. C. Reisinger, (2008) Malaria and bacterial sepsis: similar mechanisms of endothelial apoptosis and its prevention in vitro. *Crit Care Med* **36**: 2562-2568.
- Hemmer, C. J., H. A. Lehr, K. Westphal, M. Unverricht, M. Kratzius & E. C. Reisinger, (2005) Plasmodium falciparum Malaria: reduction of endothelial cell apoptosis in vitro. *Infect Immun* **73**: 1764-1770.
- Hengartner, M. O., (2000) The biochemistry of apoptosis. *Nature* **407**: 770-776.
- Ho, M., B. Singh, S. Looareesuwan, T. M. Davis, D. Bunnag & N. J. White, (1991) Clinical correlates of in vitro Plasmodium falciparum cytoadherence. *Infect Immun* **59**: 873-878.
- Ho, M., T. Schollaardt, X. Niu, S. Looareesuwan, K. D. Patel & P. Kubes, (1998) Characterization of Plasmodium falciparum-infected erythrocyte and P-selectin interaction under flow conditions. *Blood* **91**: 4803-4809.
- Hsu, L. C., J. M. Park, K. Zhang, J. L. Luo, S. Maeda, R. J. Kaufman, L. Eckmann, D. G. Guiney & M. Karin, (2004) The protein kinase PKR is required for

macrophage apoptosis after activation of Toll-like receptor 4. *Nature* **428**: 341-345.

- Hughes, K. R., G. A. Biagini & A. G. Craig, (2010) Continued cytoadherence of *Plasmodium falciparum* infected red blood cells after antimalarial treatment. *Mol Biochem Parasitol* **169**: 71-78.
- Jacobi, J., B. Kristal, J. Chezar, S. M. Shaul & S. Sela, (2005) Exogenous superoxide mediates pro-oxidative, proinflammatory, and procoagulatory changes in primary endothelial cell cultures. *Free Radic Biol Med* **39**: 1238-1248.
- Jain, V., H. B. Armah, J. E. Tongren, R. M. Ned, N. O. Wilson, S. Crawford, P. K. Joel, M. P. Singh, A. C. Nagpal, A. P. Dash, V. Udhayakumar, N. Singh & J. K. Stiles, (2008) Plasma IP-10, apoptotic and angiogenic factors associated with fatal cerebral malaria in India. *Malar J* **7**: 83.
- Jeliazkova-Mecheva, V. V. & D. J. Bobilya, (2003) A porcine astrocyte/endothelial cell co-culture model of the blood-brain barrier. *Brain Res Brain Res Protoc* **12**: 91-98.
- Jenkins, N., Y. Wu, S. Chakravorty, O. Kai, K. Marsh & A. Craig, (2007) *Plasmodium falciparum* intercellular adhesion molecule-1-based cytoadherence-related signaling in human endothelial cells. *J Infect Dis* **196**: 321-327.
- Jiang, S., S. C. Chow, P. Nicotera & S. Orrenius, (1994) Intracellular Ca<sup>2+</sup> signals activate apoptosis in thymocytes: studies using the Ca(2+)-ATPase inhibitor thapsigargin. *Exp Cell Res* **212**: 84-92.
- Jin, Z. & W. S. El-Deiry, (2005) Overview of cell death signaling pathways. *Cancer Biol Ther* **4**: 139-163.
- John, C. C., (2007) Cerebral malaria pathogenesis: what can we learn from microarray analysis? *Am J Pathol* **171**: 1729-1732.
- Joza, N., S. A. Susin, E. Daugas, W. L. Stanford, S. K. Cho, C. Y. Li, T. Sasaki, A. J. Elia, H. Y. Cheng, L. Ravagnan, K. F. Ferri, N. Zamzami, A. Wakeham, R. Hakem, H. Yoshida, Y. Y. Kong, T. W. Mak, J. C. Zuniga-Pflucker, G. Kroemer & J. M. Penninger, (2001) Essential role of the mitochondrial apoptosis-inducing factor in programmed cell death. *Nature* **410**: 549-554.
- Kaneko, Y. & A. Tsukamoto, (1994) Thapsigargin-induced persistent intracellular calcium pool depletion and apoptosis in human hepatoma cells. *Cancer Lett* **79**: 147-155.

- Karahashi, H., K. S. Michelsen & M. Arditi, (2009) Lipopolysaccharide-induced apoptosis in transformed bovine brain endothelial cells and human dermal microvessel endothelial cells: the role of JNK. *J Immunol* **182**: 7280-7286.
- Kawai, T. & S. Akira, (2006) TLR signaling. *Cell Death Differ* **13**: 816-825.
- Keller, S. A., D. Hernandez-Hopkins, J. Vider, V. Ponomarev, E. Hyjek, E. J. Schattner & E. Cesarman, (2006) NF-kappaB is essential for the progression of KSHV- and EBV-infected lymphomas in vivo. *Blood* **107**: 3295-3302.
- Kirchgatter, K. & H. A. Del Portillo, (2005) Clinical and molecular aspects of severe malaria. *An Acad Bras Cienc* **77**: 455-475.
- Kleinberg, L. & B. Davidson, (2009) Cell survival and apoptosis-related molecules in cancer cells in effusions: a comprehensive review. *Diagn Cytopathol* **37**: 613-624.
- Kniesel, U. & H. Wolburg, (2000) Tight junctions of the blood-brain barrier. *Cell Mol Neurobiol* **20**: 57-76.
- Krishnegowda, G., A. M. Hajjar, J. Zhu, E. J. Douglass, S. Uematsu, S. Akira, A. S. Woods & D. C. Gowda, (2005) Induction of proinflammatory responses in macrophages by the glycosylphosphatidylinositols of *Plasmodium falciparum*: cell signaling receptors, glycosylphosphatidylinositol (GPI) structural requirement, and regulation of GPI activity. *J Biol Chem* **280**: 8606-8616.
- Kuhnel, F., L. Zender, Y. Paul, M. K. Tietze, C. Trautwein, M. Manns & S. Kubicka, (2000) NFkappaB mediates apoptosis through transcriptional activation of Fas (CD95) in adenoviral hepatitis. *J Biol Chem* **275**: 6421-6427.
- Lackner, P., C. Burger, K. Pfaller, V. Heussler, R. Helbok, M. Morandell, G. Broessner, E. Tannich, E. Schmutzhard & R. Beer, (2007) Apoptosis in experimental cerebral malaria: spatial profile of cleaved caspase-3 and ultrastructural alterations in different disease stages. *Neuropathol Appl Neurobiol* **33**: 560-571.
- Lambros, C. & J. P. Vanderberg, (1979) Synchronization of *Plasmodium falciparum* erythrocytic stages in culture. *J Parasitol* **65**: 418-420.
- Lamikanra, A. A., M. Theron, T. W. Kooij & D. J. Roberts, (2009) Hemozoin (malarial pigment) directly promotes apoptosis of erythroid precursors. *PLoS One* **4**: e8446.

- Levick, V., H. Coffey & S. R. D'Mello, (1995) Opposing effects of thapsigargin on the survival of developing cerebellar granule neurons in culture. *Brain Res* **676**: 325-335.
- Li, L. Y., X. Luo & X. Wang, (2001) Endonuclease G is an apoptotic DNase when released from mitochondria. *Nature* **412**: 95-99.
- Liang, X., Y. Liu, Q. Zhang, L. Gao, L. Han, C. Ma, L. Zhang, Y. H. Chen & W. Sun, (2007) Hepatitis B virus sensitizes hepatocytes to TRAIL-induced apoptosis through Bax. *J Immunol* **178**: 503-510.
- Lin, K. I., S. H. Lee, R. Narayanan, J. M. Baraban, J. M. Hardwick & R. R. Ratan, (1995) Thiol agents and Bcl-2 identify an alphavirus-induced apoptotic pathway that requires activation of the transcription factor NF-kappa B. *J Cell Biol* **131**: 1149-1161.
- Liu, J. & A. Lin, (2005) Role of JNK activation in apoptosis: a double-edged sword. *Cell Res* **15**: 36-42.
- Liu, X. M., G. B. Chapman, K. J. Peyton, A. I. Schafer & W. Durante, (2002) Carbon monoxide inhibits apoptosis in vascular smooth muscle cells. *Cardiovasc Res* **55**: 396-405.
- Liu, Z. G., H. Hsu, D. V. Goeddel & M. Karin, (1996) Dissection of TNF receptor 1 effector functions: JNK activation is not linked to apoptosis while NF-kappaB activation prevents cell death. *Cell* **87**: 565-576.
- Livengood, A. J., C. C. Wu & D. A. Carson, (2007) Opposing roles of RNA receptors TLR3 and RIG-I in the inflammatory response to double-stranded RNA in a Kaposi's sarcoma cell line. *Cell Immunol* **249**: 55-62.
- Lomonosova, E., J. Ryerse & G. Chinnadurai, (2009) BAX/BAK-independent mitoptosis during cell death induced by proteasome inhibition? *Mol Cancer Res* **7**: 1268-1284.
- Lopez, M., L. M. Sly, Y. Luu, D. Young, H. Cooper & N. E. Reiner, (2003) The 19-kDa Mycobacterium tuberculosis protein induces macrophage apoptosis through Toll-like receptor-2. *J Immunol* **170**: 2409-2416.
- Lovegrove, F. E., S. A. Gharib, S. N. Patel, C. A. Hawkes, K. C. Kain & W. C. Liles, (2007) Expression microarray analysis implicates apoptosis and interferon-responsive mechanisms in susceptibility to experimental cerebral malaria. *Am J Pathol* **171**: 1894-1903.

- Loyevsky, M., C. John, B. Dickens, V. Hu, J. H. Miller & V. R. Gordeuk, (1999) Chelation of iron within the erythrocytic *Plasmodium falciparum* parasite by iron chelators. *Mol Biochem Parasitol* **101**: 43-59.
- Lytton, S. D., B. Mester, J. Libman, A. Shanzer & Z. I. Cabantchik, (1994) Mode of action of iron (III) chelators as antimalarials: II. Evidence for differential effects on parasite iron-dependent nucleic acid synthesis. *Blood* **84**: 910-915.
- Ma, Y., J. Li, I. Chiu, Y. Wang, J. A. Sloane, J. Lu, B. Kosaras, R. L. Sidman, J. J. Volpe & T. Vartanian, (2006) Toll-like receptor 8 functions as a negative regulator of neurite outgrowth and inducer of neuronal apoptosis. *J Cell Biol* **175**: 209-215.
- Mabeza, G. F., M. Loyevsky, V. R. Gordeuk & G. Weiss, (1999) Iron chelation therapy for malaria: a review. *Pharmacol Ther* **81**: 53-75.
- Marchenko, N. D., A. Zaika & U. M. Moll, (2000) Death signal-induced localization of p53 protein to mitochondria. A potential role in apoptotic signaling. *J Biol Chem* **275**: 16202-16212.
- Martikainen, P. & J. Isaacs, (1990) Role of calcium in the programmed death of rat prostatic glandular cells. *Prostate* **17**: 175-187.
- Mattson, M. P. & S. L. Chan, (2003) Calcium orchestrates apoptosis. *Nat Cell Biol* **5**: 1041-1043.
- Matusali, G., G. Arena, A. De Leo, L. Di Renzo & E. Mattia, (2009) Inhibition of p38 MAP kinase pathway induces apoptosis and prevents Epstein Barr virus reactivation in Raji cells exposed to lytic cycle inducing compounds. *Mol Cancer* **8**: 18.
- Maude, R. J., A. M. Dondorp, A. Abu Sayeed, N. P. Day, N. J. White & N. A. Beare, (2009) The eye in cerebral malaria: what can it teach us? *Trans R Soc Trop Med Hyg* **103**: 661-664.
- Medana, I. M. & G. D. Turner, (2006) Human cerebral malaria and the blood-brain barrier. *Int J Parasitol* **36**: 555-568.
- Medana, I. M. & G. D. Turner, (2007) *Plasmodium falciparum* and the blood-brain barrier--contacts and consequences. *J Infect Dis* **195**: 921-923.
- Medana, I. M., N. T. Mai, N. P. Day, T. T. Hien, D. Bethell, N. H. Phu, J. Farrar, N. J. White & G. D. Turner, (2001) Cellular stress and injury responses in the brains of adult Vietnamese patients with fatal *Plasmodium falciparum* malaria. *Neuropathol Appl Neurobiol* **27**: 421-433.

- Meguro, T., B. Chen, J. Lancon & J. H. Zhang, (2001) Oxyhemoglobin induces caspase-mediated cell death in cerebral endothelial cells. *J Neurochem* **77**: 1128-1135.
- Miu, J., N. H. Hunt & H. J. Ball, (2008) Predominance of interferon-related responses in the brain during murine malaria, as identified by microarray analysis. *Infect Immun* **76**: 1812-1824.
- Montgomery, J., F. A. Mphande, M. Berriman, A. Pain, S. J. Rogerson, T. E. Taylor, M. E. Molyneux & A. Craig, (2007) Differential var gene expression in the organs of patients dying of falciparum malaria. *Mol Microbiol* **65**: 959-967.
- Muanza, K., F. Gay, C. Behr & A. Scherf, (1996) Primary culture of human lung microvessel endothelial cells: a useful in vitro model for studying Plasmodium falciparum-infected erythrocyte cytoadherence. *Res Immunol* **147**: 149-163.
- Muller, A., D. Gunther, F. Dux, M. Naumann, T. F. Meyer & T. Rudel, (1999) Neisserial porin (PorB) causes rapid calcium influx in target cells and induces apoptosis by the activation of cysteine proteases. *EMBO J* **18**: 339-352.
- Nemajerova, A., S. Wolff, O. Petrenko & U. M. Moll, (2005) Viral and cellular oncogenes induce rapid mitochondrial translocation of p53 in primary epithelial and endothelial cells early in apoptosis. *FEBS Lett* **579**: 6079-6083.
- Neumann, M. & M. Naumann, (2007) Beyond IkappaBs: alternative regulation of NF-kappaB activity. *FASEB J* **21**: 2642-2654.
- Newbold, C., P. Warn, G. Black, A. Berendt, A. Craig, B. Snow, M. Msobo, N. Peshu & K. Marsh, (1997) Receptor-specific adhesion and clinical disease in Plasmodium falciparum. *Am J Trop Med Hyg* **57**: 389-398.
- Newhouse, K., S. L. Hsuan, S. H. Chang, B. Cai, Y. Wang & Z. Xia, (2004) Rotenone-induced apoptosis is mediated by p38 and JNK MAP kinases in human dopaminergic SH-SY5Y cells. *Toxicol Sci* **79**: 137-146.
- Newton, C. R., T. T. Hien & N. White, (2000) Cerebral malaria. *J Neurol Neurosurg Psychiatry* **69**: 433-441.
- Nishiwaki, Y., T. Yokota, M. Hiraoka, M. Miyagishi, K. Taira, M. Isobe, H. Mizusawa & M. Yoshida, (2003) Introduction of short interfering RNA to silence endogenous E-selectin in vascular endothelium leads to successful inhibition of leukocyte adhesion. *Biochem Biophys Res Commun* **310**: 1062-1066.

- Ockenhouse, C. F., M. Ho, N. N. Tandon, G. A. Van Seventer, S. Shaw, N. J. White, G. A. Jamieson, J. D. Chulay & H. K. Webster, (1991) Molecular basis of sequestration in severe and uncomplicated *Plasmodium falciparum* malaria: differential adhesion of infected erythrocytes to CD36 and ICAM-1. *J Infect Dis* **164**: 163-169.
- Ockenhouse, C. F., R. Betageri, T. A. Springer & D. E. Staunton, (1992a) *Plasmodium falciparum*-infected erythrocytes bind ICAM-1 at a site distinct from LFA-1, Mac-1, and human rhinovirus. *Cell* **68**: 63-69.
- Ockenhouse, C. F., T. Tegoshi, Y. Maeno, C. Benjamin, M. Ho, K. E. Kan, Y. Thway, K. Win, M. Aikawa & R. R. Lobb, (1992b) Human vascular endothelial cell adhesion receptors for *Plasmodium falciparum*-infected erythrocytes: roles for endothelial leukocyte adhesion molecule 1 and vascular cell adhesion molecule 1. *J Exp Med* **176**: 1183-1189.
- Oquendo, P., E. Hundt, J. Lawler & B. Seed, (1989) CD36 directly mediates cytoadherence of *Plasmodium falciparum* parasitized erythrocytes. *Cell* **58**: 95-101.
- Orrenius, S., B. Zhivotovsky & P. Nicotera, (2003) Regulation of cell death: the calcium-apoptosis link. *Nat Rev Mol Cell Biol* **4**: 552-565.
- Pamplona, A., A. Ferreira, J. Balla, V. Jeney, G. Balla, S. Epiphanyo, A. Chora, C. D. Rodrigues, I. P. Gregoire, M. Cunha-Rodrigues, S. Portugal, M. P. Soares & M. M. Mota, (2007) Heme oxygenase-1 and carbon monoxide suppress the pathogenesis of experimental cerebral malaria. *Nat Med* **13**: 703-710.
- Park, K. S., I. Jo, K. Pak, S. W. Bae, H. Rhim, S. H. Suh, J. Park, H. Zhu, I. So & K. W. Kim, (2002) FCCP depolarizes plasma membrane potential by activating proton and Na<sup>+</sup> currents in bovine aortic endothelial cells. *Pflugers Arch* **443**: 344-352.
- Parroche, P., F. N. Lauw, N. Goutagny, E. Latz, B. G. Monks, A. Visintin, K. A. Halmen, M. Lamphier, M. Olivier, D. C. Bartholomeu, R. T. Gazzinelli & D. T. Golenbock, (2007) Malaria hemozoin is immunologically inert but radically enhances innate responses by presenting malaria DNA to Toll-like receptor 9. *Proc Natl Acad Sci U S A* **104**: 1919-1924.
- Pasternak, N. D. & R. Dzikowski, (2009) PfEMP1: an antigen that plays a key role in the pathogenicity and immune evasion of the malaria parasite *Plasmodium falciparum*. *Int J Biochem Cell Biol* **41**: 1463-1466.

- Paul, F., S. Roath, D. Melville, D. C. Warhurst & J. O. Osisanya, (1981) Separation of malaria-infected erythrocytes from whole blood: use of a selective high-gradient magnetic separation technique. *Lancet* **2**: 70-71.
- Petit, P. X., H. Lecoecur, E. Zorn, C. Daguët, B. Mignotte & M. L. Gougeon, (1995) Alterations in mitochondrial structure and function are early events of dexamethasone-induced thymocyte apoptosis. *J Cell Biol* **130**: 157-167.
- Phiri, H., J. Montgomery, M. Molyneux & A. Craig, (2009) Competitive endothelial adhesion between *Plasmodium falciparum* isolates under physiological flow conditions. *Malar J* **8**: 214.
- Pietsch, E. C., S. M. Sykes, S. B. McMahon & M. E. Murphy, (2008) The p53 family and programmed cell death. *Oncogene* **27**: 6507-6521.
- Pino, P., I. Vouldoukis, J. P. Kolb, N. Mahmoudi, I. Desportes-Livage, F. Bricaire, M. Danis, B. Dugas & D. Mazier, (2003b) *Plasmodium falciparum*-infected erythrocyte adhesion induces caspase activation and apoptosis in human endothelial cells. *J Infect Dis* **187**: 1283-1290.
- Pino, P., I. Vouldoukis, N. Dugas, G. Hassani-Loppion, B. Dugas & D. Mazier, (2003a) Redox-dependent apoptosis in human endothelial cells after adhesion of *Plasmodium falciparum*-infected erythrocytes. *Ann N Y Acad Sci* **1010**: 582-586.
- Pino, P., Z. Taoufiq, J. Nitcheu, I. Vouldoukis & D. Mazier, (2005) Blood-brain barrier breakdown during cerebral malaria: suicide or murder? *Thromb Haemost* **94**: 336-340.
- Pinton, P., D. Ferrari, E. Rapizzi, F. Di Virgilio, T. Pozzan & R. Rizzuto, (2002) A role for calcium in Bcl-2 action? *Biochimie* **84**: 195-201.
- Polunovsky, V. A., C. H. Wendt, D. H. Ingbar, M. S. Peterson & P. B. Bitterman, (1994) Induction of endothelial cell apoptosis by TNF alpha: modulation by inhibitors of protein synthesis. *Exp Cell Res* **214**: 584-594.
- Pongponratn, E., G. D. Turner, N. P. Day, N. H. Phu, J. A. Simpson, K. Stepniewska, N. T. Mai, P. Viriyavejakul, S. Looareesuwan, T. T. Hien, D. J. Ferguson & N. J. White, (2003) An ultrastructural study of the brain in fatal *Plasmodium falciparum* malaria. *Am J Trop Med Hyg* **69**: 345-359.
- Potter, S. M., T. Chan-Ling, E. Rosinova, H. J. Ball, A. J. Mitchell & N. H. Hunt, (2006) A role for Fas-Fas ligand interactions during the late-stage neuropathological processes of experimental cerebral malaria. *J Neuroimmunol* **173**: 96-107.



- Potter, S., T. Chan-Ling, H. J. Ball, H. Mansour, A. Mitchell, L. Maluish & N. H. Hunt, (2006) Perforin mediated apoptosis of cerebral microvascular endothelial cells during experimental cerebral malaria. *Int J Parasitol* **36**: 485-496.
- Pouvelle, B., V. Matarazzo, C. Jurzynski, J. Nemeth, M. Ramharter, G. Rougon & J. Gysin, (2007) Neural cell adhesion molecule, a new cytoadhesion receptor for *Plasmodium falciparum*-infected erythrocytes capable of aggregation. *Infect Immun* **75**: 3516-3522.
- Prudencio, M., A. Rodriguez & M. M. Mota, (2006) The silent path to thousands of merozoites: the *Plasmodium* liver stage. *Nat Rev Microbiol* **4**: 849-856.
- Rai, N. K., K. Tripathi, D. Sharma & V. K. Shukla, (2005) Apoptosis: a basic physiologic process in wound healing. *Int J Low Extrem Wounds* **4**: 138-144.
- Rao, R. V., H. M. Ellerby & D. E. Bredesen, (2004) Coupling endoplasmic reticulum stress to the cell death program. *Cell Death Differ* **11**: 372-380.
- Robaye, B., R. Mosselmans, W. Fiers, J. E. Dumont & P. Galand, (1991) Tumor necrosis factor induces apoptosis (programmed cell death) in normal endothelial cells in vitro. *Am J Pathol* **138**: 447-453.
- Roberts, D. D., J. A. Sherwood, S. L. Spitalnik, L. J. Panton, R. J. Howard, V. M. Dixit, W. A. Frazier, L. H. Miller & V. Ginsburg, (1985) Thrombospondin binds *falciparum* malaria parasitized erythrocytes and may mediate cytoadherence. *Nature* **318**: 64-66.
- Roberts, D. J., A. G. Craig, A. R. Berendt, R. Pinches, G. Nash, K. Marsh & C. I. Newbold, (1992) Rapid switching to multiple antigenic and adhesive phenotypes in malaria [see comments]. *Nature* **357**: 689-692.
- Rock, E. P., E. F. Roth, Jr., R. R. Rojas-Corona, J. A. Sherwood, R. L. Nagel, R. J. Howard & D. K. Kaul, (1988) Thrombospondin mediates the cytoadherence of *Plasmodium falciparum*-infected red cells to vascular endothelium in shear flow conditions. *Blood* **71**: 71-75.
- Rogerson, S. J., R. Tembenu, C. Dobano, S. Plitt, T. E. Taylor & M. E. Molyneux, (1999) Cytoadherence characteristics of *Plasmodium falciparum*-infected erythrocytes from Malawian children with severe and uncomplicated malaria. *Am J Trop Med Hyg* **61**: 467-472.
- Rowe, J. A., A. Claessens, R. A. Corrigan & M. Arman, (2009) Adhesion of *Plasmodium falciparum*-infected erythrocytes to human cells: molecular mechanisms and therapeutic implications. *Expert Rev Mol Med* **11**: e16.

- Ruckdeschel, K., G. Pfaffinger, R. Haase, A. Sing, H. Weighardt, G. Hacker, B. Holzmann & J. Heesemann, (2004) Signaling of apoptosis through TLRs critically involves toll/IL-1 receptor domain-containing adapter inducing IFN-beta, but not MyD88, in bacteria-infected murine macrophages. *J Immunol* **173**: 3320-3328.
- Salanti, A., T. Staalsoe, T. Lavstsen, A. T. Jensen, M. P. Sowa, D. E. Arnot, L. Hviid & T. G. Theander, (2003) Selective upregulation of a single distinctly structured var gene in chondroitin sulphate A-adhering Plasmodium falciparum involved in pregnancy-associated malaria. *Mol Microbiol* **49**: 179-191.
- Salaun, B., I. Coste, M. C. Rissoan, S. J. Lebecque & T. Renno, (2006) TLR3 can directly trigger apoptosis in human cancer cells. *J Immunol* **176**: 4894-4901.
- Salaun, B., P. Romero & S. Lebecque, (2007) Toll-like receptors' two-edged sword: when immunity meets apoptosis. *Eur J Immunol* **37**: 3311-3318.
- Sato, K., J. Balla, L. Otterbein, R. N. Smith, S. Brouard, Y. Lin, E. Csizmadia, J. Seigny, S. C. Robson, G. Vercellotti, A. M. Choi, F. H. Bach & M. P. Soares, (2001) Carbon monoxide generated by heme oxygenase-1 suppresses the rejection of mouse-to-rat cardiac transplants. *J Immunol* **166**: 4185-4194.
- Scherf, A., J. J. Lopez-Rubio & L. Riviere, (2008) Antigenic variation in Plasmodium falciparum. *Annu Rev Microbiol* **62**: 445-470.
- Schimmer, A. D., (2004) Inhibitor of apoptosis proteins: translating basic knowledge into clinical practice. *Cancer Res* **64**: 7183-7190.
- Schroder, M. & R. J. Kaufman, (2005) The mammalian unfolded protein response. *Annu Rev Biochem* **74**: 739-789.
- Schultz, D. R. & W. J. Harrington, Jr., (2003) Apoptosis: programmed cell death at a molecular level. *Semin Arthritis Rheum* **32**: 345-369.
- Schwarzer, E., H. Kuhn, E. Valente & P. Arese, (2003) Malaria-parasitized erythrocytes and hemozoin nonenzymatically generate large amounts of hydroxy fatty acids that inhibit monocyte functions. *Blood* **101**: 722-728.
- Schwarzer, E., O. Muller, P. Arese, W. G. Siems & T. Grune, (1996) Increased levels of 4-hydroxynonenal in human monocytes fed with malarial pigment hemozoin. A possible clue for hemozoin toxicity. *FEBS Lett* **388**: 119-122.
- Serghides, L., T. G. Smith, S. N. Patel & K. C. Kain, (2003) CD36 and malaria: friends or foes? *Trends Parasitol* **19**: 461-469.

- Siano, J. P., K. K. Grady, P. Millet & T. M. Wick, (1998) Short report: Plasmodium falciparum: cytoadherence to alpha(v)beta3 on human microvascular endothelial cells. *Am J Trop Med Hyg* **59**: 77-79.
- Simak, J., K. Holada & J. G. Vostal, (2002) Release of annexin V-binding membrane microparticles from cultured human umbilical vein endothelial cells after treatment with camptothecin. *BMC Cell Biol* **3**: 11.
- Singh, B., L. Kim Sung, A. Matusop, A. Radhakrishnan, S. S. Shamsul, J. Cox-Singh, A. Thomas & D. J. Conway, (2004) A large focus of naturally acquired Plasmodium knowlesi infections in human beings. *Lancet* **363**: 1017-1024.
- Skaug, B., X. Jiang & Z. J. Chen, (2009) The role of ubiquitin in NF-kappaB regulatory pathways. *Annu Rev Biochem* **78**: 769-796.
- Skorokhod, A., E. Schwarzer, G. Gremo & P. Arese, (2007) HNE produced by the malaria parasite Plasmodium falciparum generates HNE-protein adducts and decreases erythrocyte deformability. *Redox Rep* **12**: 73-75.
- Skorokhod, O. A., L. Caione, T. Marrocco, G. Migliardi, V. Barrera, P. Arese, W. Piacibello & E. Schwarzer, (2010) Inhibition of erythropoiesis in malaria anemia: role of hemozoin and hemozoin-generated 4-hydroxynonenal. *Blood*.
- Smith, J. D., B. Gamain, D. I. Baruch & S. Kyes, (2001) Decoding the language of var genes and Plasmodium falciparum sequestration. *Trends Parasitol* **17**: 538-545.
- Soares, M. P., Y. Lin, J. Anrather, E. Csizmadia, K. Takigami, K. Sato, S. T. Grey, R. B. Colvin, A. M. Choi, K. D. Poss & F. H. Bach, (1998) Expression of heme oxygenase-1 can determine cardiac xenograft survival. *Nat Med* **4**: 1073-1077.
- Song, R., Z. Zhou, P. K. Kim, R. A. Shapiro, F. Liu, C. Ferran, A. M. Choi & L. E. Otterbein, (2004) Carbon monoxide promotes Fas/CD95-induced apoptosis in Jurkat cells. *J Biol Chem* **279**: 44327-44334.
- Springer, A. L., L. M. Smith, D. Q. Mackay, S. O. Nelson & J. D. Smith, (2004) Functional interdependence of the DBLbeta domain and c2 region for binding of the Plasmodium falciparum variant antigen to ICAM-1. *Mol Biochem Parasitol* **137**: 55-64.
- Stark, L. A., K. Reid, O. J. Sansom, F. V. Din, S. Guichard, I. Mayer, D. I. Jodrell, A. R. Clarke & M. G. Dunlop, (2007) Aspirin activates the NF-kappaB signalling pathway and induces apoptosis in intestinal neoplasia in two in vivo models of human colorectal cancer. *Carcinogenesis* **28**: 968-976.

- Sutherland, C. J., N. Tanomsing, D. Nolder, M. Oguike, C. Jennison, S. Pukrittayakamee, C. Dolecek, T. T. Hien, V. E. do Rosario, A. P. Arez, J. Pinto, P. Michon, A. A. Escalante, F. Nosten, M. Burke, R. Lee, M. Blaze, T. D. Otto, J. W. Barnwell, A. Pain, J. Williams, N. J. White, N. P. Day, G. Snounou, P. J. Lockhart, P. L. Chiodini, M. Imwong & S. D. Polley, (2010) Two nonrecombining sympatric forms of the human malaria parasite *Plasmodium ovale* occur globally. *J Infect Dis* **201**: 1544-1550.
- Swerlick, R. A., K. H. Lee, T. M. Wick & T. J. Lawley, (1992) Human dermal microvascular endothelial but not human umbilical vein endothelial cells express CD36 in vivo and in vitro. *J Immunol* **148**: 78-83.
- Takeda, K., T. Kaisho & S. Akira, (2003) Toll-like receptors. *Annu Rev Immunol* **21**: 335-376.
- Taoufiq, Z., F. Gay, J. Balvanyos, L. Ciceron, M. Tefit, P. Lechat & D. Mazier, (2008) Rho kinase inhibition in severe malaria: thwarting parasite-induced collateral damage to endothelia. *J Infect Dis* **197**: 1062-1073.
- Taoufiq, Z., P. Pino, N. Dugas, M. Conti, M. Tefit, D. Mazier & I. Vouldoukis, (2006) Transient supplementation of superoxide dismutase protects endothelial cells against *Plasmodium falciparum*-induced oxidative stress. *Mol Biochem Parasitol* **150**: 166-173.
- Taylor, T. E., W. J. Fu, R. A. Carr, R. O. Whitten, J. S. Mueller, N. G. Fosiko, S. Lewallen, N. G. Liomba & M. E. Molyneux, (2004) Differentiating the pathologies of cerebral malaria by postmortem parasite counts. *Nat Med* **10**: 143-145.
- Thompson, C. B., (1995) Apoptosis in the pathogenesis and treatment of disease. *Science* **267**: 1456-1462.
- Thumwood, C. M., N. H. Hunt, I. A. Clark & W. B. Cowden, (1988) Breakdown of the blood-brain barrier in murine cerebral malaria. *Parasitology* **96** ( Pt 3): 579-589.
- Toure, F. S., O. Ouwe-Missi-Oukem-Boyer, U. Bisvigou, O. Moussa, C. Rogier, P. Pino, D. Mazier & S. Bisser, (2008) Apoptosis: a potential triggering mechanism of neurological manifestation in *Plasmodium falciparum* malaria. *Parasite Immunol* **30**: 47-51.
- Trager, W. & J. B. Jensen, (1976) Human malaria parasites in continuous culture. *Science* **193**: 673-675.

- Treeratanapiboon, L., K. Psathaki, J. Wegener, S. Looareesuwan, H. J. Galla & R. Udomsangpetch, (2005) In vitro study of malaria parasite induced disruption of blood-brain barrier. *Biochem Biophys Res Commun* **335**: 810-818.
- Treiman, M., C. Caspersen & S. B. Christensen, (1998) A tool coming of age: thapsigargin as an inhibitor of sarco-endoplasmic reticulum Ca(2+)-ATPases. *Trends Pharmacol Sci* **19**: 131-135.
- Treutiger, C. J., A. Heddini, V. Fernandez, W. A. Muller & M. Wahlgren, (1997) PECAM-1/CD31, an endothelial receptor for binding Plasmodium falciparum-infected erythrocytes. *Nat Med* **3**: 1405-1408.
- Tripathi, A. K., D. J. Sullivan & M. F. Stins, (2006) Plasmodium falciparum-infected erythrocytes increase intercellular adhesion molecule 1 expression on brain endothelium through NF-kappaB. *Infect Immun* **74**: 3262-3270.
- Tripathi, A. K., D. J. Sullivan & M. F. Stins, (2007) Plasmodium falciparum-infected erythrocytes decrease the integrity of human blood-brain barrier endothelial cell monolayers. *J Infect Dis* **195**: 942-950.
- Tripathi, A. K., W. Sha, V. Shulaev, M. F. Stins & D. J. Sullivan, Jr., (2009) Plasmodium falciparum-infected erythrocytes induce NF-kappaB regulated inflammatory pathways in human cerebral endothelium. *Blood* **114**: 4243-4252.
- Turner, G. D., H. Morrison, M. Jones, T. M. Davis, S. Looareesuwan, I. D. Buley, K. C. Gatter, C. I. Newbold, S. Pukritayakamee, B. Nagachinta & et al., (1994) An immunohistochemical study of the pathology of fatal malaria. Evidence for widespread endothelial activation and a potential role for intercellular adhesion molecule-1 in cerebral sequestration. *Am J Pathol* **145**: 1057-1069.
- Udomsangpetch, R., P. H. Reinhardt, T. Schollaardt, J. F. Elliott, P. Kubes & M. Ho, (1997) Promiscuity of clinical Plasmodium falciparum isolates for multiple adhesion molecules under flow conditions. *J Immunol* **158**: 4358-4364.
- Van Antwerp, D. J., S. J. Martin, T. Kafri, D. R. Green & I. M. Verma, (1996) Suppression of TNF-alpha-induced apoptosis by NF-kappaB. *Science* **274**: 787-789.
- van der Heyde, H. C., J. Nolan, V. Combes, I. Gramaglia & G. E. Grau, (2006) A unified hypothesis for the genesis of cerebral malaria: sequestration, inflammation and hemostasis leading to microcirculatory dysfunction. *Trends Parasitol* **22**: 503-508.

- van Loo, G., M. van Gurp, B. Depuydt, S. M. Srinivasula, I. Rodriguez, E. S. Alnemri, K. Gevaert, J. Vandekerckhove, W. Declercq & P. Vandenabeele, (2002) The serine protease Omi/HtrA2 is released from mitochondria during apoptosis. Omi interacts with caspase-inhibitor XIAP and induces enhanced caspase activity. *Cell Death Differ* **9**: 20-26.
- van Zyl, R. L., I. Havlik, E. Hempelmann, A. P. MacPhail & L. McNamara, (1993) Malaria pigment and extracellular iron. Possible target for iron chelating agents. *Biochem Pharmacol* **45**: 1431-1436.
- Vayssiere, J. L., P. X. Petit, Y. Risler & B. Mignotte, (1994) Commitment to apoptosis is associated with changes in mitochondrial biogenesis and activity in cell lines conditionally immortalized with simian virus 40. *Proc Natl Acad Sci U S A* **91**: 11752-11756.
- Vermes, I., C. Haanen, H. Steffens-Nakken & C. Reutelingsperger, (1995) A novel assay for apoptosis. Flow cytometric detection of phosphatidylserine expression on early apoptotic cells using fluorescein labelled Annexin V. *J Immunol Methods* **184**: 39-51.
- Vermeulen, K., D. R. Van Bockstaele & Z. N. Berneman, (2005) Apoptosis: mechanisms and relevance in cancer. *Ann Hematol* **84**: 627-639.
- Viebig, N. K., M. C. Nunes, A. Scherf & B. Gamain, (2006) The human placental derived BeWo cell line: a useful model for selecting Plasmodium falciparum CSA-binding parasites. *Exp Parasitol* **112**: 121-125.
- Viebig, N. K., U. Wulbrand, R. Forster, K. T. Andrews, M. Lanzer & P. A. Knolle, (2005) Direct activation of human endothelial cells by Plasmodium falciparum-infected erythrocytes. *Infect Immun* **73**: 3271-3277.
- Vogt, A. M., A. Barragan, Q. Chen, F. Kironde, D. Spillmann & M. Wahlgren, (2003) Heparan sulfate on endothelial cells mediates the binding of Plasmodium falciparum-infected erythrocytes via the DBL1alpha domain of PfEMP1. *Blood* **101**: 2405-2411.
- Vousden, K. H. & X. Lu, (2002) Live or let die: the cell's response to p53. *Nat Rev Cancer* **2**: 594-604.
- Wada, T. & J. M. Penninger, (2004) Mitogen-activated protein kinases in apoptosis regulation. *Oncogene* **23**: 2838-2849.
- Wagner, E. F. & A. R. Nebreda, (2009) Signal integration by JNK and p38 MAPK pathways in cancer development. *Nat Rev Cancer* **9**: 537-549.

- Walker, T., H. P. Wendel, L. Tetzloff, C. Raabe, O. Heidenreich, P. Simon, A. M. Scheule & G. Ziemer, (2007) Inhibition of adhesion molecule expression on human venous endothelial cells by non-viral siRNA transfection. *J Cell Mol Med* **11**: 139-147.
- Walker, T., H. P. Wendel, L. Tetzloff, O. Heidenreich & G. Ziemer, (2005) Suppression of ICAM-1 in human venous endothelial cells by small interfering RNAs. *Eur J Cardiothorac Surg* **28**: 816-820.
- Wang, C. Y., M. W. Mayo & A. S. Baldwin, Jr., (1996) TNF- and cancer therapy-induced apoptosis: potentiation by inhibition of NF-kappaB. *Science* **274**: 784-787.
- Wang, S., Z. Liu, L. Wang & X. Zhang, (2009) NF-kappaB signaling pathway, inflammation and colorectal cancer. *Cell Mol Immunol* **6**: 327-334.
- Warren, M. C., E. A. Bump, D. Medeiros & S. J. Braunhut, (2000) Oxidative stress-induced apoptosis of endothelial cells. *Free Radic Biol Med* **29**: 537-547.
- Wassmer, S. C., C. Lepolard, B. Traore, B. Pouvelle, J. Gysin & G. E. Grau, (2004) Platelets reorient Plasmodium falciparum-infected erythrocyte cytoadhesion to activated endothelial cells. *J Infect Dis* **189**: 180-189.
- Wassmer, S. C., J. B. de Souza, C. Frere, F. J. Candal, I. Juhan-Vague & G. E. Grau, (2006b) TGF-beta1 released from activated platelets can induce TNF-stimulated human brain endothelium apoptosis: a new mechanism for microvascular lesion during cerebral malaria. *J Immunol* **176**: 1180-1184.
- Wassmer, S. C., V. Combes, F. J. Candal, I. Juhan-Vague & G. E. Grau, (2006a) Platelets potentiate brain endothelial alterations induced by Plasmodium falciparum. *Infect Immun* **74**: 645-653.
- Wei, Y., P. Chen, M. de Bruyn, W. Zhang, E. Bremer & W. Helfrich, Carbon monoxide-releasing molecule-2 (CORM-2) attenuates acute hepatic ischemia reperfusion injury in rats. *BMC Gastroenterol* **10**: 42.
- White, N. J., G. D. Turner, I. M. Medana, A. M. Dondorp & N. P. Day, (2009a) The murine cerebral malaria phenomenon. *Trends Parasitol* **26**: 11-15.
- White, V. A., S. Lewallen, N. A. Beare, M. E. Molyneux & T. E. Taylor, (2009b) Retinal pathology of pediatric cerebral malaria in Malawi. *PLoS One* **4**: e4317.
- Wilson, C., G. H. Foster & M. Bitzan, (2005) Silencing of Bak ameliorates apoptosis of human proximal tubular epithelial cells by Escherichia coli-derived Shiga toxin 2. *Infection* **33**: 362-367.

- Wilson, N. O., M. B. Huang, W. Anderson, V. Bond, M. Powell, W. E. Thompson, H. B. Armah, A. A. Adjei, R. Gyasi, Y. Tettey & J. K. Stiles, (2008) Soluble factors from *Plasmodium falciparum*-infected erythrocytes induce apoptosis in human brain vascular endothelial and neuroglia cells. *Mol Biochem Parasitol* **162**: 172-176.
- Win, T. T., A. Jalloh, I. S. Tantular, T. Tsuboi, M. U. Ferreira, M. Kimura & F. Kawamoto, (2004) Molecular analysis of *Plasmodium ovale* variants. *Emerg Infect Dis* **10**: 1235-1240.
- Wu, G. D., H. J. Zhou & X. H. Wu, (2004) Apoptosis of human umbilical vein endothelial cells induced by artesunate. *Vascul Pharmacol* **41**: 205-212.
- Yang, Y., R. Sharma, A. Sharma, S. Awasthi & Y. C. Awasthi, (2003) Lipid peroxidation and cell cycle signaling: 4-hydroxynonenal, a key molecule in stress mediated signaling. *Acta Biochim Pol* **50**: 319-336.
- Yipp, B. G., M. J. Hickey, G. Andonegui, A. G. Murray, S. Looareesuwan, P. Kubes & M. Ho, (2007) Differential roles of CD36, ICAM-1, and P-selectin in *Plasmodium falciparum* cytoadherence in vivo. *Microcirculation* **14**: 593-602.
- Yu, C., Y. Minemoto, J. Zhang, J. Liu, F. Tang, T. N. Bui, J. Xiang & A. Lin, (2004) JNK suppresses apoptosis via phosphorylation of the proapoptotic Bcl-2 family protein BAD. *Mol Cell* **13**: 329-340.
- Zang-Edou, E. S., U. Bisvigou, Z. Taoufiq, F. Lekoulou, J. B. Lekana-Douki, Y. Traore, D. Mazier & F. S. Toure-Ndouo, (2010) Inhibition of *Plasmodium falciparum* field isolates-mediated endothelial cell apoptosis by Fasudil: therapeutic implications for severe malaria. *PLoS One* **5**: e13221.
- Zeng, H., H. Wu, V. Sloane, R. Jones, Y. Yu, P. Lin, A. T. Gewirtz & A. S. Neish, (2006) Flagellin/TLR5 responses in epithelia reveal intertwined activation of inflammatory and apoptotic pathways. *Am J Physiol Gastrointest Liver Physiol* **290**: G96-G108.
- Zimmermann, K. C. & D. R. Green, (2001) How cells die: apoptosis pathways. *J Allergy Clin Immunol* **108**: S99-103.